THERMOMECHANICAL AND RHEOLOGICAL PROPERTIES OF INVESTMENT CASTING PATTERNS

This dissertation is submitted in fulfilment of the requirement for the Doctor of Philosophy (PhD): Engineering: Chemical

ROBERT KIMUTAI TEWO
217054242

Vaal University of Technology, Main Campus
Private Bag X021, Vanderbijlpark-1900, South Africa

Supervisor: Prof. H.L. Rutto
Co-supervisor: Prof. W. Focke
Dr. T. Seodigeng

DECLARATION BY CANDIDATE

"I hereby declare that the thesis submitted for the degree Doctor of Philosophy: Chemical Engineering, at the Vaal University of Technology, is my own original work and has not previously been submitted to any other institution of higher education. I further declare that all sources cited or quoted are indicated and acknowledged by means of a comprehensive list of references".

Robert Kimutai Tewo 2nd October 2019

DEDICATION

Dedicated to

My parents:

Alexander Chepsergon Tewo

Margaret Mokiyo Chepsergon

and siblings

for all their love and support throughout my life.

ACKNOWLEDGEMENTS

First and foremost, I would like to extend my sincere gratitude and appreciation to my able and approachable supervisor professor Hilary Rutto for giving me an opportunity to be part of his research team. Thanks for the intellectual guidance all through my studies and caring about my general wellbeing while in South Africa. I extend my deepest gratitude to my co-supervisor professor Walter Focke for his exceptional research philosophy and high standard of excellence that he has instilled in me. Thank you for allowing me to use all the facilities at the Institute of Applied Materials and treating me on par with your own students at the University of Pretoria. You introduced me to the world of applied materials and widened my knowledge to visualize the formulations of new polymers mechanisms in order to get a great understanding of what I was expected of. Your glimmers of hope during the experimental work in the smallest steps of progress was tremendously motivational, and taught me to take pride in everything I do. Thanks also goes to Dr. Tumisang Seodigeng, my co-supervisor, you have always been part of this work.

Special thanks to Dr. Isbe Van Der Westhuizen for the help with TGA/DSC/TMA analysis, you contributed immensely to the completion of this work. Dr. Shatish Ramjee for the rheology analysis.

I would also like to acknowledge my colleagues, especially Dr. Benjamin Mapossa, you were part of every step of my research, we always called each other a brother. Thanks also goes to Alcides Sitoe, Katlego Mphahlele, Baatseba Nkgabane, Lucky Malise and Moshe Mello my office mates, you guys were a source of encouragement all through. Al though we were researching on different research areas, the talk, the discussions and the laughter we had sometimes kept me going.

My family has always been the best and most devoted set of supporters I could have ever asked for. My parents instilled in me a great deal of hard work, discipline, humbleness and endurance from a tender age. My sister Jacqueline has amazed me with her prayers and encouragement in every step of my life. Her great believe in God and her constant prayers has always given me a sense of cover and protection. My other brothers and sisters, you have been with me through the ups and downs of undergraduate and graduate school, in the country and out of the country, your backing has been incredibly worthwhile and enabling for me.

I am deeply indebted to Lawrence Koech, we have walked this journey together for 11 years as members of one family it has been a roller coaster, Gideon Koech you joined us and the family grew. My mentees Isaac Mbucho and Nthabeleng Mokoteli, you two have been a younger brother and a sister at the University of Pretoria, you guys brought levity to the many stressful parts of a Ph.D. studies, as you were a source of encouragement and perspective and I wish you well as you finish your undergraduate and Honours degree. Housemates Mr. Francis Nturanabo, Leonard Onyango, Dr. Wesley Omwoyo and Wilson Webo, thanks for the great time we spent together. I will surely miss you.

PREFACE

The central theme of the study was to explore the thermal, mechanical, surface and rheological properties of wax/ethyl vinyl acetate (EVA) and wax/linear low-density polyethylene (LLDPE) blends and how it can be further modified by incorporating acrylics. The first phase of the project involved studying the wax/EVA and wax/LLDPE blends i.e. from 10-40% EVA/LLDPE and fully characterizing them in terms of their thermal, mechanical, surface and flow characteristics. EVA and LLDPE were chosen due to their compatibility with wax which is brought by the presence of CH_2 chains in both wax, EVA and LLDPE. The second and third phase of the project entailed the incorporation of acrylic (PMMA) into the wax/EVA and wax/LLDPE polymer blend matrix. The thermal, mechanical, surface and flow characteristics of both wax/EVA/PMMA and wax/LLDPE/PMMA was also investigated. The thesis is structured in a way that all the three research areas are captured in chapters 3-5. The highlight of the work is the improvement of the mechanical properties of the wax/EVA/PMMA and wax/LLDPE/PMMA polymer blends.

The thesis has six chapters each with the list of references and the appendices all combined together after the conclusions and recommendations chapter.

Chapter 1 is an introduction to the study; it contains a brief overview and the history of investment casting patterns and how wax properties can be improved by incorporating additives into its matrix.

Chapter 2 highlights the history of investment casting process, patterns for investment casting process, comparisons between investment casting process and other casting techniques. It also gives comprehensive details of previous studies involving the development of investment casting pattern material where several additives have been incorporated into wax. The methods used to

characterize investment casting pattern as well as factors affecting investment casting process are also mentioned in detail.

Chapter 3 examines the properties of wax/EVA and wax/LLDPE blends prepared by conventional extrusion process. The chapter presents a full characterization of the wax/EVA and wax/LLDPE blends in regards to its thermal properties, mechanical properties, surface properties and its flow properties.

Chapter 4 provides the effects of incorporating of PMMA into the wax/EVA blend by extrusion process on the thermal properties, mechanical properties, surface properties and its flow properties.

Chapter 5 highlights the effects of incorporating of PMMA into the wax/LLDPE blends by extrusion process and the effects of incorporation on the thermal properties, mechanical properties, surface properties and its flow properties.

Chapter 6 gives a summary of the study and provides all the key findings. As the concluding chapter, it highlights all the recommendations on the future research studies and other possible application of incorporating polymers into blends.

The **References** provide all the literature material used in the course of this study which was also used to elucidate the findings of the study.

The **Appendices** give the complementary data generated from the study as well as other important data.

ABSTRACT

Investment casting process is the most suitable technique for producing high quality castings which are dimensionally accurate with excellent surface finish and complex in nature. Recently with the ever-changing manufacturing landscape, the process has been increasingly used to produce components for the medical, aerospace and sports industry. The present study looked at three investigative scenarios in the development of a pattern material for investment casting process: (i) the development of wax/ethyl vinyl acetate (EVA) and wax/linear low-density polyethylene (LLDPE) blends as the carrier vehicle materials for the development of pattern material for investment casting; (ii) the development of wax/EVA/polymethyl methacrylate (PMMA) based investment casting pattern and lastly (iii) the development of wax/LLDPE/PMMA based investment casting pattern material.

The **first part** of the studies elucidates the effects in terms of the thermal, mechanical, surface and rheological properties when paraffin wax in blended with poly EVA and LLDPE. The developments involved the extrusion of seven formulations for EVA and also LLDPE using a twin-screw extrusion compounder. The paraffin wax weight percent investigated ranged from 33% to 87% thus encompassing both low and high wax loading ratios. The thermal properties of the developed binary blends were characterized via thermogravimetric analysis (TGA) and differential scanning calorimetry (DSC). The mechanical properties were characterized using three-point bending test. The thermo-mechanical and rheological properties were determined using thermomechanical analysis (TMA) and a rheometer respectively. A scanning electron microscope (SEM) was used to study the surface texture of the extruded blends. The thermal properties indicated that the thermal stability of paraffin wax is improved when it is blended with both EVA and LLDPE. DSC curves showed two endothermic melting peaks and two exothermic

crystallisation peaks. In the case of wax/EVA blends, there was no distinct peak showing the independent melting of neat wax and EVA. The peak at a temperature of 50 – 72 °C corresponds to the melting of the wax/EVA blend. In the case of wax/LLDPE blends, the peak at 50 -66 °C corresponds to the melting of wax whereas the large peak at 112 - 125°C corresponds to the melting of the LLDPE. Wax/EVA and wax/LLDPE had improved mechanical properties as compared to that of neat wax. The rheological properties of both the EVA based and LLDPE based blends indicated that the viscosity of the blends increased as compared to that of neat wax. SEM confirmed that EVA alters the wax crystal habit at higher concentrations. In the case of wax/LLDPE blends, at 20-30 % wax content, a heterogeneous surface was observed, indicating the immiscibility of the paraffin wax within the LLDPE matrix. At a high wax content, there was agglomeration of wax. LLDPE allows amorphous structure of wax to disperse easily between the chains.

The **second part** of the studies focussed on the wax/EVA filled with poly (methyl methacrylate) (PMMA) microbeads. TGA behaviour on the pyrolysis of wax/EVA/PMMA showed that the compounds volatilise readily with virtually no residue remaining above 500 °C. The DSC curves indicated that, the incorporation of PMMA reduced the crystallinity of wax/EVA blend. A distinct endothermic peak and another small peak was observed in all the formulations. The mechanical properties of wax/EVA/PMMA improved significantly. The methylene group present in both wax and EVA combined to form a blend with enhanced mechanical properties whereas the PMMA microbeads improved the needle penetration hardness. The melt viscosity of wax/EVA/PMMA increased as the EVA and/or the PMMA content is increased. The rheological experimental data fitted with the data predicted using the modified Krieger and Dougherty expression. The maximum attainable volume fraction of suspended PMMA particles was at $\varphi_{max} = 0.81$. The SEM micrograph

of wax/EVA/PMMA revealed a near perfect spherical nature for the filler particles in the wax/EVA polymer matrix. It further shows that the PMMA microbeads were weakly bonded and well distributed in the wax/EVA matrix.

The **third part** of the studies focussed on the wax/LLDPE filled with Poly (methyl methacrylate) (PMMA) microbeads. The incorporation of LLDPE and PMMA into paraffin wax had a strong influence on the thermal properties, tensile properties, flow properties and its morphology. The TGA analysis showed that there was a slight observable decrease in the melting onset temperatures when the wax content was increased. From the DSC curves, the corresponding values of onset temperatures observed are between melting and crystallization temperature of neat paraffin wax and neat LLDPE. The short chains of the paraffin wax and the fragments formed by scission of wax chain have sufficient energy to escape from the matrix at lower temperatures. The slight decrease in peak temperatures associated with melting and crystallization could be attributed to the decrease in the average lamellar thickness of the blends. The tensile properties by three-point bending tests indicated an increase in the stress with an increase in the LLDPE content. This can be attributed to the formation of paraffin wax crystals in the amorphous phase of the blend which may influence the chain mobility. Since the paraffin wax used for this study had a low viscosity as compared to LLDPE, both LLDPE or PMMA had an influence on the viscosities of the blends. The data obtained from the experiments fitted with the data predicted obtained from the modified Krieger and Dougherty expression. The maximum attainable volume fraction of suspended PMMA particles was at $\varphi_{max} = 0.74$. Similar observation with that of wax/EVA/PMMA was made in terms of the morphology of the wax/LLDPE/PMMA blends.

The excellent thermal stabilities, the superior mechanical strength of wax/EVA/PMMA and wax/LLDPE/PMMA and the flow properties with relatively high EVA and also with high PMMA

loadings, open new opportunities for EVA and LLDPE based pattern material for in investment casting process. It is worth pursuing further comprehensive studies since it offers a strong potential for realizing further technological improvement in the field of investment casting and rapid prototyping technologies.

Keywords:

Paraffin wax, ethylene vinyl acetate, linear-low density polyethylene, poly methyl methacrylate, investment casting, rheology, thermal stability, three-point bending tests.

GRAPHICAL ABSTRACT

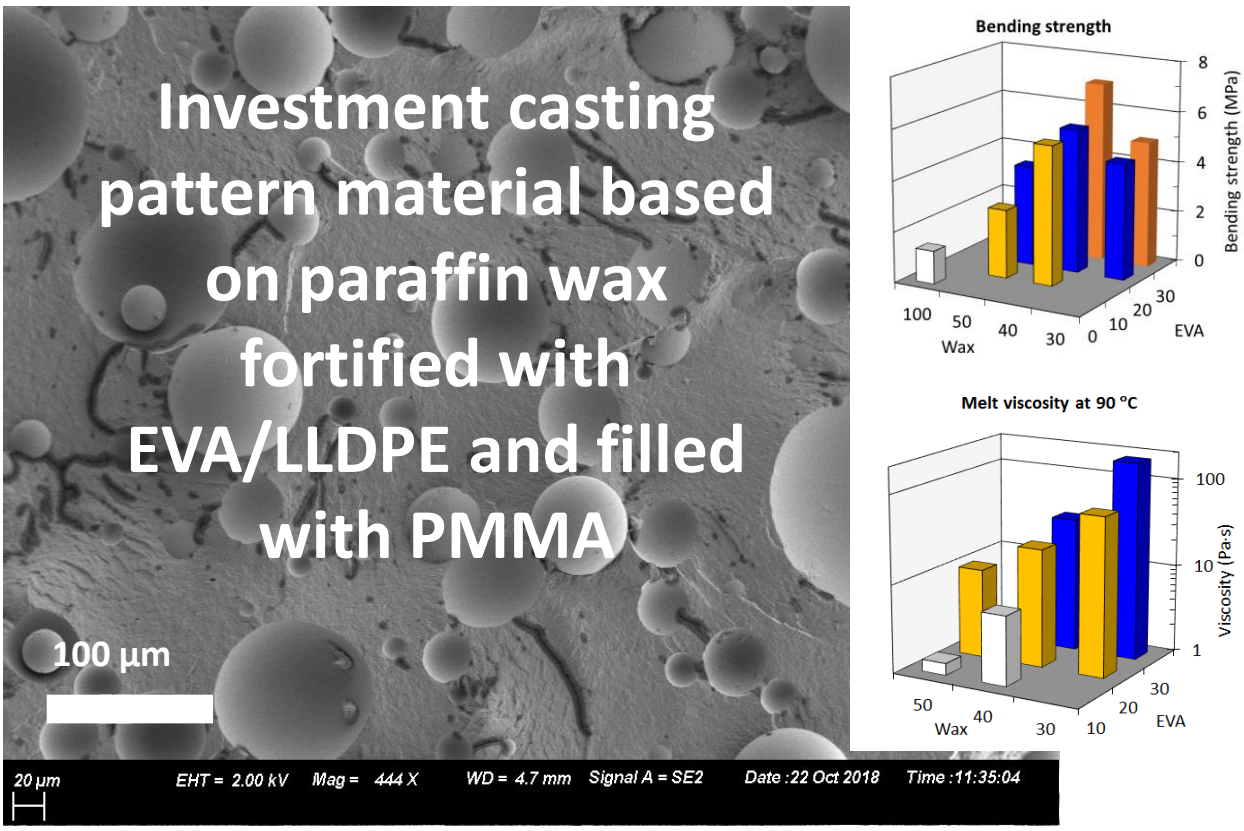

TABLE OF CONTENTS

LIST OF FIGURES

LIST OF TABLES

LIST OF EQUATIONS

$$\eta = \eta_s(1 + 2.5\varphi) \tag{2.1}$$

$$\frac{\eta}{\eta_o} = (1 - \frac{\varphi}{\varphi_{max}})^{-2.5k\varphi_{max}} \tag{2.2}$$

$$\mathrm{M} = \frac{-\mathrm{L}(\mathrm{F} + \frac{\mathrm{wL}}{2})}{4} \tag{2.3}$$

$$\mathrm{w_o} = \frac{\mathrm{WL^3}}{48\mathrm{EI}} \tag{2.4}$$

$$\text{Solidification time} = \mathrm{C}\left(\frac{\text{Volume}}{\text{Surface area}}\right)^{\mathrm{n}} \tag{2.5}$$

$$\mathrm{Q} = -\mathrm{kA}\frac{\mathrm{dT}}{\mathrm{dx}} \tag{2.6}$$

$$\mathrm{Re} = \frac{\mathrm{vD\rho}}{\eta} \tag{2.7}$$

$$\Delta\mathrm{V} = \beta\mathrm{V_i}(\mathrm{T_i} - \mathrm{T_f}) \tag{2.8}$$

$$\sum_{\mathrm{i=1}}^{\mathrm{q}} \mathrm{x_i} = 1 \; ; x_i \geq 1 \; ; \mathrm{i} = 1 \ldots, \mathrm{q} \tag{2.9}$$

$$\mathrm{x_1} + \mathrm{x_2} + \mathrm{x_3} = 1 \tag{2.10}$$

$$\mathrm{F_{Elong}} = 6\pi\eta\varepsilon\gamma^2 \tag{2.11}$$

$$\mathrm{F_{Shear}} = 3\pi\eta\,\dot{\gamma}\mathrm{r}^2 \tag{2.12}$$

$$\mathrm{E} = \frac{\mathrm{L^3m}}{4\mathrm{bd^3}} \tag{3.1}$$

$$\sigma_f = \frac{3PL}{2bd^2} \tag{3.2}$$

$$\varepsilon_f = \frac{6Dd}{L^2} \tag{3.3}$$

$$\eta_{mix} = \exp\left(w_{wax} ln\eta_{wax} + 2\, w_{wax} w_{EVA} ln\eta_{Int} + w_{EVA} ln\eta_{EVA}\right) \tag{4.1}$$

$$\frac{\eta}{\eta_o} = \left(1 - \frac{\varphi}{\varphi_{max}}\right)^{-2.5k\varphi_{max}} \tag{4.2}$$

LIST OF ABBREVIATION

ANOVA - Analysis of variance

ASTM - American society for testing and materials

ATR - Attenuated total reflectance

CSIR - Council for scientific and industrial research

DMA - Dynamic mechanical analysis

DSC - Differential scanning calorimeter

DTG - Derivative thermogravimetry

EVA - Ethylene vinyl acetate

FESEM - Field emission scanning electron microscope

HTMA - Hexamethylene tetramine

KD - Krieger Dougherty

KN - Kilo Newtons

LDPE - Low density polyethylene

LLDPE - Linear-low density polyethylene

LVDT - Linear variable displacement transducer

MCR - Modern control register

MFI - Melt flow index

MIM - Metal injection moulding

MPA - Mega pascals

PET - Polyethylene terephthalate

PM- Powder metallurgy

PMMA - Polymethyl methacrylate

PSD -	Particle size distribution
PVOH -	Polyvinyl alcohol
RP -	Rapid prototyping
SEM -	Scanning electron microscope
TGA-	Thermogravimetric analysis
TMA -	Thermomechanical analysis
VA -	Vinyl acetate
3D -	3 Dimension

LIST OF SYMBOLS

A	m^2	Cross-sectional area
B	K^{-1}	Volumetric coefficient of thermal expansion
b	m	Specimen width
D	m	Maximum deflection of the centre of the beam
d	m	Specimen thickness
D_m	m	Diameter of the channel
Dt/dx	Dimensionless	Temperature gradient.
E	GPa	Young's modulus of bending
F	N	Force
$\Delta H_{(pm)}$	kJ/kg	Specific enthalpy of melting
$\Delta H_{(pc)}$	kJ/kg	Specific enthalpy of crystallization
h	m	Height
I	m^2	Second moment area
k	W/m. K	Thermal conductivity of the body;
k	Dimensionless	Particle shape factor
L	m	Length of support span
M	Nm	maximum bending moment
m	Dimensionless	Slope of the gradient to the initial load deflection curve
P	N	Maximum load
Q	W/m^2	Heat flow rate;
r	m	radii of the particles
ΔT	° C	Change in temperature

T_f	° C	Final temperature.
T_g	° C	Glass transition temperature
T_i	° C	Initial temperature
T_{pc}	° C	Peak crystallization temperature
T_{pm}	° C	Peak melting temperature
T_{oc}	° C	Onset crystallization temperature
T_{om}	° C	Onset melting temperature
ΔV	m^3	Change in volume
V_i	m^3	Initial volume
V_o	m^3	Occupied volume
v	m/s	Velocity of the liquid
w_{wax}	g	Wax weight fraction
$w_{EVA/LLDPE}$	g	EVA/LLDPE mass fraction

Greek

η	Pas	Viscosity
ε	Dimensionless	Strain
ρ	Kg/m^3	Density of the sample
η_{mix}	Pas	Viscosity of the binary mixture,
η_{wax}	g	Viscosities of the neat wax
$\eta_{EVA/LLDPE}$	Pas	Viscosity EVA/LLDPE.
η_s	Pas	Viscosity of the suspension
η_o	Pas	Viscosity of pure fluid

φ -	Dimensionless	Volume fraction of suspended particles
φ_{max}	Dimensionless	Maximum volume fraction of suspended particles.
γ	N/m	Surface tension
α	K^{-1}	Coefficient of linear thermal expansion
σ	N/m^2	Stress
σ_0	N/m^2	Maximum stress
$\dot{\gamma}$	s^{-1}	Shear rate

Chapter 1 . BACKGROUND AND INTRODUCTION

Investments casting produced metal parts currently play an important role in enhancing our daily lives through medical implants, power generation, air travel and other diverse myriad components (Upadhya *et al.*, 1995 ; Jones & Yuan, 2003). The demand for investment casting metals that are of high quality, low cost and with the ability to perform well under extreme operating conditions has increased in the competitive market in the recent past (Biernacki *et al.*, 2015). The growth in the sector has led to increased manufacture of sophisticated and lightweight engineering components as a way of reducing the production costs as well improving the overall efficiency of investment casting engineering systems.

Investment casting process, also known as "lost wax process" is used to produce ferrous and non-ferrous metal parts. Investment casting process is an ancient method employed by early man in the production of primitive tools. The process involves four stages; (i) injecting wax into a metal mould, (ii) building of a ceramic shell mould around the wax by the application of a series of ceramic coatings to the wax pattern, (iii) dewaxing of the ceramic shell mould and (iv) Casting of the alloy into the shell mould (Taylor, 1983). Investment casting process is significant over sand casting due to its ability to produce components of excellent dimensional accuracy, perfect surface finish and complex shapes. The process also produces parts of great precision, reliability, and flexibility (Jones and Yuan, 2003; Sabau and Viswanathan, 2003; Pattnaik *et al.*, 2012).

Sand casting has been the most extensively used technology to produce various large metal and alloy parts mainly from iron, aluminium and brass. However, due to the advancement in the production of complex parts, the process is hampered by a number of serious problems such as difficulty to produce components with predetermined weight and size specification, a trend of

yielding products with a comparatively rough surface finish and also the process produces metal parts with a lower degree of accuracy and precision as compared to other casting technologies such as investment casting (Williamson, 2005).

The wax pattern used in investment casting process has the exact geometry of the required final cast part with dimensional allowances to compensate for its own volumetric shrinkage as well as the solidification shrinkage of the cast metal in the ceramic mould. Wax, fillers, resins and additives are the common materials used for pattern making, but wax has been widely used (Vekariya and Ravani, 2013). The pattern material used for investment casting should have the following characteristics: (i) low thermal expansion so that it can form a shape with highest dimensional accuracy; (ii) smooth and wettable surface in order to obtain a smooth finished surface; (iii) resistance to breakage to obtain sufficient strength at room temperature; (iv) high melting point than the ambient temperature to prevent distortion of thick sections and surface cavitation; (v) low viscosity when melted in order to fill the thinnest sections of the die; (vi) residual ash content of $\leq 0.05\%$ and (vii) environmentally safe to avoid the formation of environmentally hazardous or carcinogenic materials upon combustion (Singh *et al*., 2006).

The drawbacks associated with the use of wax only for investment casting patterns is that, conventionally, during investment casting process, wax must be injected at temperatures above room temperature i.e. temperatures above 40 °C. Waxes being Non- Newtonian fluid exhibit elasto-viscoelastic characteristics and are subjected to shearing forces that make them become more of a fluid when they are injected in the extrusion moulding machine under pressure (Zhang and Gilchrist, 2012). In addition, the use of wax pattern for a small number of investments casting pieces as well as for products with thin geometry that readily break or deform when handled is not economically viable due to its precision casting application limitations. The use of fillers, additives

and resins based investment casting pattern gives a better dimensional accuracy and a better quality of the final investment casting product (Zhang and Gilchrist, 2012). Muschio III (1996) researched and invented the use of thermoplastic cellulosic acetate resin powders as a useful filler material to improve wax properties for investment casting.

The performance of investment casting pattern is directly dependent on the addition of fillers, resins, and other additives. There have been significant strides recently in the use of wax blends to produce an improved investment casting pattern material with improved properties such as better surface finish, minimum shrinkage and moderate hardness. The use of fillers and resins have enhanced effects on the thermal, physical, shrinkage characteristics and mechanical properties such as thermal conductivity of wax, wax heat capacity, and mechanical strength of investment casting pattern. Paraffin wax, beeswax, montan wax, and carnauba wax have been blended to produce a pattern with improved properties (Bemblage and Karunakar, 2011). Other additives such as oils and plasticizers addition in small quantities have also been found to increase the pattern mechanical strength. Examples of resins that have been used for investment casting pattern include ester gum, evaflex V-577. Mostly, fillers consist of fine powder materials. The most commonly used fillers include isophthalic polystyrene, bisphenol A and hydro-fill (Kawano *et al*., 1988).

A lot of research and development has been conducted to develop processes to produce an investment casting patterns with better physical, thermal and mechanical properties (Guler *et al*., 2011). The last four decades has seen a continuous development of noble investment casting patterns by using blend of waxes, polymers, oils, plasticizers, solid organic fillers, and resins. Uram (1969) studied the use of thermoplastic resin polystyrene for pattern production to blend wax. He concluded that, plastic materials have good hot strength properties, ease of assembly and handling and dimensional stability, however, the challenge associated with plastic materials is the

distortion of the green investment. Merges et al. (1972) investigated the use of 25- 65% petroleum wax, 25 – 55% solid chlorinated polyphenyl, 5 – 15% acid type montan wax and 0.1 – 5% stearic acid. Guinn (2002) investigated the use of 5 – 50% (weight percent) polyethylene terephthalate as a filler material. Guinn (2002) also concluded that, filler materials are effective in controlling the expansion and contraction properties of the blended wax material. Rutto and Focke (2009) investigated on the formulation of urea-based investment casting pattern using low polarity ethylene vinyl acetate (EVA) and a highly hydrophilic plasticized poly vinyl alcohol (PVOH), the study concluded that, addition of urea brought about enhanced mechanical properties of the pattern, however, its shortcoming is that, urea tends to decompose when the wax is melted. Though there was an improvement of pattern characteristics in terms of shrinkage and penetration, most of these blended patterns exhibit distortion tendencies, some high thermal expansion tendencies, and thus it is important to do more studies to develop an investment casting pattern material by incorporating fillers material and resins to develop a pattern that would overcome most of the limitations if not all.

Rheological study is an important aspect in the formulation and development of investment casting pattern. Rheology is the study of science that deals with the flow and deformation of matter under controlled testing conditions. Rheology is significant in the determination of melt process ability of pattern material as well as the waxes chemical and physical properties (Cassagnau, 2008; Zapata *et al*., 2015). Generally, when pressure and thermal application is exerted on most plastics materials, because of extrusion process, there is a significant reduction in its molecular weight. The reduction of molecular weight is associated with an increase in melt flow index (MFI) which in turn leads to polymer chain degradation. In addition, when virgin thermoplastics are processed into any product, by overheating and application of excessive shear the initial antioxidant present

in it is largely depleted. The main purpose of rheometry is to establish the apparent viscosity in extrusion machines or injection moulding machines, this will in turn help in the behavioural understanding of different wax types, fillers and additives melts flows during its manufacture, hence, making injection moulding a measurable process for manufacturing high-quality parts (Zhang and Gilchrist, 2012).

The present study seeks to focus on the development and formulation of compoundable investment casting pattern using Sasol Fischer – Tropsch waxes, resins and binders (ethyl vinyl acetate – EVA and linear low- density polyethylene (LLDPE)) and poly methyl methacrylate (PMMA) as a filler. The study will explore ways of optimization relating to the content in terms of percentages of wax, fillers, resins, and binders. The study will also consider the development of novel compounding techniques using vibrating ring droppo pelletizer to utilize different wax types, fillers, resins, additives and binders based moulding compounds for investment casting processes. Thermal, rheological, mechanical and surface morphology characterization of the formulated investment casting pattern was conducted.

1.1 PROBLEM STATEMENT

The use of wax as the only pattern material for investment casting process to produce advanced and light weight engineering components has been hindered by: (i) dimensional accuracy control due to wax hot deformation and thermal expansion; and (ii) wax rigidity and strength deficiency properties for highly fragile patterns (Sabau and Viswanathan, 2003). The demand for complex, advanced and light weight engineering components has increased worldwide in the recent past. In addition, the need to develop ready for use, soft pattern material for investment casting, has led to increased research and development for a more suitable material to be used for investment casting

pattern. There is need to develop an improved investment casting pattern material by incorporation and application of thermoplastic materials such as fillers, additives and resins for investment casting pattern. Although considerable development has been done on the use of polymers such as poly(ethylene-co-vinyl acetate) (EVA) and poly vinyl alcohol (PVOH) for investment casting patterns, further investigation on the practical application of the use of blended wax types, filler material, resins and its integration to produce a better investment casting pattern needs to be done. The study seeks to evaluate the use of Sasol Fischer - Tropsch waxes combined with poly (ethylene-co-vinyl acetate) (EVA), linear low-density polyethylene (LLDPE) and poly methyl methacrylate (PMMA) as a filler material to formulate a new investment casting pattern.

1.2 OBJECTIVES

1.2.1 Main Objective:

This study aims to develop a new investment casting pattern using Sasol waxes and organic fillers as physical, thermal and mechanical properties enhancing compounds. The developed new pattern material will be capable of satisfying the functional requirements of the investment casting process. The study will seek to evaluate and integrate the application of Sasol Fischer Tropsch wax, EVA, LLDPE and PMMA as a filler material for the formulation of a new investment casting pattern.

1.2.2 Specific Objectives

1) To develop a baseline data in terms of the thermal, mechanical, rheological and surface characterization techniques on filled industrial pattern material (Hyfill B 289) and non-filled industrial pattern (Castylene B97) used for investment casting process;

2) To develop, determine the thermal, mechanical, rheological properties and surface morphology of paraffin wax (Sasol Fischer Tropsch wax) and EVA binary blends using formulation mixture model;
3) To develop, determine the thermal, mechanical, rheological properties and surface morphology of paraffin wax (Sasol Fischer Tropsch wax) and LLDPE binary blends using formulation mixture model;
4) To develop, determine the thermal, mechanical, rheological properties and surface morphology of paraffin wax (Sasol Fischer Tropsch wax) fortified using EVA and filled with PMMA using formulation mixture model;
5) To develop, determine the thermal, mechanical, rheological properties and surface morphology of paraffin wax (Sasol Fischer Tropsch wax) fortified with LLDPE and filled with PMMA using formulation mixture model.

Chapter 2 . LITERATURE REVIEW

2.1. INTRODUCTION

The recent development in metal alloy casting, manufacturing processes has escalated the perplexity faced by designers to manage the track of the prevailing competence of metal casting manufacturing processes and single out the relevant ones. The advancements brought about by recent industrialization in developed countries and developing countries call for new technological developments to handle the growing demand for intricate and complex metal parts. Investment casting technology has had a huge improvement from the ancient times when it was used to produce rudimentary tools till recently where the technology has had a huge positive impact in the casting industries. Today, the use of advanced technologies such as rapid tooling technology and rapid prototyping combined with investment casting process produce metal parts which are relatively cheap with better quality.

2.2. CASTING TECHNIQUES

2.2.1 Sand casting

Sand casting technology is one of the most extensively used casting process. Sand casting technique is used to make large metal and alloys parts mainly of aluminium, brass, bronze and iron 123a duplicate shape of the real part to be produced (Figure 2.1). The cavity where the molten metal is poured, is formed by extracting a pattern from sand that has been filled throughout it. Natural, synthetic or artificially blended material can be used (Campbell, 2015; Ogunwole *et al.*, 2007). Sand casted metallic and alloys parts have shape complexity challenges due to the difficulty in controlling the flow of the metallic liquid into the cavities and the uneasy task of managing

gating. The metal casting parts made by sand casting techniques as compared to other casting processes have the lowest accuracy in terms of its tolerance (Saikaew & Wiengwiset, 2012).

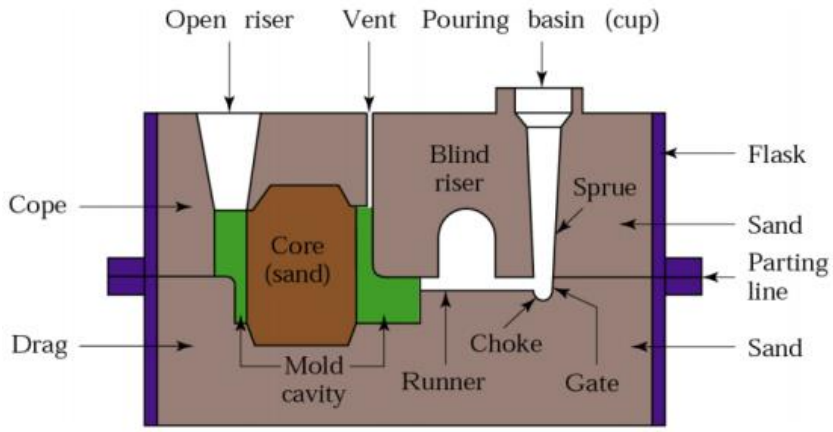

Figure 2.1: Sand casting mould (Campbell, 2015)

2.2.2 Investment casting

Investment casting" lost wax process" as often referred, is an ancient process where ferrous and non-ferrous metals are made from alloys (Sin & Dube, 2004). The process produces metallic parts with pleasing excellent surface finish, complex shapes and dimensional accuracy. Investment casting involves injecting wax or other material into a metallic mound to form a disposable pattern (Karwiński *et al*., 2011; Shivappa *et al*., 2014). A series of shell coatings (composed of ceramic material such as zirconium oxide; a binder which can be either water based binder such as colloidal silica, methyl cellulose, and alcohol based binders such as ethyl silicate and alumina- silicates) is applied on the pattern and is dried in a controlled temperature and humidity oven adiabatically (Li & Zhang, 2003). The ceramic shell mound is then dewaxed and the alloy is casted into the shell to

produce a metallic part. Doli Rani & Karunakar (2013) illustrated investment casting process in eight steps involved, which include: (i) pattern production; (ii) pattern assembly; (iii) investment; (iv) dewaxing; (v) casting; (vi) shell removal; (vii) cut-off and (viii) finishing and inspection as shown in Figure 2.2.

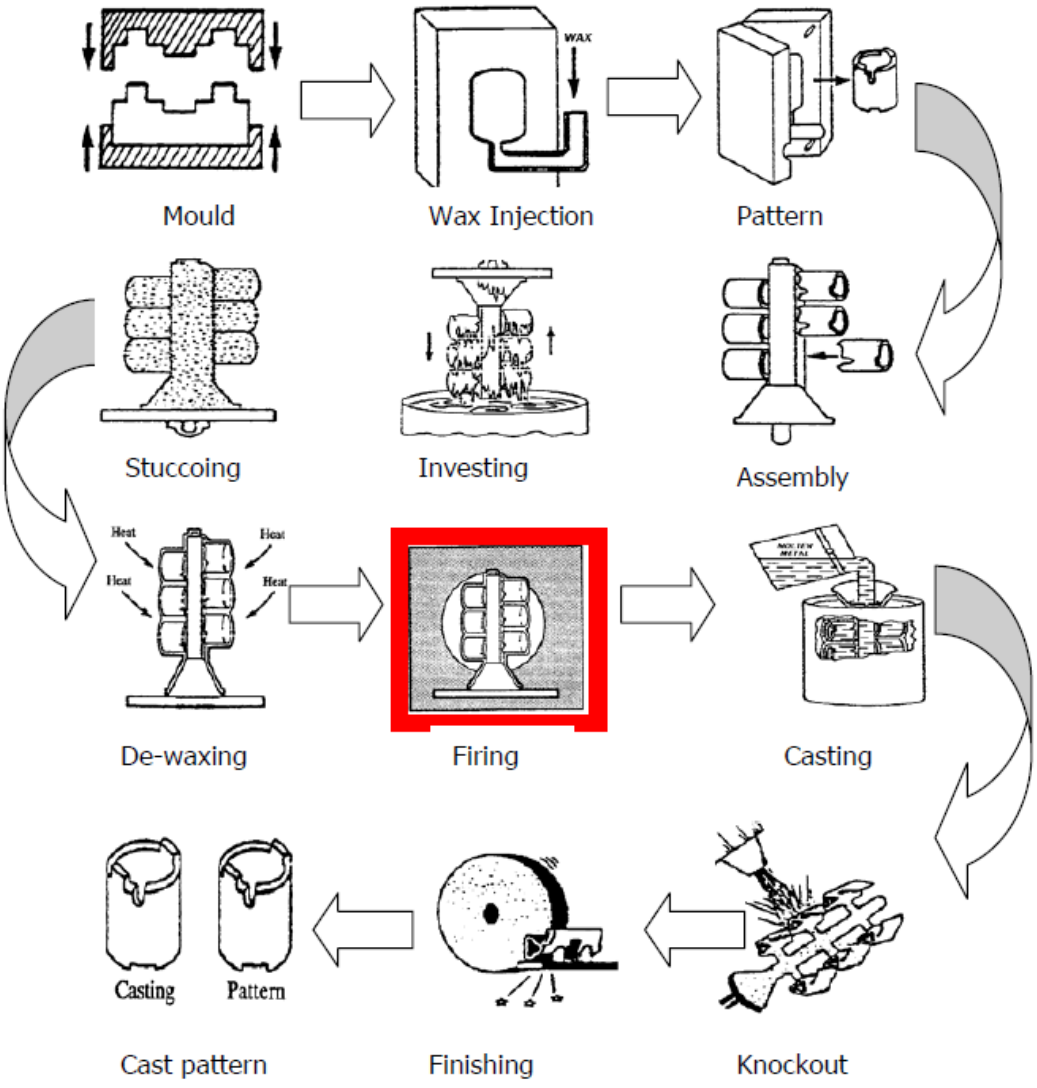

Figure 2.2: Investment casting process (adapted from (Jones & Yuan, 2003).

2.2.3 Pressure die casting

Pressure die casting process is a casting process used to produce non-iron casting alloys for high detail, high volume and economically priced casting metal and alloy parts (Dargusch *et al*., 2006; Güner *et al*., 2015). The metal or alloy part casted is injected at a high pressure into the mould. Die casting utilizes metal moulds or permanent dies to produce a moulded metallic part. The die casting process has three main sub-processes. These are: (i) permanent mould casting, also called gravity die casting, (ii) low-pressure die casting, and (ii) high-pressure die casting (Butler, 2001).

2.2.4 Plaster casting

Plaster mould casting process is used widely in the production of alloys of aluminium, zinc, copper and magnesium. The technique uses gypsum or plaster of Paris as the main materials for casting process (Pawlak & Władysiak, 2009). To regulate the settling time and the contraction characteristics in plaster casting process, additives such as silica flour, asbestos, talc, fibres etc. are added to the gypsum or plaster used. A slurry of plaster of Paris is drained to a metallic pattern bound in a flask. Brass in half portions linked to a match plate (bottom of the moulding flask) is always used as the pattern material (Kim *et al*., 2006). Air trapped in the slurry is removed by vibrating the slurry as well as ensuring the mould is filled up completely. The produced plaster mould is dried in an oven at a temperature of between 200 - 700 °C. The fundamental sprue, runner etc. are cut before joining them (Pastirčák *et al*., 2015).

2.2.5 Permanent and semi-permanent mould casting

Permanent and semi-permanent mould casting is sometimes referred as gravity casting. Permanent mould casting is where a permanent mould or non-expandable mould is used to cast a metallic

part. In permanent and semi-permanent mould casting, the flow of the metal into the mould is due to gravity (Zhang *et al*., 2016). The cores used in this technique are either simple removable cores usually made of metals or sand or plaster cores. Semi-permanent mould casting technique is where sand or plaster cores are used, whereas for permanent mould casting techniques, is whereby the metal core is used and the technique is convenient casting metallic parts with even wall dimension, complex enclosed coring and large number of casting items (Tyler *et al*., 2008). Permanent and semi-permanent mould casting technique gives metals parts with excellent surface finish, better mechanical properties as compared to parts produced by sand casting process given that the alloys used display hindrance to hot tearing and with good fluidity (Bhardwaj *et al*., 2014). Table 2.1 highlights the advantages, disadvantages and application of various casting techniques.

Table 2.1: Advantages, disadvantages and application of types of casting processes (Hamilton, 1989).

	Advantages	Disadvantages	Applications
Sand Casting	❖ Less expensive for small items quantities (<100); ❖ Both ferrous and non - ferrous metals produced; ❖ Very large parts can be casted.	❖ inferior dimensional accuracy as compared to alloys produced by other casting processes; ❖ The process gives castings with poor surface finish	❖ Used for parts with low tolerances levels, surface finish and low machining.
Plaster Casting	❖ Parts with closer dimensional tolerance are obtained; ❖ Parts with intricate shapes and fine details can be produced; ❖ Large parts which cannot be produced by investment casting with less cost to cast can be produced.	❖ expensive when compared to sand or permanent mould-casting;	❖ Used to produce parts with smooth surface finish and with a closer dimensional tolerance.
Permanent and semi-permanent mould casting	❖ Less expensive than Investment or die castings; ❖ Parts produced has a dimensional tolerance closer than sand castings;	❖ Non-ferrous metals can be produced by this process; ❖ A higher tooling cost required for this process than sand cast.	❖ Used for parts that are subjected to hydrostatic pressure; ❖ Excellent for parts having low profile, no cores and quantities in more than 300.

Investment casting	❖ close dimensional tolerance parts are produced; ❖ Complex shape parts with fine details and intricate nature are produced; ❖ Parts with excellent surface finish are produced.	❖ The casting process is expensive as compared to permanent mould, sand casting, or plaster process.	❖ Used for complex and intricate shapes that precludes the use of sand or permanent mild castings; ❖ Has a high cost requirement
Die casting	❖ Good dimensional tolerances parts can be produced; ❖ Parts with excellent surface finish can be produced; ❖ The parts produced require minimal post machining.	❖ Economical for only very large quantities due to high tool cost; ❖ Parts produced are not recommended for hydrostatic pressure applications;	❖ Used for a larger quantity of parts justifies the high tooling cost.

From Figure 2.3, it can be seen that conventional machining processes are well-developed technologies with the capability of employing a wide range of materials in the creation of highly accurate components (Kochan *et al*., 1999). It can also be seen that investment casting process, layer manufacturing and metal injection moulding (MIM) are used to produce metal parts with medium to high geometric complexity whereas MIM and investment casting process can be used to produce a higher quantity of products as compared to layer manufacturing process (Frank *et al*., 2009).

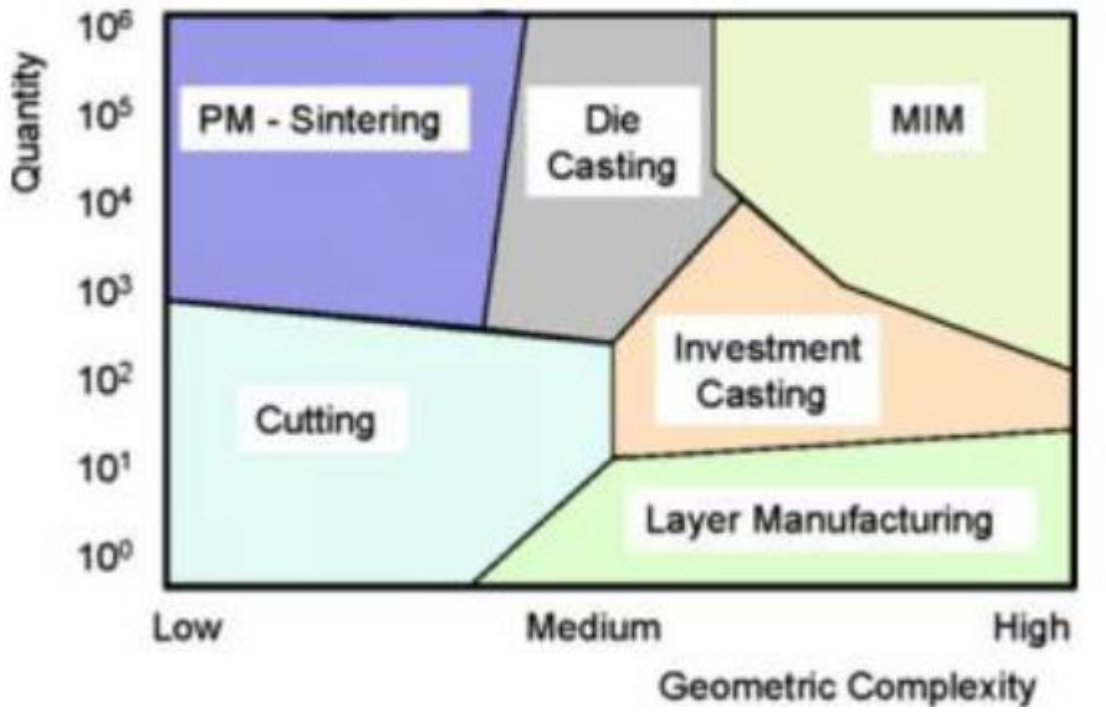

Figure 2.3: Assessment of methods available for metal production

2.3. APPLICATION OF INVESTMENT CASTING PROCESS

Currently investment casting process plays an important role in the various industries. Some of the industries that investment casting parts are utilized include medical industry, power generation, and aerospace as shown in Table 2.2 (Prasad, 2012).

Table 2.2: Industries that use investment casting parts and its applications

Industry	**Application**
Aerospace	Jet engines, aero plane air frames, aircraft fuel systems, aircraft communication systems, aircraft hydraulic systems, aerospace missiles and ground support systems.
Industrial and automotive applications	Industrial gas turbines, oil well drilling and auxiliary equipment, diesel engines, pneumatic systems, machine tools, material handling equipment, valves, packaging equipment.
Medical	Prosthetic appliances, dentistry and dental tools, optical equipment.

2.4. MANUFACTURING ROUTES FOR INVESTMENT CASTING PATTERNS

The production of patterns for investment casting process is characterized into two categories namely (i) indirect approach and (ii) direct approach. In the case of indirect approach, also referred to as the conventional pattern making process, the die is produced under the normal conventional

production techniques (Muller & Sladojevik, 2001). In the case of the direct approach, rapid prototyping systems are used to make patterns. 3D objects are created using RP manufacturing techniques. The 3D created objects are usually used as sacrificial pattern for investment casting process. The only shortcoming associated with this technique is that the technique is used for low volume production of small parts with high geometrical complexities (Frank *et al*., 2009; Medell & Potos, 2016).

2.5. INVESTMENT CASTING PROCESS CAPACITY IN SOUTH AFRICA

Investment casting and rapid prototyping in South Africa is widely used in the aerospace, small arms, mining, medical, pumps and valves, petrochemical and other general engineering fields (Nyembwe, 2007). South Africa currently has three investment casting companies specializing in various investment casting components. There are three well-known companies in South Africa specializing in investment casting process namely: (i) Rely Precision Casting, (ii) IntraCast Precision Casting and (iii) Castco Precision Castings (Crawford, 2017). Also, Council for Scientific and Innovation Research (CSIR) plays a crucial role in the provision of investment casting research facilities.

2.6. INVESTMENT CASTING PROCESS MOULDING COMPOUNDS

2.6.1. Introduction

Wax has been the mostly used as a pattern material for investment casting process mounding compounds. The advantages of wax use include its nature to be easily deformed, easily hardened and wax melts easily at low temperature. The use of wax as a pattern material for complex shapes has been hindered by several defects when it comes to pattern production which can affect the flow

of wax, its solidification time and wax shrinkage. In order to reduce the limitation of the use of wax for investment casting process, various compounds have been incorporated with wax to produce a pattern with better thermal, mechanical, surface and flow properties and with wide range of application in the investment casting industry. Some of the additives incorporated include fillers, resins, plasticizers, emulsifiers etc.

2.6.2. Formulation of investment pattern

Conventionally, wax has been used as the only thermoplastic material for making investment casting pattern material. Beeswax was the major wax for pattern making during the ancient times (Singh *et al*., 2014). With advancement in technology over the years, the term wax refers to any material which has properties like wax material or blends of wax with other components that give an improves pattern material for investment casting (Pankaj Sharma *et al*., 2013). The complex nature and the chain length of carbon essentially are the major factors that influence investment casting pattern properties. Inclusion of other components into investment casting wax material gives variation to its properties such as its viscosity, contraction and expansion, melting point, hardness etc. (Patel, 2016). The above-named properties have great influence on the composition and structure of the final pattern material. The use of filler materials in investment pattern production is mainly to improve the shrinkage tendency of pattern material such as its strength, volumetric expansion and cavitation propensity whereas, the use additives aids in improving the strength and rigidity of investment casting pattern material (Pattnaik *et al*., 2012; Pankaj Sharma *et al*., 2013).

2.6.2.1. Unfilled wax produced investment casting pattern

Several researchers have studied on the use of unfilled wax as a pattern material for investment casting pattern. Doli Rani & Karunakar (2013) from their studies reported that, the use of bee wax and paraffin wax for investment casting pattern gives a better surface finish to the produced alloys. The authors went on to highlight the constituent of bee wax, carnauba wax, montan wax and paraffin wax as follows: (a) bee wax (esters of fatty acids and long chain alcohols with, palmitate, hydroxy palmitate and oleate alcohol chains esters of $C_{30} – C_{32}$); (b) carnauba wax (41%; diesters of 4- hydroxycinnamic acid (21%); fatty acid alcohol $C_{26} – C_{30}$ (12%) and ω – hydroxycarboxylic acids (13%)); (c).Montan wax (non-glyceride carboxylic acid esters (62 – 68 % w/w; long chain free acids (22 – 26% w/w); hydrocarbons (7 – 15 % w/w) and resins); (d) paraffin wax (alkane category of hydrocarbons with a general formula (C_nH_{2n+2})). The properties of the wax types are summarized in Table 2.3 and a general hardness versus temperature curve is described in Figure 2.4.

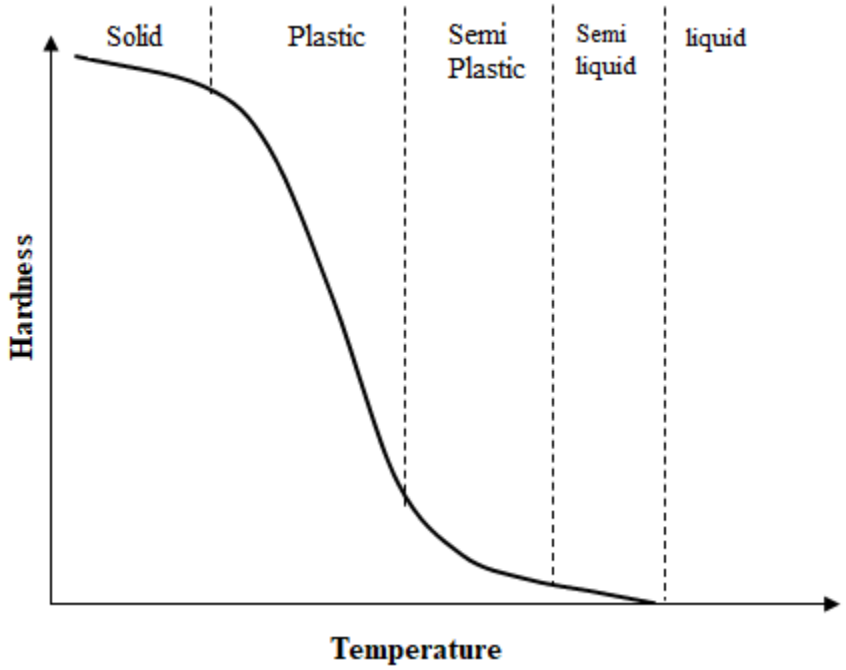

Figure 2.4: Wax hardness depending on temperature change

Table 2.3: Properties of different types of waxes (Doli Rani & Karunakar, 2013)

Type of wax	Density (g/cm^3)	Melting point (° C)	Volumetric shrinkage	Flash point (° C)
Paraffin wax	0.78	52 – 74	6.20	275
Bee wax	0.958 -0.97	62 – 64	7.25	204.4
Carnauba wax	0.97	82 – 86	5.45	300
China wax	0.82	62 – 75	6.28	318
Montan wax	1.02	82 – 95	2.45	300.26

Sabau & Viswanathan (2003) further studied the use of an industrial wax referred to as Cerita^{TM} 29 – 51 for investment casting pattern development. As per their conclusion on the use of computer models for dimensional analysis of Cerita^{TM} 29 – 51, their studies on rheological and thermophysical properties indicated that Cerita^{TM} 29 – 51 pattern material has low thermal diffusivity hence, the wax cools slowly which in turn leads to the formation of a small thickness on the pattern surface. Bemblage & Karunakar (2011) developed a wax blend using five mass ratios as described in Table 2.4 to produce an improved pattern material for investment casting process. Blend 2(paraffin: beeswax: Montan: Carnauba of 50: 30:20:0) produced a pattern material with the best properties with better surface finish and minimum shrinkage. Bemblage & Karunakar (2011) further used Taguchi experimental analysis technique as a way of designing the experiments as well as to develop the suitable experimental condition by optimizing all the process parameters varied in the experiments. From Taguchi method, the best most suitable ratio gave a

linear shrinkage (0.75%); volumetric shrinkage (2.25%); and surface roughness (0.7 µm) from the paraffin: beeswax: Montan: Carnauba of 50: 30:20:0) weight ratios.

Table 2.4: Wax blends proportions (% weight) (Bemblage & Karunakar, 2011)

Blend	Paraffin wax (%)	Beeswax (%)	Montan wax (%)	Carnauba wax (%)
1	50	30	0	20
2	50	30	20	0
3	50	30	10	10
4	60	20	10	10
5	70	10	10	10

Karwiński *et al.* (2011) prepared an improved wax pattern using paraffin wax, Stearin, and polyethylene wax. The studies focused on a typical composition (weight percent) of paraffin wax (70%), stearin (20%) and 10% polyethylene wax. Polyethylene wax and stearin addition reduce the shrinkage capacity of the pattern material and it also preserves the plastic properties of the pattern as well as increase its hardness. The summarized physico-chemical properties of the produced pattern are described in Table 2.5.

Table 2.5: Physico- chemical properties of PET, Paraffin and stearin produced pattern (Karwiński *et al*., 2011)

Parameter	Experiment Number		
	1	2	3
Solidification Temp (° C)	71.4	68.6	71.6
Dropping point (°C)	76.0	68.0	74.0
Penetration at 25 °C (-)	9	9	8
Kinematic viscosity at 100 °C (mm^2/s)	9.11	6.42	8.52
Carbon residue (wt. %)	0.0025	0.0028	0.0018

Shivappa *et al.* (2014) used the factorial method to blend carnauba wax, montan, paraffin and bee wax. The authors emphasis was to consider improved investment casting pattern production and the recyclability of the reclaimed wax. Paraffin wax is required in bulk and was used as the primary wax component and factorial statistical technique was used to vary the other three wax components; hence the other 3 waxes are used as variables. The authors blended the different waxes to get a formulation that gives minimum melting point and congealing point values. The three wax variables (bee wax, carnauba wax, and Montan wax) were coded with letters B, C and D and taken at two level factorials which forms 2^3 factorial experiments. Using ANOVA to interpret the factorial experimental data, the authors concluded that, the independent effects of waxes B, C and D were significant at 99% and 95% confidence levels. (Guinn (2002) concluded that the best formulation which gave an improved investment casting pattern as well a high degree of recyclability composed of 80% paraffin wax, 8% wax B, 8% wax C and 4% wax D.

Recent studies by Patel (2016) elaborated on how to develop an enhanced investment casting pattern with superior mechanical and physical properties basing on volumetric shrinkage, surface finish and tensile properties of the pattern. The author explored the use of commercial wax mixtures (Paraffin wax, Irani wax, Rosin wax, Mointan wax and microchip wax) and innovative additives (charcoal powder) for investment casting pattern. The results affirmed that the combination of distinctive commercial wax and charcoal powder presented an improved volumetric, surface roughness and linear shrinkage to a greater extend. Patel (2016) further found out that temperature influenced the surface roughness of the pattern.

2.6.2.2. Filled wax produced investment casting pattern

Unfilled or straight pattern waxes were used in the ancient early days of investment casting process to produce metals parts of desired shapes (Wang *et al*., 2010). However, with the recent demand for more complex and tightly dimensional casting metal parts, unfilled waxes exhibited performance limitations hence, the research and development of filled pattern material with suitable properties (Rutto & Focke, 2009). Filled investment casting patterns consists of filler materials incorporated either into wax or any other material used for producing pattern. The filler material consists of solid or liquid compounds (Gebelin *et al*., 2003). The solid particles are discrete particles that do not melt during investment casting process. The physical and mechanical properties of polymeric compounds are improved by addition of particulate fillers. Polymeric materials are the ideal filler materials due to: (i) low coefficient of friction as glazing compounds; (ii) polymeric compounds are resistant to corrosion; (iii) polymeric materials have low density and (iv) high transparency properties (Groover, 2010; Pattnaik *et al*., 2012). According to Pankaj Sharma *et al.* (2013); Rutto & Focke (2009), a good filler material should have the following characteristics: (i) a filler material should be inert to the base material used; (ii) a filler material

should have a low ash content (≤ 0.05%); (iii) a filler material should be thermally stable; (iv) a filler material should have a density like that of the molten base wax; (v) a filler material should be relatively cheap and easily found.

Several researchers have investigated on the addition of several filler materials on wax patterns to improve its properties. Vihtelic *et al.* (1999) stated that filler materials in the wax pattern should be in the range of 35 - 40% weight percent. The authors further elaborated that the particle size of the solid filler material should be between 25 – 35 microns preferably (27 to 33 microns) to give a particle size distribution that is narrowly relative hence, reduce the surface depression on the surface of the investment casting pattern. This will improve the surface texture and uniformity of the investment casting wax. Muschio (1996) further added that the use of solid particles as filler materials produce no carcinogenic material during combustion hence, becoming an important ingredient in improving the properties of investment casting pattern. Sabau & Viswanathan (2003) classified filler materials into several categories which include resins such as polyterpene resin, Ciba-Geigy XB5131 acrylate ester blend; plastics/polymers such as polystyrene beads, polyethylene carbonate, polypropylene carbonate, polymethylmethacrylate (PMMA); oils such as castor, organic acids such as adipic acid, isophthalic acid, stearic acid and terephthalic acid. A summary of functional properties and advantages and disadvantages of filled pattern material is described in Table 2.6.

Table 2.6: Filled and unfilled wax pattern advantages and disadvantages (Rajagopal *et al*., 2012)

Criteria	Filled wax	Unfilled wax
Simplicity in wax pattern production	Can be worked with wide range of injection temperature;	Proper wax conditioning needs to be done for proper wax production.
Productivity	Low cycle time are required hence, better productivity;	Due to higher cycle time, unfiled wax results to low productivity.
Surface sinking	For wide range of thickness, surface chills are not required;	For thick cross sections, chills must be used to avoid surface chills.
Flow lines	Better surface quality, no flow lines;	Flow lines or non-fills are always experienced.
Ovality and shape sustaining	Complete solidification is experienced during injection;	Due to uneven cooling, variation in cross section include: bending of wax pattern, ovality chances and variations in dimensions.
Process control	Wide range of injection parameters hence better reliability in dimensional consistency and quality;	Close injection parameters hence frequent injection and process control required.
Dewaxing and burn out	High temperature and time required for complete burn out;	Easy and fast burn out while shell sintering.

2.6.2.2.1. Chlorinated polyphenyl acid type filled investment casting pattern

Research by Merges et al. (1972) investigated the use of chlorinated polyphenyl acid type, Montan wax, Stearic acid and petroleum wax. The resulting investment casting pattern resulting from the combination of the four materials, produced a pattern with low penetration and low shrinkage properties. The use of petroleum wax is limited by volume change and its gradual softening characteristics also referred as slow setup during melting. Slow setup requires a significant amount of time before wax hardens enough to be handled. Ware & Merges (1972), did some studies on the change of petroleum wax volume during heating. The authors concluded that, when petroleum wax is heated from a temperature of 15 °C to 43 °C, it undergoes a volumetric expansion of 14%. He summarized that, a composition (weight %) consisting of 35 – 65% paraffin wax, 25 – 55% solid chlorinated polyphenyl, 5 – 15% Montan wax (acid type) and 0.1 – 5% stearic acid produced an improved investment casting pattern.

2.6.2.2.2. Combustible polyhydric alcohol filled investment casting pattern

Studies done by Speyer (1974) researched on the use of combustible polyhydric alcohol as a filler material for investment casting pattern. The melting point of polyhydric alcohol is higher than the melting point of most wax types hence, the filler material will remain in its particulate existence during injection moulding process. The inventor used a petroleum wax weight composition of at least 40%; pentaerythritol as a polyhydric alcohol (5 – 50% weigh percent); a fatty acid, stearic acid preferred (5 -15%). The significance of a particulate filler is that; it has a reduction in contraction of the pattern tendencies as well as most of them are non-corrosive to ceramic mounds. The use of fatty acids acts as a suspending agent for polyhydric alcohol. Ionic suspension rather

than particulate filled melt is usually obtained with the use of polyhydric alcohol as a filler material.

2.6.2.2.3. Alpha- alkylstrenes polymers filled investment casting pattern

McLaren *et al.* (1975) made some investigation on how polymers of alpha- alkylstrenes, or polystyrene copolymers with vinyl alkyl benzene or α -alkyl styrene or the two copolymers, substituted as polystyrene fillers can be used to produce an innovative pattern material for investment casting. A combination of the copolymers of styrene, a fatty acid and a petroleum wax gives a material which can be injected at lower temperature of 50 – 80 °C and a pressure of 0 – 34 atm. Pattern stiffness and shrinkage can also be controlled with the use of styrene material. The pattern will have an increased shrinkage as well as a lower shrinkage characteristic. In general, the use of polystyrene materials has homogenous sufficient flow tendencies, the pattern material can be removed freely from the metal without damaging the metal part and the material has a good stability during heating and it cannot be oxidized in the presence of air.

2.6.2.2.4. Hexamethylenetetramine (HMTA) filled investment casting pattern

Investigation by Koenig (1979) affirmed that the introduction of hexamethylenetetramine (HMTA) and methenamine into wax material produces a pattern material with low shrinkage properties. HTMA remains in suspension due to its low specific gravity hence, injected non-clogging uniform material is produced. The author concluded that 5 – 50% HTMA and 55 - 80% petroleum wax weight composition gives an improved investment casting pattern compared to the conventional unfilled wax pattern.

2.6.2.2.5. Thermoplastic resins filled investment casting pattern

Muschio (1996) demonstrated a new approach where thermoplastic resin 80% or more powders of cellulosic acetate is incorporated as a filler material for investment casting pattern. Cellulosic resin thermoplastic powders on combustion are environmentally safe since no carcinogenic substances are produced. Cellulose acetate containing 45 weight percent acetyl, up to 52 weight percent propionyl and which has a specific gravity of between 1.31 – 1.32 is preferred. A composition of 15 – 25% (weight percent) thermoplastic acetate powder and 75 – 75% (weight percent) base wax gave the best combination for a suitable investment casting pattern. A pattern material with a low shrinkage capacity, fast setting and dimensional stability is produced.

2.6.2.2.6. Polymeric organic carbonate filled investment casting pattern

Sturgis *et al.* (2001) proposed an improved process whereby polymeric organic carbonate are used as a filler material for investment casting pattern. Polymeric organic carbonate used include polyethylene carbonate, poly (cyclohexane carbonate), polypropylene carbonate and poly (cyclohexane propylene carbonate). The authors from their findings noted that, polymeric organic carbonates decompose completely to give carbon dioxide gas and water. This leads to no residual ash content produced hence, almost no surface flaws on the investment casting produced metallic part. Uygunoglu *et al.* (2015) made further investigation on the physical and mechanical properties of polymeric organic carbonates and affirmed to the findings of (Sturgis *et al*., 2001). The authors further added that polymeric organic carbonates increase the thermal stability as well as the comprehensive strength of the investment casting pattern formed.

2.6.2.2.7. Polyethylene terephthalate filled investment casting pattern

Guinn (2002) proved that the use polyethylene terephthalate as a filler material for investment casting pattern is efficient for controlling the contraction and expansion characteristics of wax patterns. The author alluded that, the advantages associated with the use of polyethylene terephthalate include: (i) polyethylene terephthalate being cheap to some extent, (ii) it also provides a pattern material with a high dimensional preciseness, (iii) it is non-reactive hence, it does not chemically attack the refractory mound, (iv) its high thermal conductivity properties allows quick cooling of the pattern material, (v) it produces no substantial ash content on ignition due to it being able to flow easily during dewaxing and (vi) it has reduced shell cracking tendencies. A composition of (weight percent) 5 – 50% polyethylene terephthalate and 50 – 95% wax gives a pattern material with the highlighted improved properties.

2.7. OTHER MOULDING COMPOUNDS FOR INVESTMENT CASTING PROCESS

2.7.1. Urea filled investment casting pattern

Rutto & Focke (2009) studied the use of urea with poly (vinyl alcohol) plasticized with glycerol or ethylene vinyl acetate (EVA) together with wax to produce an investment casting pattern which can produce a near net shape metal parts. The authors explained that urea being a material with good mechanical and thermal properties, in addition to its low toxicity level and its low melting point, the material is attractive for investment casting process. Jang & Lee (2003) on their studies further revealed that PVOH interacts strongly with urea. Due to its hydrophilic nature and since, the melting point of poly vinyl alcohol exceeds the thermal degradation onset temperature, plasticizing it with compatible and high boiling point glycerol lowers its melting point. In conclusion, the difference in the interaction and affinities between polymer phases, urea, wax, poly

vinyl alcohol formulated investment casting pattern exhibited elevated mechanical properties such as impact resistance, strength and stiffness as compared to ethylene vinyl acetate formulated investment casting pattern. The authors conclusively discussed about the degradation of urea to ammonia and carbon dioxide gas at a temperature above its melting point as the greatest impediment to its use in investment casting pattern formulation process.

2.7.2. Ice based investment casting pattern material

Many researchers in the casting industries have been concerned with the emission of CO_2 and volatile organic matter from melted wax patterns which raises issues on ventilation and environmental regulatory compliance. In addition, the expansion of wax due to stresses from the mound causes cracking. Huang *et al.* (2004) studied the possibility of using ice patterns instead of wax patterns for commercial use. The authors further specified three benefits of ice patterns as (i) environmental benignity of the process; (ii) ready availability of ice than wax brings the economic aspect of the process and (iii) ice shrinks during melting hence, averting the chance of mound cracks. This was further studies to earlier studies done by (Pham *et al.*, 2008). Huang *et al.* (2004) further studied on how catalysts and binders are vital constituents used to improve dimensional accuracy of the pattern. Binders bond refractory material for mound formation whereas catalysts addition into the slurry reduces the gelling time of the pattern. The authors finally concluded that an increase in catalyst to binder ratio improves the dimensional accuracy.

2.8. WAX/POLYMER-FILLER INTERACTION

Wax – filler/polymer interaction at macroscopic and microscopic scale depends on the wax content as well as temperature. Wax -filler interaction produce complex aggregates with its structure dependant on precipitation temperature of the two mixtures(Molaba *et al.*, 2015; Reddy *et al.*,

2018). The co-crystallization of wax-fillers/polymer occurs because of the van der Waals interaction and the changes in polymer interaction in the system. In investment casting pattern, the nature of wax -filler interaction determine the mechanical properties of the pattern (Ansarifar & Saeed, 2012).

2.8.1. Suspension rheology

When solid materials are incorporated into polymers, a suspension of polymer blends plus the solids is formed. Suspension can be defined as a mixture which has solid particles in a liquid. Suspension rheology occurs practically in many industries currently which include the food industry, concrete etc. viscosity measurements in pattern waxes for investment casting is important when it comes to understanding the rheological behaviour of the formulations used (Mueller *et al*., 2010; Ochowiak & Rozanski, 2012). Suspension rheology models are based on the mixture viscosity and the way in which the suspended fluid is affected by the volume of solids suspended in its matrix. The physical characteristics of the suspended solids such as (i) suspended solids shape; (ii) suspended solid sizes and (iii) the distribution of the suspended solids in the fluid matrix. Figure 2.5 summarizes the effect of temperature, pressure, filer material addition, shear rate and molecular weigh on the viscosity of polymeric materials and how a solid particle is sheared in a polymer matrix. Filler material addition has a great increase on viscosity, polymeric materials with narrow molecular weight distribution are more viscous as compared to polymeric materials with broad molecular distribution. The use of additives such as lubricants decrease viscosity whereas pressure, being an important factor in extrusion conditions has an increase in viscosity (Rides, 2005; Sęk *et al*., 2019).

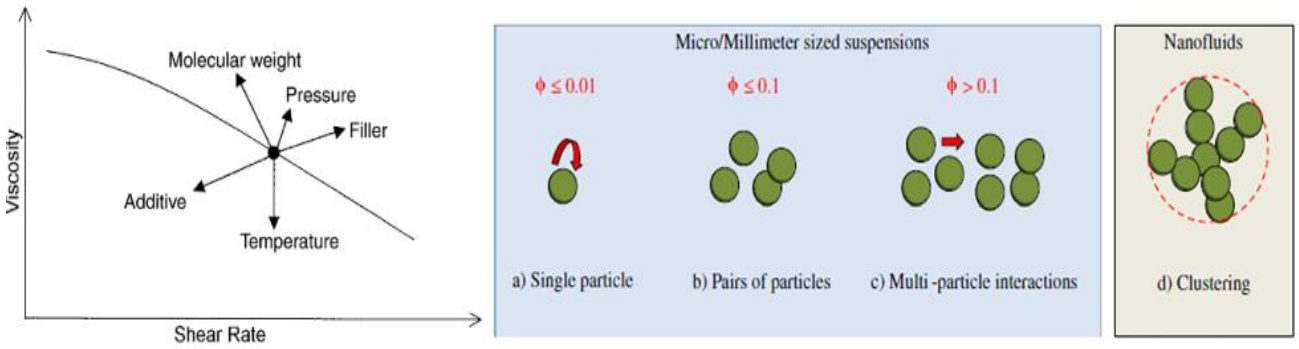

Figure 2.5: The influence of various parameters on polymer viscosity and the interaction of solid particles in a shear flow (Schramm, 1994; Selvakumar & Dhinakaran, 2016)

Equations have been used to describe the viscosity of a suspension when Newtonian fluid flows around a single phase. In the case where the volume fraction of the solid particles is low, Einstein Equation as shown in Equation 2.1 is normally used (Aldin & Christian, 2015).

$$\eta = \eta_s(1 + 2.5\varphi) \tag{2.1}$$

Where η is the intrinsic viscosity; η_s is the viscosity of the suspension and φ is the closed packing value.

In the case of higher order volume fraction of suspended solids, Krieger and Dougherty expression (Krieger, 1972) is modified to Equation 2.2 (Wang *et al*., 2012; Selvakumar & Dhinakaran, 2016).

$$\frac{\eta}{\eta_o} = (1 - \frac{\varphi}{\varphi_{max}})^{-2.5k\varphi_{max}} \tag{2.2}$$

2.8.2. Wax/EVA and wax/LLDPE compatibility

Theories on EVA and LLDPE compatibility is explained by EVA and LLDPE in nature, acting as a nucleating agent for wax crystals and as well as being a crystal inhibitor (Su *et al*., 2017). The compatibility of wax, EVA and LLDPE resins is due the presence of long sequences of $–CH_2–$ units linked together in both EVA, LLDPE and wax. Co-crystallization of wax, LLDPE and EVA occurs when the crystallization temperature of EVA and LLDPE overlap with that of wax hence enabling the EVA and LLDPE resin to reinforce wax forming a compatible blend with improved thermal and mechanical properties (Krupa & Luyt, 2001a; Hato & Luyt, 2006). In the case of EVA, as the vinyl acetate is >28% weight percent the wax- EVA compatibility decrease hence vinyl acetate units are not blended into the wax crystals due to the reduction in the chains of $–CH_2–$ units as well as the change in its freezing point (Krupa & Luyt, 2000). The compatibility relationship between vinyl acetate content using differential scanning calorimetry by freezing and cloud point is shown in Figure 2.6.

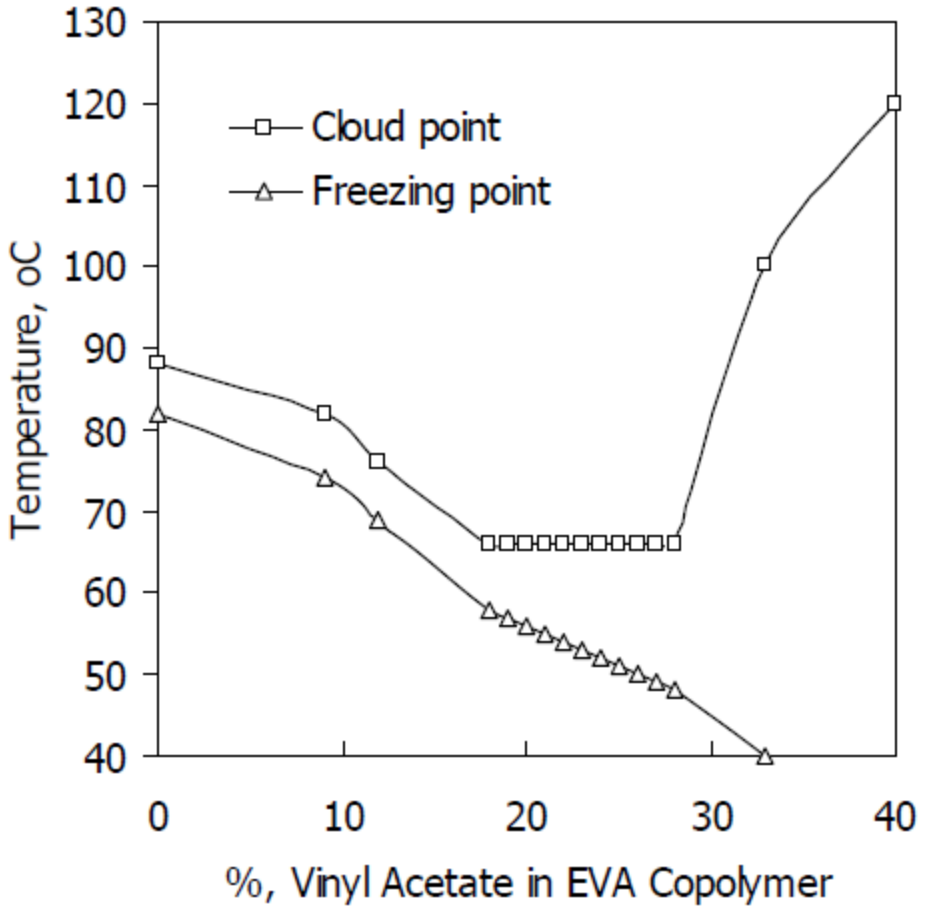

Figure 2.6: Cloud and freezing point for 10% EVA, with different VA contents, dissolved in paraffin wax (Rutto, 2007)

2.8.3. Ethyl Vinyl Acetate (EVA)

EVA is a copolymer resin of ethylene and vinyl acetate used in sealants, coatings and adhesives. Vinyl acetate is distributed arbitrary in the long polymer chains and its percentage as well as its melt flow rate are always used to distinguish the grade of EVA. The vinyl acetate (VA) content of commercial EVA copolymers range from 9 -30% whereas its melt flow index ranges from 0.4 - 500. EVA resin wide application in the industry is due to the following properties: (i) Excellent

adhesion to a wide range of substrates, (ii) high resistance to rupture, (iii) flexibility and (iv) lower coefficient of thermal expansion (Czaniková *et al*., 2012; Tham *et al*., 2015). Figure 2.7 shows the chemical structure and a picture of EVA and the physical and mechanical properties of selected EVA grades are shown in Appendix IV in Appendices section.

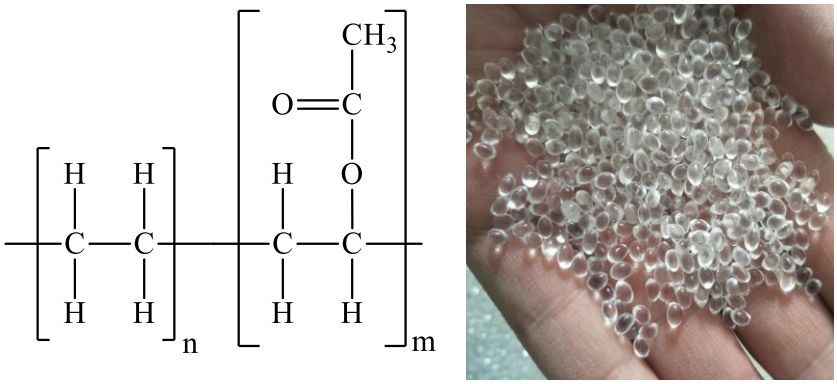

Figure 2.7: EVA chemical structure and picture of EVA pellets

2.8.4. Poly methyl methacrylate (PMMA)

Poly (methyl methacrylate) (PMMA) is a low-cost thermoplastic acrylic polymer with wide application in everyday life. (PMMA) is a transparent low crystallinity polymer with good mechanical strength and electrical properties. Its formation is through emulsion polymerization of methacrylic acid. PMMA industrial application include its use in fibre optics, 3D illuminated panels, orthodontic equipment and solar deflectors just to name a few (Pachamuthu & Hatna, 2005; Alshamari & Sayed, 2016). Figure 2.8 shows the chemical structure of PMMA and a picture.

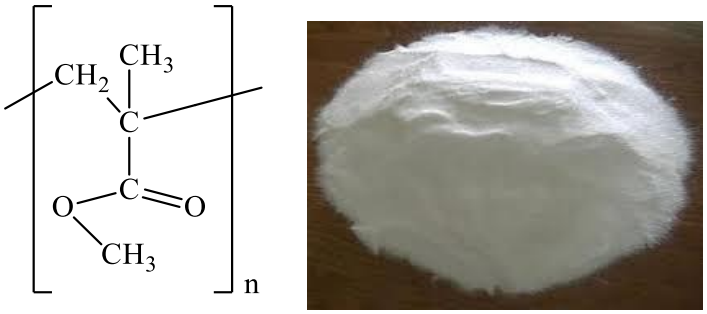

Figure 2.8: Chemical structure of PMMA and picture of PMMA powder

2.9. INVESTMENT CASTING PATTERN CHARACTERIZATION TECHNIQUES

Characterization techniques in investment casting involves the pattern material and the produced metallic part. The importance of characterization techniques is to determine the structure, properties and the composition of the material (Sabau & Viswanathan, 2003). In investment casting process, the pattern mechanical properties, flow properties are so crucial hence, the most important characterization techniques involved in in investment casting process are (i) thermal characterization techniques, (ii) mechanical properties characterization technique and (iii) flow properties.

2.9.1. Thermal characterization techniques

The primary purpose of investigating the thermal characteristic of investment casting pattern material is majorly to establish the thermal stability information of the pattern material and the material composition (Kodre *et al*., 2014). In theory, the flow of thermal energy is by the movement of electrons and its collisions with atoms coupled by lattice vibrations. The vibration

quantum that conducts heat is referred to as a phonon. Phonon quantity in a system is directly proportional to temperature. In most ceramic systems, the interaction of phonons plays a crucial role for its conduction mechanisms. The scattered characteristic behaviour of phonons at high temperature causes a reduction in thermal conductivity (Klancnik *et al*., 2010; Shekhawat, 2013).

Thermal characterization techniques on investment pattern material aid in establishment of its physical and thermal properties. Thermal characterization plays an important role in relation to the melting and crystallization of the materials used in the wax injector as well is removal from the mould. The techniques which are vital in the investigation of the thermal characteristics of investment casting pattern are (a)Thermo Gravimetric Analysis (TGA); (b) Differential Thermo-Gravimetric (DTG) and (c) Differential Scanning Calorimetry (DSC) (Kumar, 2014).

2.9.1.1.Thermogravimetric analysis (TGA)

Thermogravimetric Analysis (TGA) is a thermal analytical technique used to study the physical and chemical properties of a material as a function of temperature at a constant heating rate. TGA measures the change in the sample mass (loss or gain) that occur while the sample temperature is varied during a controlled temperature program (Januszewicz *et al*., 2017). TGA analysis relies on a high degree of precision in three measurements: weight, temperature and temperature change (Abu-Bakar & Moinuddin, 2012). The weight/mass change is obtained as a function of temperature, time and atmosphere. The weight loss/gain observed during TGA analysis can be due to volatiles sorption/desorption process, decomposition process, oxidation and reduction processes (Rafat, 2014; Yazmin *et al*., 2016). TGA characterization technique on investment casting pattern determines the decomposition change on the pattern material with change in temperature. The thermal stability and composition of the blend is obtained from TGA analysis (Xu *et al*., 2017).

2.9.1.2.Differential scanning calorimetry (DSC)

Differential scanning calorimetry (DSC) is one of the thermo-analytical techniques used to measure the energy required to provide approximately zero temperature variations between a substance and an inert reference material, as the two compounds are conducted in identical temperature system in an environment heated or cooled at a controlled rate (Kodre *et al*., 2014). The degree of temperature difference for a given supply of heat will vary between the two pans. This difference depends on the composition of the pan contents and the physical changes that occur on the sample such as phase changes (Kannan *et al*., 2012). Figure 2.9 shows the effect a filler material has on a pure paraffin wax when a filler material is incorporated into the paraffin wax. The melting point as well as the heat flow is affected by the addition of fillers to paraffin wax. The characteristic temperature change during DSC analysis can be attributed to reaction changes due to phase changes or exothermic and endothermic reaction transitions (Pu *et al*., 2007; Xu, 2015).

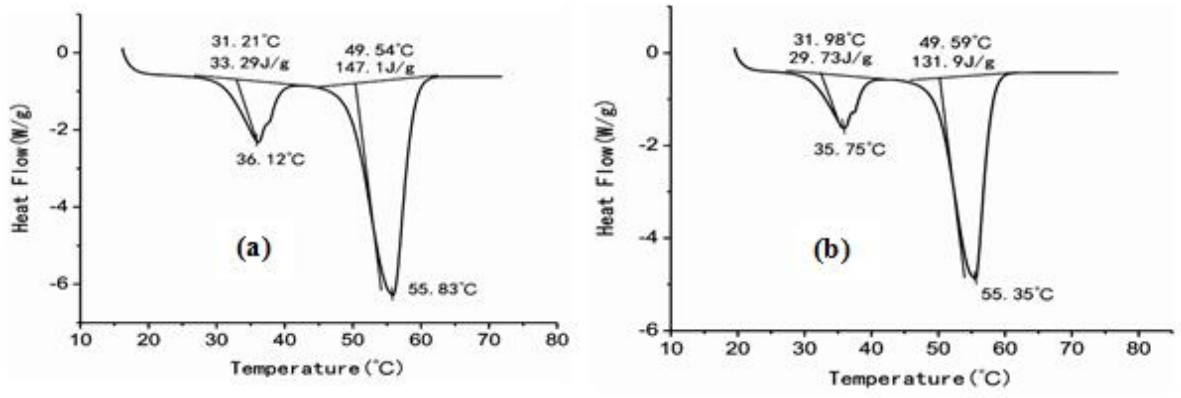

Figure 2.9: Shows DSC analysis (a) pure paraffin wax, (b) pure paraffin wax with a filler material

2.9.2. Mechanical characterization techniques

Mechanical characterization of investment casting pattern material is a crucial component for the development of a suitable pattern material with sustainable properties (Patel, 2016). The two most preferred mechanical characterization techniques are (a) the dynamic mechanical analysis and (b) the tensile testing technique. The study of mechanical properties of investment casting patterns gives a substantial estimation of majorly the shrinkage factors and pattern deformation tendencies hence, a better understanding of the pattern process design aspects (Kumar *et al*., 2016). Some of the most identified scenarios where mechanical analysis is important is where a pattern material is hard and brittle hence, may be damaged during assemble as well to flexible pattern hence, may not retain its shape during investment process. Tensile properties and hardness are the most common mechanical analysis done on pattern material (Sabau, 2005).

2.9.2.1.Three-point bending testing

Three-point bending test technique is a method utilized to test the flexural properties of a brittle material (Azzam & Li, 2014). Flexural strength can be defined as the capacity of a material to resist deformation when load is applied. The determination of ultimate stress, elastic modulus and the ultimate strain of investment casting pattern material is done by three-point bending testing analysis which is a destructive testing technique (Novais *et al*., 2011). Three-point bending elaborates on the elongation, yield strength and the ultimate tensile strength of the pattern. In three-point testing techniques, Three-point flexural test are performed as per American Society for Testing and Materials 790 (ASTM 790). Rectangular specimens with dimensions of 10 by 4 by 80 mm is obtained by casting in an Amsil 25 cure silicone mould. The load cell is a precisely calibrated transducer that gives a specific evaluation of the load applied. In three-point bending test, a beam which has bisymmetrical cross-section held on supports at the ends is loaded by a constant force, the deformation on the sample produces a couple in the plane

of symmetry which is called the bending moment as shown in Figure 2.10 (Azzam & Li, 2014). The deflection (w_o), second moment area (I) and the maximum bending moment (M) is calculated using Equation 2.3 and 2.4 respectively (Sorn, 2011). The mentioned parameters occur at x = L/2 i.e. the centre of a symmetrical beam.

Table 2.*7* gives the summary of mechanical characterization techniques of polymeric compounds.

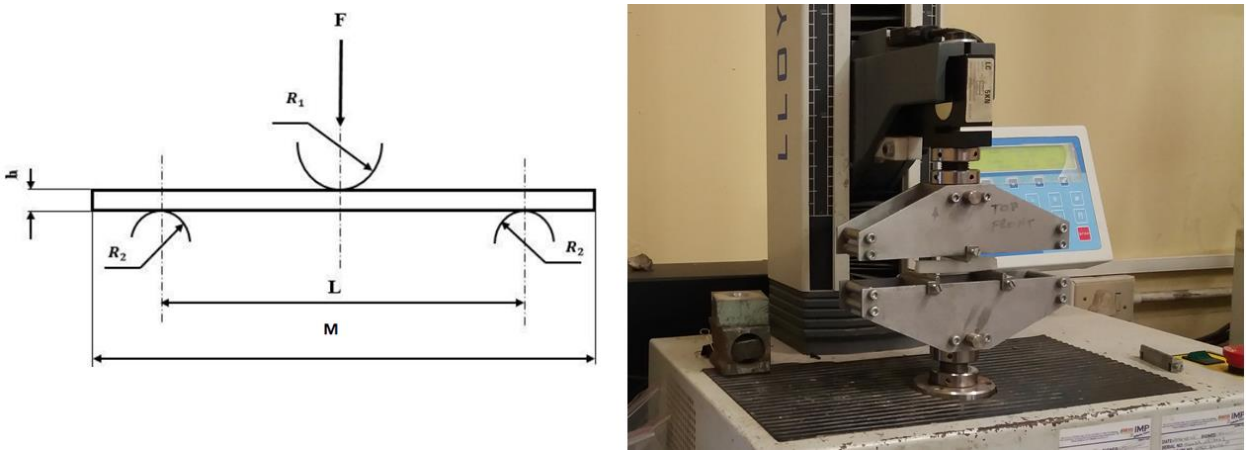

Figure 2.10: Three-point bending of a beam and a picture of universal tensile tester

$$M = \frac{-L(F + \frac{wL}{2})}{4} \quad (2.3)$$

$$w_o = \frac{WL^3}{48EI} \quad (2.4)$$

Where M is the bending moment, L is the length of the beam, F is the force and w are the weight of the beam, E is the Young Modulus, (I) is the second moment of area.

Table 2.7: Mechanical tests done on investment pattern materials

Material form	Analysis	Equipment	Sample
Solid	3-point bending test	Bending beam equipment	Rectangular solid bars
Hard paste	Torsion oscillatory	DMA	Rectangular solid bars
Soft paste	Shear oscillatory	DMA	Paste
Liquid	Shear oscillatory	Melt rheometer	Paste

2.9.2.2.Thermomechanical analysis (TMA)

Thermomechanical analysis (TMA) is a technique used in thermal studies to study the properties of materials as they change with temperature. The fundamental investigation signal in TMA is the sample dimensional change when heated or cooled (Haines, 1995). In TMA, the sample to be analysed is placed on top of a support material and a probe is always above the sample. The probe is usually connected to a Linear Variable Displacement Transducer (LVDT) which gives the sample dimensional change when heated or cooled. TMA measurement are carried under inert atmosphere to avoid air oxidation when heating and heating the sample (Fifield & Kealey, 2000). TMA measurements are always done under zero load by ensuring that the probe comes in contact with the sample. The probes used can be in penetration mode, expansion mode, tension mode or

flexure mode depending on what is being investigated. Penetration probe is used to determine the sample glass transition temperature, expansion probe is used measure the coefficient of thermal expansion. TMA measurement can also be performed under varied load such as incremental forces technique (Brown, 1988).

2.9.3. Surface characterization techniques

2.9.3.1.Fourier transform infrared spectroscopy (FT-IR)

Fourier transform infrared (FTIR) is a technique used in organic chemistry for the identification of functional groups in a molecule. The technique can also be used to collect adsorption bands to confirm a pure compound or detect the presence of impurities (Christy *et al*., 2001; Stuart, 2004). In FTIR, infrared radiation is passed through the sample, some infrared radiation is absorbed and some is transmitted through the sample. The resulting spectrum gives a representation of magnetic absorption and transmittance giving a molecular fingerprint of the sample (Smith, 2011).

2.9.3.2.Scanning electron microscopy (SEM)

Scanning electron microscopy (SEM) is a surface characterization technique used to give the morphology structure of many materials. SEM uses a focused beam of high-energy electrons to generate a variety of signals at the surface of solid specimens (Dehm *et al*., 2012). The signals that are derived from electron-sample interactions reveal information about the sample which include the external morphology (texture), chemical composition, and crystalline structure and orientation of materials making up the sample (Magampa *et al*., 2013). Accelerated electrons in a SEM carry significant amounts of kinetic energy, and this energy is dissipated as a variety of signals produced by electron-sample interactions when the incident electrons are decelerated in the solid sample.

These signals include secondary electrons (that produce SEM images), backscattered electrons (BSE), diffracted backscattered electrons that are used to determine crystal structures and orientations of minerals and photons (characteristic x-rays that are used for elemental analysis and continuum x-rays) (Dehm *et al*., 2012). Secondary electrons and backscattered electrons are commonly used for imaging samples which include morphology and topography on samples and contrast in composition in multiphase samples.

2.9.4. Flow and rheological characterization techniques

The flow of fluids can be either Newtonian flow or Non-Newtonian flow which is well elaborated by the Newton's Law of Viscosity (Holman & Lloyd, 2010). Newtonian fluid flow is whereby, when the fluid viscosity is independent of the shear rate, i.e. the flow curve of Newtonian fluid is straight and the shear stress – shear rate cannot be influenced by its shear rate, whereas when fluid flow viscosities is dependent on shear rate it is referred to being a Non-Newtonian fluid. Polymeric fluids exhibit a shear-thinning behaviour, its shear rate in inversely proportional to viscosity as shown in Figure 2.11 (Brennen, 2005). This is attributed to the molecular alignment and detachment from the long polymer chains hence, a higher shearing rates a lower viscosity hence easy flow of the fluid through dies and process equipment.

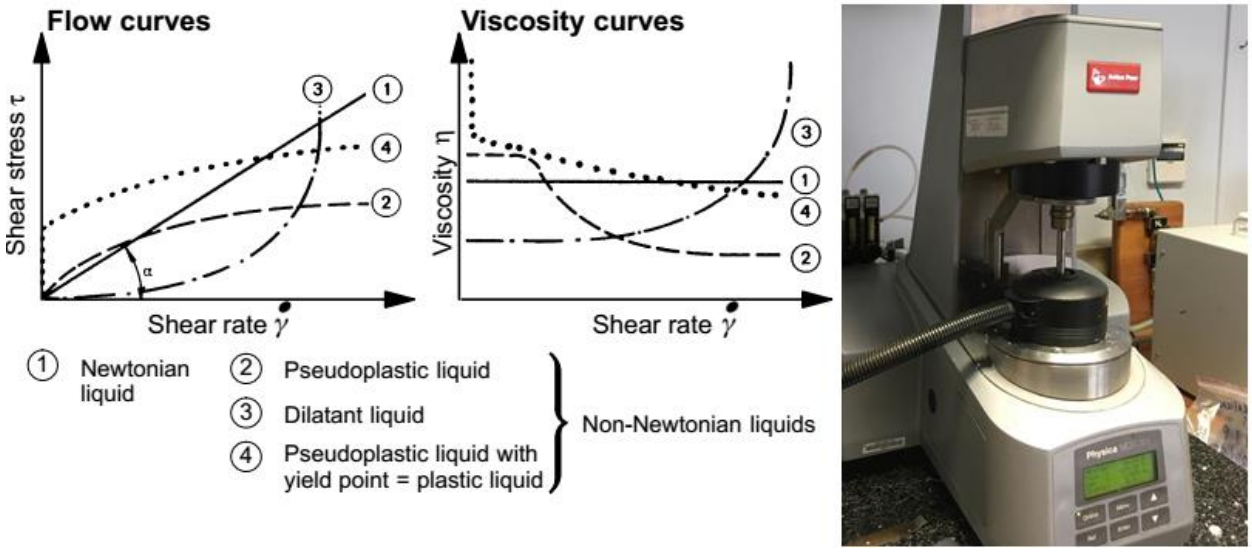

Figure 2.11: Newtonian and Non-Newtonian flow behaviour characteristics and a picture of Anton Paar rheometer (Schramm, 1994))

2.10. FACTORS AFFECTING INVESTMENT CASTING PROCESS

2.10.1. Solidification of metals

Metal solidification in investment casting process involves a phase transformation from liquid phase to solid phases through solute diffusion and latent heat. The process is dependent on temperature (Conti & Marconi, 2000; Anjo, 2012). For pure metals, solidification process occurs at a constant temperature whereas for alloys, solidification occurs over a temperature range (Raza, 2015). The theory of solidification process involves two stages namely: (i) grain nucleation and (ii) growth kinetics. During grain nucleation, the molten metal in liquid phase cools, hence there is a change of state from liquid to solid. This phase change is due to the corresponding discontinuity in free energy. Grain growth mechanisms takes place through diffusion process when the temperature is high enough and the time of heat treatment is long enough. This will result in small

particles surrounding the liquid being formed (Tiaden, 1999; Yang *et al*., 2014). The freezing point of pure metals are well-defined; the metal starts to solidify when the operating temperature drops to its freezing point (Dai, 2009). The solidification process occurs isothermally. The mechanical properties of pure metals can be enhanced and modified by alloying techniques to improve its properties and its suitability. The time taken by solidification process is described by Equation 2.5. (Ilangovan, 2014).

$$\text{Solidification time} = C\left(\frac{\text{Volume}}{\text{Surface area}}\right)^{n} \qquad (2.5)$$

Where C – Represents a constant that reflect properties of the mould material, molten metal as well as the temperature; n – represents a constant.

2.10.2. Fluid flow and heat transfer

The materials used for investment casting pattern are always complex in nature. The flow kinetics of most of these materials is dependent on temperature and shear rate (Upadhya *et al*., 1995; Rafique, 2015). Investment casting waxes display elasto-visco-plastic characteristics in solid state and visco-plastic tendencies at liquid state (Teng & Zhang, 2013). Most thermoplastic materials used for investment pattern are compressible materials hence, they are pressure and temperature dependent (Mendes, 2015). Compressibility and viscosity are temperature dependent hence, pattern flow must consider heat transfer mechanisms (Lee, 2008). Heat transfer mechanisms of investment casting process is based on the first Fourier law (Equation 2.6) for both conduction and convection to be factored in (Raza, 2015). The heat capacity, thermal conductivity of the pattern

material and the heat transfer coefficient are the thermo – physical needed for the establishment of the heat transfer mechanism of investment casting process (Ridge, 2004; Welty *et al*., 2008). The heat transfer mechanisms and flow pattern for investment casting process inside the cavity influences the solidification pattern inside the cavity of the mould. Its control is so crucial to avert inter-dendritic shrinkage, gas porosity, grain structure and miss-runs during the investment casting process (Bonilla *et al*., 2001).

$$Q = -kA\frac{dT}{dx} \tag{2.6}$$

Where Q – is the heat flow rate; k – thermal conductivity of the body; A- is the cross-sectional area and Dt/dx – is the temperature gradient.

Fluid flow characteristics in investment casting process depends mainly on its Reynold's Number which is described by Equation 2.7.

$$Re = \frac{vD\rho}{\eta} \tag{2.7}$$

Where v - is the velocity of the liquid; D - is the diameter of the channel; ρ - is the density; η – is the viscosity (Al-Shemmeri, 2012).

Typically, for Re up to 2300, the flow characteristics is laminar whereas for Re ($2300 \leq 4000$), the flow characteristics is a mixture of both laminar and turbulent flow. For Re > 4000, the flow is a turbulent. Surface tension, heat of fusion, viscosity, mould material, rate of pouring inclusions and design are the additional factors that affect fluidity (Hallquits, 2011). Viscosity being dependent on temperature, the molten metal fluidity characteristics is affected by heat transfer mechanisms. Additionally, in the case of alloys, the intensity of superheat above its melting point causes solidification delay hence, affecting fluidity. During the casting process, from when the molten metal is poured through solidification and cooling, heat transfer occurs all through (Bala & Khan, 2014; Bala *et al.*, 2013).

During heating and cooling of solids including pattern materials for investment casting, most solids have a trend of expanding during the heating process and contracting during the cooling process. The extend of dimensional change depends on the change in temperature. The volume change of the solid can be described by Equation 2.8. (Das & Himte, 2013; Muthuraman *et al*., 2017).

$$\Delta V = \beta V_i (T_i - T_f) \qquad (2.8)$$

Where.ΔV- is the change in volume; $\beta -$ is volumetric coefficient of thermal expansion; V_i - is the initial volume; T_i - is the initial temperature and T_f – is the final temperature.

2.10.3. The use of additives

Additives are compounds that are used in small amounts to complement the properties of a material hence, improve its performance, appearance, and its process ability (Patel, 2016). The use of wax

as a pattern material lacks (a) dimensional accuracy and (b) strength and rigidity (Pattnaik *et al*., 2012). The use of additives in investment casting pattern material helps in improving the thermal and thermochemical behaviour of investment casting pattern. Horton & Tetlow (2005) from their research findings alluded that, the two most common shortcomings associated with the use of wax only as an investment casting pattern material can be reduced by the inclusion of additives such as fillers, resins, plasticizers and oils in the parent wax material. In the case of the use of filler material, its selection criteria are: (i) it should have a higher melting point; (ii) it should be non-reactive towards the base wax and the ceramic materials; (iii) it should have fine particle size distribution; (iv) its specific gravity should be close to that of the base wax; (v) it should have low ash content. Extensive research findings by Borcherding & Luck (2000) alluded and affirmed that, the use of soybeans as a filler material improve wax properties by reducing shrinkage, improving surface roughness and tensile strength of the pattern. Soybean is combustible hence; it has an appropriate ash content ($\leq 0.05\%$). Further investigation by Taşcıoğlu & Akar (2003) revealed that pattern properties such as coefficient of thermal expansion, tensile strength, surface roughness and viscosity can be improved using additives such as activated charcoal, palmitic acid, cross-linked polyvinyl-polypyrrolidone, and some surface-active agents. The addition of rigid fillers to polymeric material increase its modulus, while the addition of soft microscopic particles lowers the modulus and increases its toughness (Taşcıoğlu & Akar, 2003). The use of fillers in powder form decrease the polymer elongation and its ultimate strength whereas, the use of long fibres causes both the modulus and the ultimate strength to increase. The addition of plasticizers into polymers brings changes same as changes witnessed with temperature increase. The effect of adding fillers and plasticizers on stress strain curve on polymeric materials is described in Figure 2.12 (Menard, 1999). The use of resins in investment casting pattern material aid in increasing the

strength and body of the pattern (Sabau & Viswanathan, 2003). Solidification shrinkage which causes surface cavitation of pattern material is lessened by the addition of little amount of resin material into the parent pattern material. The most preferred resins used for investment casting pattern include acrylate functional oligomers such as acrylate resins of bisphenol. Resins such as coal tar resins, terpene resins and rosin derivatives have fluctuating viscosities and expanded softening points at different temperatures which needs to be factored during its addition to pattern material (Prasad, 2012). Examples of resins which improve the patterns' mechanical strength, hardness and its softening and have been practically incorporated into pattern material include acrylic resins such as ethyl and butyl methacrylate, thermoplastic resins such as polyvinyl alcohol and polyvinyl acetate and thermosetting resin for instance phenol formaldehyde (Horton & Tetlow, 2005). The choice of a resin used as an additive to investment casting pattern primarily depends on its interaction with the filler and the primary pattern material (Menard, 1999; Rutto & Focke, 2009). The use of plasticizers in investment casting pattern improve the static nature of the pattern material and plasticizers also have a functionality in pattern material as a lubricating agent.

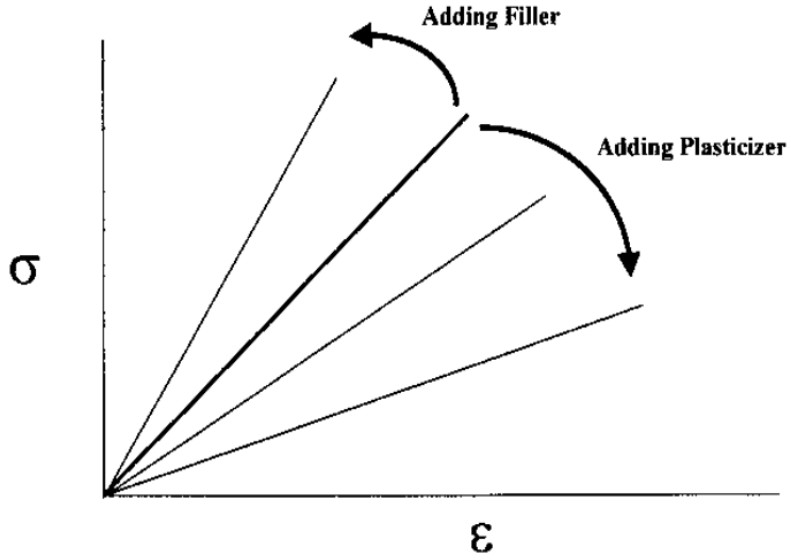

Figure 2.12: Effect of addition of filler and plasticizers on polymer stress - elongation relationship (Menard, 1999)

2.11. MIXTURE PROCESS EXPERIMENTS

Investment casting pattern production involves the proportion variation of different materials. Investment casting pattern workability depends on the proportions of wax present, fillers added and other additives (Horton & Tetlow, 2005; Higgins *et al*., 2010). Mixture models aids in the optimizing mixture ratio formulation as well as optimization of the process. In ternary investment casting, experimental mixture (where wax, fillers and additives are used), the factors of the three components varied mixture proportions and its response in terms of the measured parameters always give the characteristics of the investment casting pattern (Nascimento *et al*., 1997; Gonzalez-leon & Mayes, 2003; Tewo *et al*., 2018). The general equation for mixture experiments, considering x_i as proportion representation, and q as the component mixture is described and shown by Equation 2.9 and Figure 2.13.

$$\sum_{i=1}^{q} x_i = 1 \; ; x_i \geq 1 \; ; i = 1 \ldots . , q \qquad (2.9)$$

For a ternary system (Figure 2.13), The summarized representation is described by Equation 2.10.

$$x_1 + x_2 + x_3 = 1 \qquad (2.10)$$

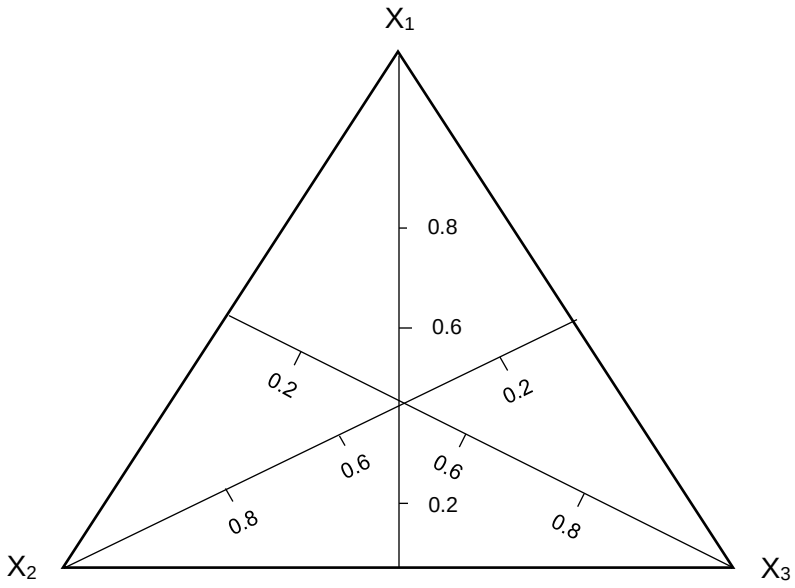

Figure 2.13: Three coordinate ternary phase system

2.12. EXTRUSION PROCESS

Extrusion process has been widely used for a long time to produce polymeric compounds. Generally, extrusion is divided into (i) the extruder section and (ii) the die section as shown in Figure 2.14. The extruder section is where the raw materials are melted, mixed and converted into the final product whereas the die section is where the shape of the final product is formed (Osswald, 2011). The produced material is forced under controlled conditions to a narrow section to form the required shape. Conventionally, extruders are categorized into two categories namely: (i) single screw and (ii) double screw extruders. The reciprocating screw helps with shearing and the heater in form of an electrical element helps with plasticizing polymers hence, causing a shearing reaction on the material which further causes friction and melting of the material. Advantages associated

with extrusion process include processing versatility, short residence time and self-wiping adjustable screw profile. Twin screw extruders have been preferred over single screw extruders due to its superior mass and heat transfer mechanisms (Breitenbach, 2002; Siaotong *et al*., 2005).

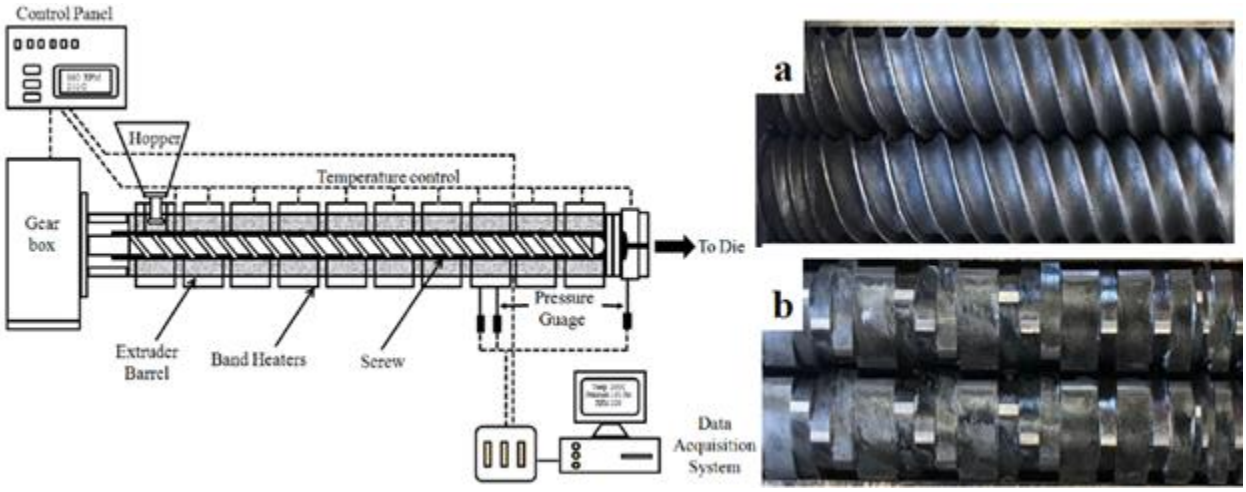

Figure 2.14: Typical extrusion process and (a) conveying element (b) kneading element

2.12.1. Mixing polymers and additives

In order to obtain reproducible results when it comes to polymer blends, mixing plays an important role especially in the case of highly filled energetic materials that exhibit a high melt viscosity whereby there is no mixing by turbulence and eddy diffusion. Generally, the mixing process is split into two categories namely: (i) distributive mixing and (ii) dispersive mixing (Huang *et al*., 2014; Dombe *et al*., 2015).

2.12.1.1. Distributive mixing

Distributive mixing also referred as laminar mixing refers to de-agglomerated particulates distributed evenly within space. It can also be defined as rearrangement of minor units to increase

the system special homogeneity. In the case of polymer melts, distributive mixing distributes miscible fluids or particles within the polymer matrix. Distributive mixing can be achieved by imposing large strains on the system which leads to increases in the interfacial area (Wang & Kaufman, 2001; Osswald, 2011).

2.12.1.2. Dispersive mixing

Dispersive mixing or intensive mixing in polymer processing that generally ruptures of agglomerates formed by a solid phase or fluid droplets and distributes them throughout the polymer matrix. After the break up process, the separated particles or droplets are distributed of through the polymeric matrix. Figure 2.15 better explains dispersive mixing. It is described using only two spherical particles (Zloczower *et al*., 1983; Williams, 1989; Osswald, 2011).

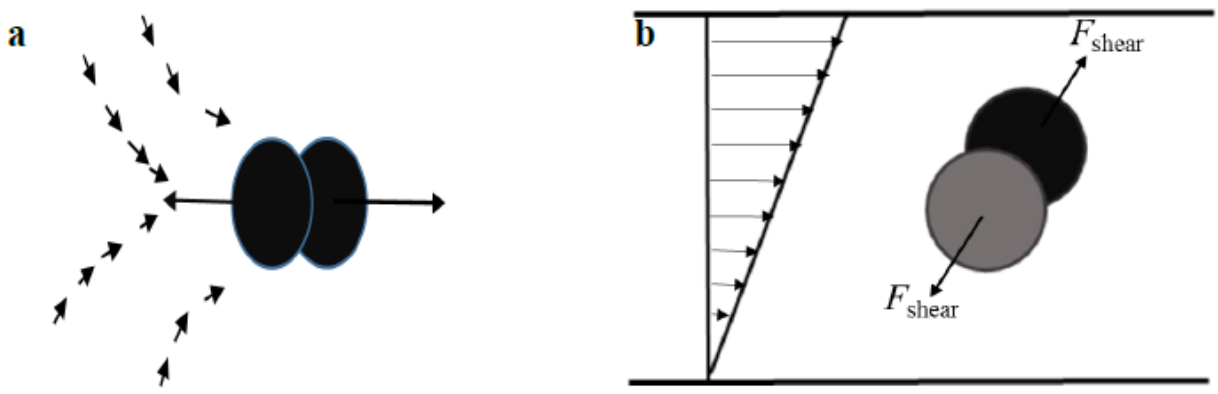

Figure 2.15: Elongational and shear forces applied to two particle agglomerates during flow (Osswald, 2011).

Figure 2.15 illustrates the effect of both elongational flow and (b) shear flow patterns. As it can be seen from Figure 2.15, the maximum shear force will be in effect when the units are positioned at a 45° C angle. In the case of elongational force, the shear force will be maximum at 0° C angle. Equation 2.11 and 2.12 describes the magnitude of the maximum separation forces applied to separate the particles (Osswald, 2011).

$$F_{Elong} = 6\pi\eta\varepsilon\gamma^2 \quad (2.11)$$

$$F_{Shear} = 3\pi\eta\,\dot{\gamma}r^2 \quad (2.12)$$

Where η is the viscosity of the carrier fluid, $\dot{\gamma}$ is the magnitude of the strain rate tensor between the two particle radii. In instances where the elongational flow and the shear are the same, then maximum elongational force is double that of the shear force. This shows that elongational flow is preferred when mixing and breakup of agglomerated particles is required (Osswald, 2011)

Chapter 3 : THERMAL, MECHANICAL SURFACE CHARACTERIZATION AND RHEOLOGY OF WAX/EVA AND WAX/LLDPE BLENDS.

ABSTRACT

Different ratios of wax and EVA blends and wax and LLDPE were prepared using one-step extrusion process to investigate their potential for as carrier vehicles for investment casting pattern. The thermal, mechanical, surface and rheology properties were characterized. Thermal properties were done using thermogravimetric analysis (TGA) and differential scanning calorimetry (DSC), mechanical properties was done by three-point bending and thermomechanical analysis (TMA), whereas the chemical interaction was done by Fourier transform infrared (FT-IR), surface properties by scanning electron microscopy (SEM) and rheology was characterized by the viscosity of the blends. Experimental results showed that incorporation of EVA into wax influences its thermal, rheological, surface and mechanical properties. The thermal results confirmed that the thermal stability of the wax-EVA blend decreased with an increase in the amount of wax. The following findings were made: (i) The TGA analysis showed that the incorporation of EVA/LLDPE into wax improved the thermal stability properties of the blend which can be attributed to enhanced phase adhesion; (ii) the melting and solidification behaviour of the blends had intermediate temperatures between that of wax and EVA; (iii) the wax/EVA blends displayed evident viscosity shifts as compared to the viscosity of wax; (iv) incorporation of EVA into wax significantly alters its mechanical properties; (v) FTIR spectrometry of both wax/EVA and wax/LLDPE has shown the predominant presence of CH_2 and carbonyl group in the blend; (vi) the mechanical properties of neat wax was improved when EVA and LLDPE was incorporated into wax; (ii) SEM confirmed that EVA and LLDPE alters the wax crystal habit at higher concentrations due to the immiscibility nature at a higher EVA and LLDPE loading.

KEY WORDS: *ethyl vinyl acetate, wax, rheology, three-point bending, penetration, deflection.*

3.1. INTRODUCTION

Recently, there has been immense concern in the development of wax blends or polymer blends with good stabilities thermal and mechanical strength for investment casting patterns (Rajendran *et al*., 2008). With an increase in demand for tightly dimensional and complex shapes, various materials such as fillers, resins, plasticizers have been blended with wax to develop a more suitable pattern for investment casting process over the recent years to overcome performance limitation exhibited by unfilled wax (Rutto & Focke, 2009; Tomasik *et al*., 2009). The identification of new materials to replace improve the properties of conventional materials through blending technique has drawn lots of research and development of new polymer blends/material blends (Azimi *et al*., 2009; Wawulska-marek *et al*., 2015; Ferreira *et al*., 2018).

Fischer-Tropsch waxes are synthetic waxes produced by gas-liquid technology by polymerization of synthetic gas under elevated temperature and pressure into hydrocarbons (Leviness *et al*., 2011; Hassankiadeh *et al*., 2012). Fischer-Tropsch waxes are characterized by low viscosity, high degree of linear molecular structure, high crystallinity and high congealing point (Hu *et al*., 2012). Ethylene vinyl acetate (EVA) is a commercial random copolymer consisting of ethylene and vinyl acetate (VA) units which has lots of application such as a medium for filler dispersion and polymer compatibilization. The VA content in EVA varies from 3 to 50 weight percent (Nordqvist *et al*., 2009; Róz *et al*., 2012).

Blends produced from wax and EVA have increased hardness with the copolymer concentration and decreases with decreasing VA content (Nebykov *et al*., 1985). Thermal stability studies and the crystallization behavior of materials, polymers and polymer blends is valuable in the field of

material, applied materials, science and technology (Kannan *et al*., 2012). In order to develop durable industrial products, it is necessary to investigate the thermal stability of these blends. Thermal analysis studies such as investigation of the change in heat flow and stability of materials will give some idea on the extent of chemical interaction occurring between the components, bond strength, activation energy, melting temperature, and degradation kinetics (Bonilla *et al*., 2001).

The thermal stability of the material used as pattern material for investment casting process depends greatly on the addition and compatibility of the mixtures used to make the pattern material. Thermal degradation characteristics of pattern material is analyzed by thermogravimetry (Kumar *et al*., 2009). Thermogravimetric analysis epitomizes the variation of sample mass with a change in temperature. The stages of thermal break down, thermal stability and its degree of degradation, as well as temperature threshold is well illustrated in thermogravimetric curves (Jesiotr & Myszka, 2013). The melting, crystallization and miscibility of pattern samples for investment casting is an important criterion used to characterize polymers can be achieved by using DSC characterization techniques (Tiwari & Hihara, 2012).

Mechanical properties of industrial pattern waxes are crucial properties when describing pattern performances during moulding and when under temperature change. Pattern material with good mechanical properties should be easy to handle during investment casting. The estimation of shrinkage factors and pattern deformation tendencies gives a better understanding of investment casting pattern design. Pattern hardness, ultimate tensile strength, yield strength is determined by three-point bending test and hardness test.

The objective of this chapter was to study the composition effect of EVA and LLDPE in wax matrix and come up with the effects of blending EVA and LLDPE into wax with varied proportions

on the thermal, mechanical, morphological and rheological properties of wax/EVA blends prepared in a twin corotating twin screw extruder.

3.2. MATERIALS AND METHODS

3.2.1. Materials

Sasol Fischer-Tropsch wax (Melting point = 55 °C, average molecular weight = 785g/mol, density at 25 °C = 0.9 g/cm^3, soft, brittle straight hydrocarbon wax) was supplied by Sasol SA. Elvax 250 (28 % vinyl acetate – melting point = 71 °C and density at 25 °C= 0.926 g/cm3, melt flow index (MFI) =25) was supplied by Carst&Walker SA, LLDPE (density at 25 °C= 0.93 g/cm3, melt flow index (MFI) =50) was supplied by Sabric, SA . The samples were developed according to the procedure described in Figure 3.1. The compounds were tested as received initially prior to development. Nitrogen gases used in the thermal characterization techniques of the pattern material were of high purity (99.99 %) analytical grade sourced from Air Liquid SA and Afrox SA.

3.2.2. Method

The formulations were developed according to the procedure described in Figure 3.1.

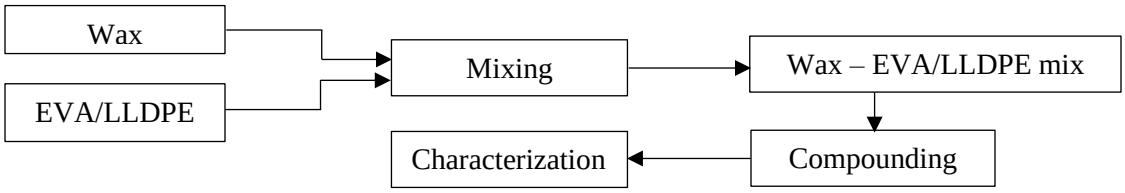

Figure 3.1: Development scheme for wax/EVA and wax/LLDPE binary blends

3.2.3. Characterization and testing methods

3.2.3.1. Thermogravimetric analysis (TGA)

The thermal characterization studies by thermogravimetric analysis (TGA) on the wax /EVA and wax/LLDPE blends were performed by TGA analysis isothermally and at a constant heating rate using Advanced Laboratories Solutions SDT Q 600 TGA analyser. The TGA analyser had a microprocessor controller, a heat and balance controller, furnace and an integration connecting the furnace with the plotter and the computer. A mass of 5-10 mg was degraded in a 70 µL alumina pan under nitrogen and air at a flow rates of 50ml/min in the thermo balance under dynamic conditions at a heating rate of 20 °C/min. The wax/EVA blends were scanned from 30 °C to 900 °C. Three experimental runs were performed to realize consistent data.

3.2.3.2. Differential scanning calorimetry (DSC)

DSC analysis of the EVA/wax and LLDPE/wax blends were performed using Mettler Toledo DSC 1 and Perkin Elmer DSC 4000 Analyzer under a constant dry nitrogen purge introduced into the DSC cell at 50 mL/min. The sample mass used was between 10- 20 mg. The samples were weighed and filled into an aluminium pan. An aluminium lid which was then sealed hermetically on to the pan. All analyses were performed in the scanning mode from 20 to 200 °C at the heating rate of 10 C/min. During the first heating process while holding for one minute at 20 °C, at 200 °C, the sample was hold for one minute then cooled from 200 °C to 20 °C at 10 °C/minute. Thermal characteristics such as melting, crystallization temperatures and its subsequent heat flow were determined. The DSC curves were normalized with respect to the sample mass and three experimental runs were performed to realize consistent data.

3.2.3.3. Fourier transform infrared (FT-IR)

Fourier transform infrared spectroscopy (FT-IR) of the samples was performed in transmission mode detection. The EVA/wax and LLDPE/wax blends were analysed using Perkin Elmer spectrum 100 FT-IR spectrometer from 4000 - 550 cm^{-1}at a resolution of 4 cm^{-1} spectra representing an average of 16 scans. About 1 mg of each wax/EVA and wax/LLDPE blends were placed in the accessory as the spectra was recorded.

3.2.3.4. Mechanical testing

Mechanical testing of the blends was performed by three-point flexural test as per American Society for Testing and Materials 790 (ASTM 790) using an Instron 5564 twin column tensile tester with a 5 kN load cell. Rectangular specimens with dimensions of 10 by 10 by 80 mm were obtained by casting in an Amsil 25 cure silicone mould (Appendix I). At least 5 samples were tested for each specimen at a crosshead speed of 1.8 mm/min and the load applied over a 64 mm support span. The maximum load obtained was used to calculate the modulus of elasticity (E), flexural strength (σ_f) and flexural strain (ε_f) at break according to Equation 3.1, 3.2 and 3.3.

$$E = \frac{L^3 m}{4bd^3} \quad (3.1)$$

$$\sigma_f = \frac{3PL}{2bd^2} \quad (3.2)$$

$$\varepsilon_f = \frac{6Dd}{L^2} \quad (3.3)$$

Where L is the support span, m is the slope of the gradient to the initial load deflection curve, b is the specimen width, d is specimen thickness, P is maximum load and D is the deflection at break point.

3.2.3.5. Thermomechanical analysis (TMA)

Thermomechanical analysis (TMA) of the blends was carried out using Advanced Laboratories TMA Q 400 analyser according to ASTM D696. The analysis was done at a force of 0.02N – 0.1N, the measurements were conducted at 30 °C, the TMA probe was fitted with a needle with a tip radius of 1.4 mm under Nitrogen gas at 50 ml/min (Appendix II). The penetration measurement was obtained on the immediate direction of compacts.

3.2.3.6. Scanning electron microscope (SEM)

To determine morphology of the EVA/wax and LLDPE/wax blends, surface characterization was observed using Zeiss Ultra FESEM (high resolution micrograph) scanning electron microscope. The EVA/wax and LLDPE/wax specimens were placed on a double-sided tape fixed on a metallic plate. Acceleration voltage of 2 kV was used and the samples were coated with gold by sputtering to give a conductive coating onto the samples.

3.3. RESULTS AND DISCUSSION

3.3.1. Thermogravimetric analysis (TGA)

Figure 3.2 (a) and (b) shows the TGA curves of EVA/wax and LLDPE/wax blends and Figure 3.3 (a) and (b) shows the corresponding DTG curves. From Figure 3.2 (a) and (b) it can be seen that both EVA and LLDPE exhibit a higher thermal stability as compared to neat wax. This can be attributed to the higher molecular weight of EVA and LLDPE than neat wax. As it can be seen

from Figure 3.2 (a), wax decomposes continuously from a temperature of 220 °C to around 400 °C. This can be attributed to the differing chains. EVA has two mass loss peaks. The first mass loss peak at a temperature of around 345 °C could be due to the disintegration of acetic acid and another mass loss peak at around 450 °C. The second mass loss peak can be attributed to the loss of methylenic chain (Ray *et al*., 1994). From Figure 3.2 (b), it is also evident that LLDPE has one mass loss peak, the mass loss can be ascribed to the degradation of the long chains. Also, from Figure 3.2 (a) and (b) it is also evident that the different EVA/wax and LLDPE/wax blends have intermediate thermal stabilities with two mass loss distinct peaks at 265 °C and 342 °C for EVA/wax blends and 245 °C and 365 °C for LLDPE/wax blends. The first mass loss could be due to the evaporation of wax and the second mass loss peak can be ascribed to the degradation of EVA and LLDPE in the case of Figure 3.2 (b). EVA/wax and LLDPE/wax binary blends decompose fully at temperatures above 480 °C. The interaction between the wax and EVA and LLDPE and wax could be associated with the tie molecules of CH_2 chain interaction and better interfacial adhesion.

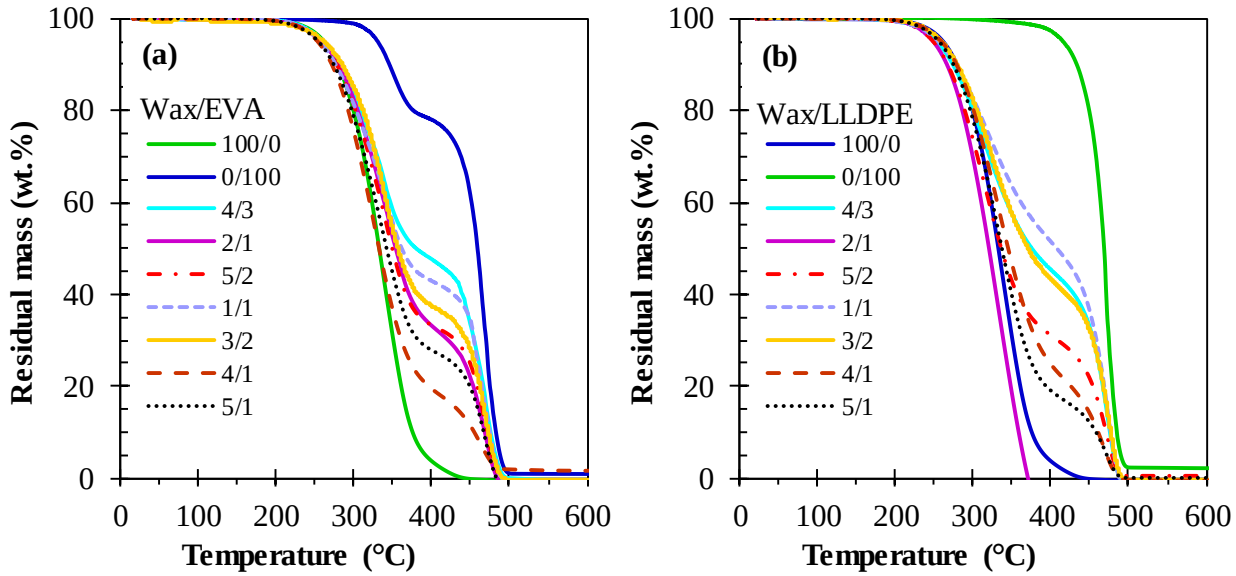

Figure 3.2: (a) TGA mass loss curve of EVA and EVA/wax blends (b) LLDPE and LLDPE/ wax blends

Figure 3.3 (a) and (b) shows the DTG curves of wax, EVA, LLDPE wax/EVA and wax/LLDPE binary blends. From the DTG curve as shown in Figure 3.3 (a) and (b) in the case of wax suggests that the apparent mass loss occurred, for the most part, as a one-step process. However, the mass loss happened over a large temperature interval from about 200 to 450 °C. However, the wax mass loss was most likely dominated by concurrent evaporation and thermal degradation events. In the case of EVA, the highest thermal stability was witnessed due to the loss of vinyl acetate units via a de-acylation process and due to the degradation of resulting partially unsaturated polyethylene material polymer as shown in Figure 3.2 (a) (Zanetti *et al*., 2001). Wax/EVA blends showed apparent two-step mass loss profiles with thermal stabilities intermediate to those of wax and EVA behaviours. As it can be seen from Figure 3.3 (b), the LLDPE mass loss happened in one step over a large temperature interval from about 400 to 480 °C. This can be attributed to the degradation of polyethylene polymer material chains. In the case of wax/LLDPE blends, in all the blends, two mass loss steps were observed at temperature from 220 °C to 390 °C and 400 °C to 500 °C. The thermal stabilities values of the blends are intermediates to those of wax and LLDPE.

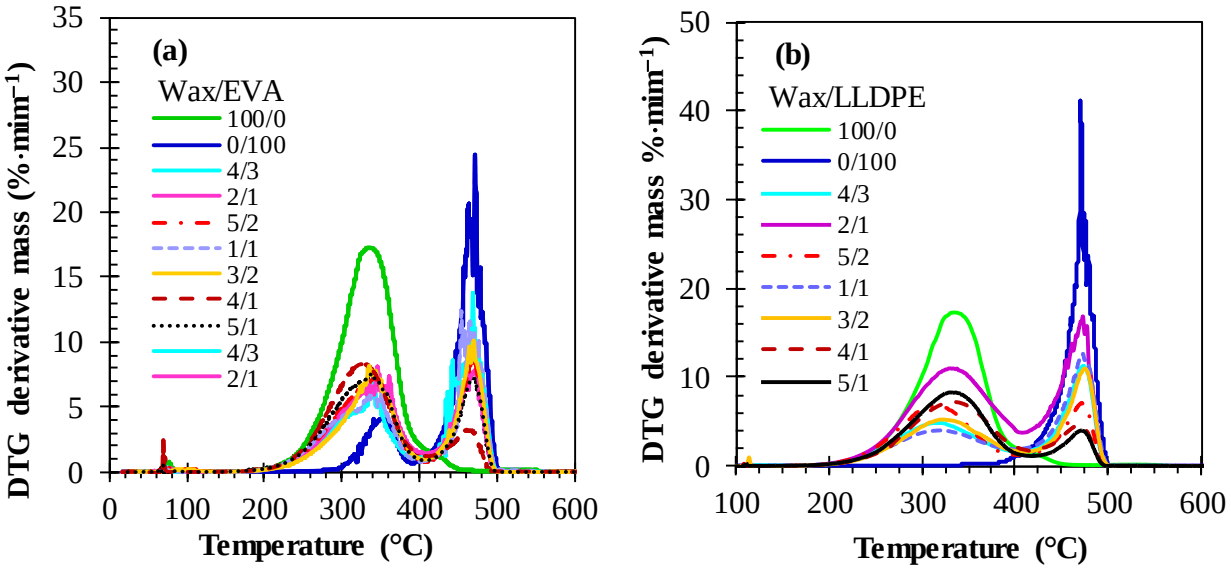

Figure 3.3: (a) DTG curve of EVA and wax and wax/EVA blends and (b) LLDPE and wax/LLDPE blends

3.3.2. Differential scanning calorimetry (DSC)

Figure 3.4 (a) and (b) show the DSC curves for neat EVA, wax, LLDPE, wax/EVA and wax/LLDPE blends during heating and Figure 3.5 (a) and (b) during cooling. Heating was done to 150 °C and cooled to 30 °C and reheated to 150 °C. From Figure 3.4, it can be seen that thermal profile curves for wax has two distinct endothermic peaks whereas LLDPE has one distinct peak. It can also be observed that the solid–solid transition peak of wax/EVA decreases in magnitude as the EVA content increases. This was also observed in the case of wax/LLDPE binary blends. In the case of wax/EVA blends, the separate peaks of wax were not observed since similar melting characteristics was witnessed due to wax and EVA melting point being in the same temperature range. From Figure 3.4 (b), wax/LLDPE has two distinct peaks associated with the melting of wax and LLDPE. It can be said that LLDPE and wax are not miscible with each other in the crystalline

phase. Generally, the lower temperature peaks are due to a solid–solid phase transformation. The other peaks are due to the solid–liquid melting or crystallization transitions. During cooling as shown in Figure 3.4 (b), wax, EVA and wax/EVA binary mixtures showed two exothermic peaks. Figure 3.5 (a) and (b) shows the cooling of wax, LLDPE, wax/EVA and wax/LLDPE blends. From Figure 3.5 (a) and (b), it can be concluded that at a higher wax contents, there is a possibility of the larger part of wax not co-crystallizing with both EVA and LLDPE. Wax will crystallize in LLDPE amorphous phase.

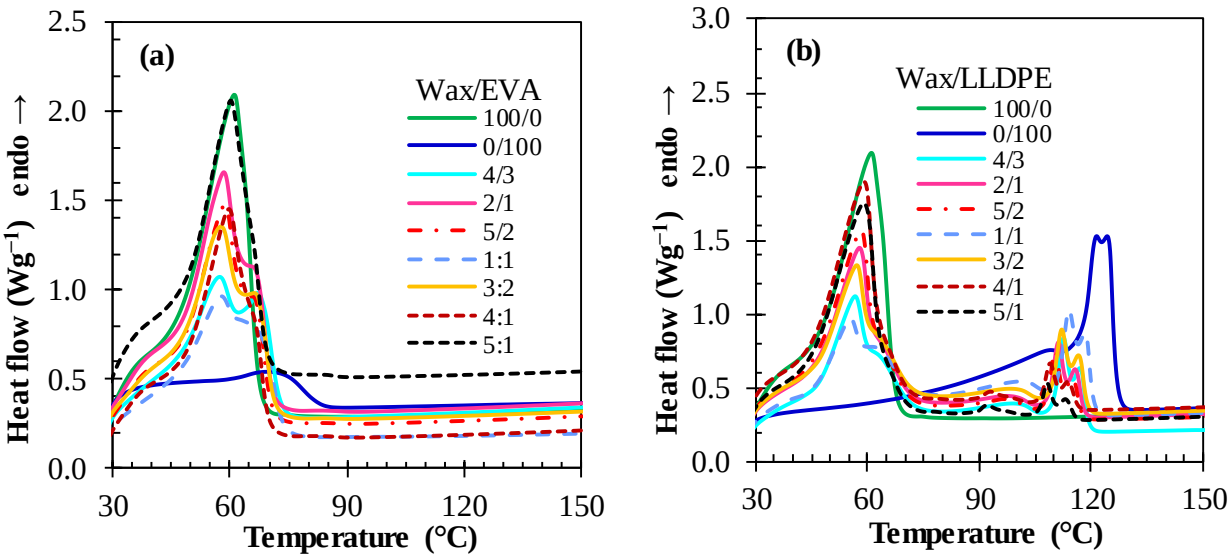

Figure 3.4: (a) DSC heating curves for wax, EVA and wax/EVA blends (b) DSC heating curves for wax, LLDPE and wax/LLDPE blends

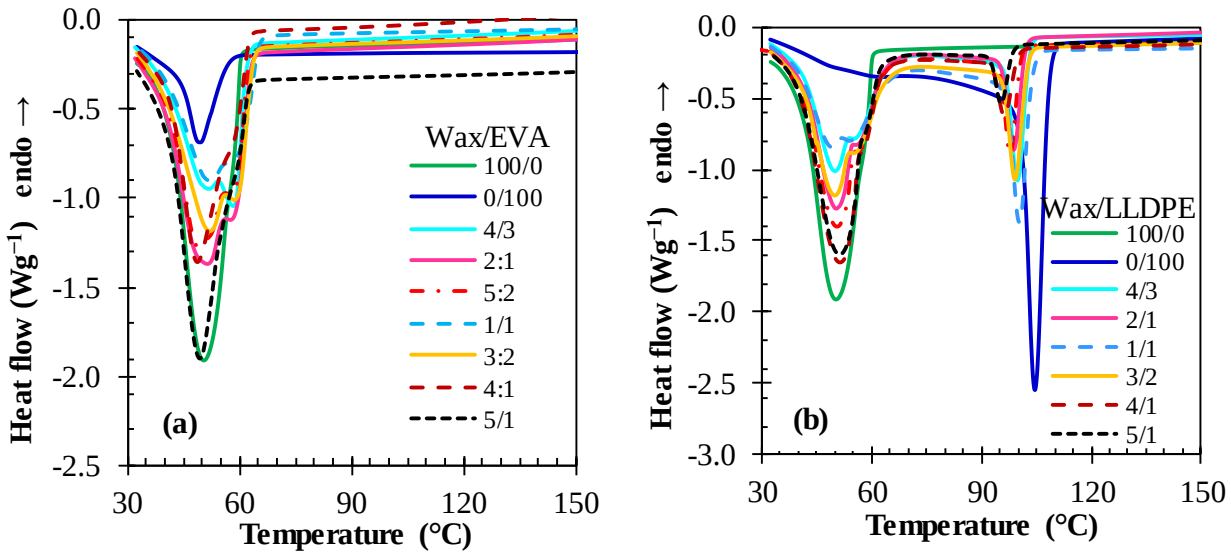

Figure 3.5: (a) DSC cooling curves for wax, EVA and wax/EVA blends (b) DSC cooling curves for wax, LLDPE and wax/LLDPE blends

Table 3.1 and

Table 3.2 shows the summarized DSC results for wax/EVA and wax/LLDPE binary blends. It shows the melting, crystallization peaks and enthalpies for wax, EVA wax/EVA and wax/LLDPE binary blends. As it can be seen from and

Table 3.2, the incorporation of EVA and LLDPE into wax has a slight effect on the melting temperature and the crystallization temperature as well as the enthalpy of melting and crystallization. EVA and LLDPE binary blends have lower enthalpies as compared to the neat compounds. This can be primarily due to better interaction of EVA phase with wax phase hence, as it can also be seen, the recrystallization peaks of wax/EVA binary blends have a lower shift in terms of melting and crystallization temperatures. In the case of LLDPE, two melting and two crystallization peaks are observed. This can be ascribed to phase separation. At a higher amount of LLDPE, there is a phase separation and an immiscible wax/LLDPE binary blend is formed.

Table 3.1: DSC parameters obtained for wax, EVA and wax/EVA binary blend

Sample Wax/EVA	T_{om} (°C)	T_{oc} (°C)	T_{pm} (°C)	T_{pc} (°C)	$\Delta H_{(pm)}$ (J/g)	$\Delta H_{(pc)}$ (J/g)
100/0	42.74	60.22	60.98	50.26	195.20	-156.62
0/100	58.26	56.89	72.42	49.76	56.24	-36.36
57/43	42.32	62.05	57.16	58.53	104.97	-99.52
67/33	43.88	63.33	58.37	51.63	153.81	-125.66
71/29	43.81	62.70	58.55	49.24	137.13	-121.29
50/50	27.32	65.07	57.66	52.20	121.69	-92.91
60/40	44.05	63.41	57.59	51.93	130.02	-111.23
80/20	45.11	62.81	59.56	49.09	128.54	-118.03
83/17	27.11	63.34	60.03	49.16	191.95	-129.94

Table 3.2: DSC parameters obtained for wax, LLDPE and wax/LLDPE binary blend

Sample Wax/LLDPE	T_{om} (°C)	T_{oc} (°C)	T_{pm} (°C)	T_{pc} (°C)	$\Delta H_{(pm)}$ (J/g)	$\Delta H_{(pc)}$ (J/g)
100/0	42.74	60.22	60.98	50.26	195.20	-156.62
0/100	58.26	56.89	72.42	49.76	56.24	-36.36
57/43	45.79	59.25	56.65	49.95	58.858	-89.793
	109.73	103.01	112.72	99.83	19.412	-21.379
67/33	45.23	58.15	57.96	50.26	80.556	-110.131
	108.46	101.85	111.24	98.78	15.348	-17.616
71/29	44.93	57.50	58.35	50.53	83.590	-117.873
	107.82	100.65	110.37	97.83	13.226	-15.043
50/50	45.92	64.32	55.48	49.19	45.752	-74.528
	110.93	103.75	114.14	100.44	23.853	-32.170
60/40	45.51	57.73	57.24	49.88	66.150	-95.121
	109.30	102.54	112.17	99.21	18.318	-21.601
80/20	44.34	58.31	59.29	51.43	105.938	-135.468
	106.55	99.75	109.06	96.29	9.149	-10.836
83/17	43.28	58.81	59.14	51.24	115.702	-131.732
	105.96	98.44	108.25	95.42	6.855	-8.255

3.3.3. Fourier Transform infrared (FT-IR)

Figure 3.6 (a) and (b) shows the FTIR spectra of wax/EVA blends and wax LLDPE blends respectively. Wax/EVA blends has five main bands in the wavelength range of 4000–500 cm^{-1}

whereas wax/LLDPE has three main peaks. Both EVA and LLDPE blends has a wide band in the region of 2919-2842 cm^{-1} and in the region of 1459–1480 cm^{-1} attributed to the deformation vibrations stretch of a long-chain aliphatic hydrocarbon denoted by (C-H) and $-C-H-$ bend of the alkane's hydrocarbons respectively. The less sharp bend indicated by both wax/EVA and wax/LLDPE at a band of between 700 cm^{-1} to 634 cm^{-1} can be ascribed to $-C-H-$ bend of the alkane's hydrocarbons. The wax/EVA spectra further showed a sharper peak at a band in the region of 1760 - 1665. This peak can be ascribed to the presence of carbonyls absorption group denoted by $-C=O-$ stretch.

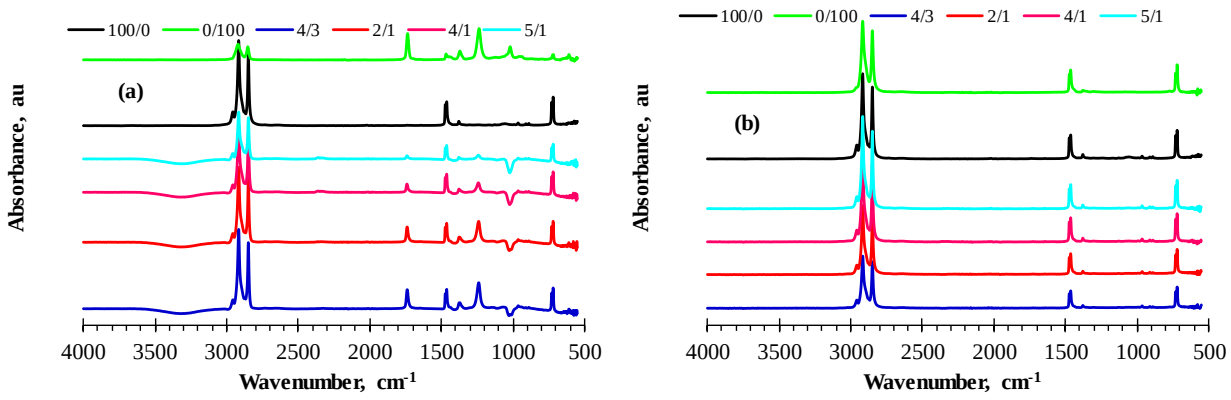

Figure 3.6: FT-IR spectra (a) wax/EVA blends and (b) wax/LLDPE blends

3.3.4. Three-point bending test

Figure 3.7 (a) and (b), Figure 3.8 (a) and (b), Figure 3.9 (a) and (b) and

Table 3.3 shows typical three-point bending results of wax/EVA and wax/LLDPE binary blends. From Figure 3.7 (a) and (b), it can be seen that an increase in EVA and LLDPE content in the binary blends leads to a marginal increase in bending strength. This can be attributed to EVA and LLDPE chains being interlinked in the blends. There is also a slight increase in the resistance to crack propagation. Generally wax experiences brittle failure at small flexural strains caused by easy propagation of cracks through its crystalline structure.

Table 3.*3* report on the mechanical properties of the wax and the formulated blends. The neat wax is very brittle with an average strain at break of just 1.7 ± 0.5 %. Most samples showed similar brittle failure behaviour with an abrupt fracture observed when the maximum load is reached.

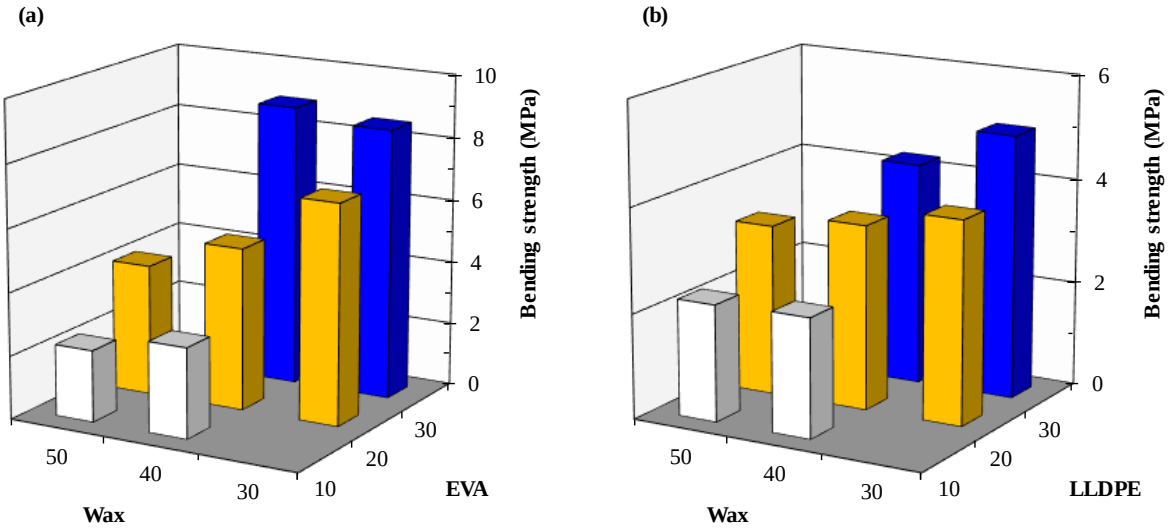

Figure 3.7: (a) Bending strength of wax/EVA blends (b) Bending strength of wax/LLDPE blends

Table 3.3: Mechanical properties of wax/EVA and wax/LLDPE blends obtained from tensile measurements

Wax	EVA	Stress (MPa)	Strain (%)	Modulus (MPa)	Wax	LLDPE	Stress (MPa)	Strain (%)	Modulus (MPa)
100	0	1.3±0.1	1.7±0.5	38±20	100	0	1.3±0.1	1.7±0.5	38±20
30	20	7.0±0.5	13.5±0.8	179±21	30	20	3.9±1.0	1.6±0.2	384±123
30	30	5±0.4	14.1±0.0	179±19	30	30	5.0±1.1	1.8±0.4	493±196
40	10	2.9±0.1	3.4±0.2	138±12	40	10	2.3±0.2	1.4±0.4	266±68
40	20	5.1±0.5	9.1±0.9	160±28	40	20	3.8±0.4	1.5±0.2	318±35
40	30	8.9±0.3	13.4±1.4	201±11	40	30	4.3±0.6	1.5±0.1	477±145
50	10	2.3±0.3	2.7±0.3	159±29	50	10	2.2±0.4	1.0±0.1	302±55
50	20	4.1±0.2	4.6±0.2	238±88	50	20	3.3±0.6	1.5±0.3	309±41

Figure 3.8 (a) and (b) shows the effect of EVA and LLDPE weight variation on the strain of the blends. It can be seen that in the case of EVA, the change in the bending strain as the EVA content increases is in magnitude. Also, as the wax content in the blend increases, the strain increases. The increase in the strain in both EVA and LLDPE wax blends could be attributed to the increasing amorphous nature of both the blends hence, plastic deformation nature is witnessed before the macroscopic yield point. In general, the structural realignment of amorphous fraction of the blends induced by the applied stress increases the amorphous fraction which yields an increase in the strain with plastic deformation starting to take place. LLDPE is a more brittle polymer blend with a lower strain as compared to EVA based wax blend. This can be related to the decrease in the tie-

chain fraction in the blends caused by a high number of wax chains that do not contribute to the tie chain in the case of LLDPE.

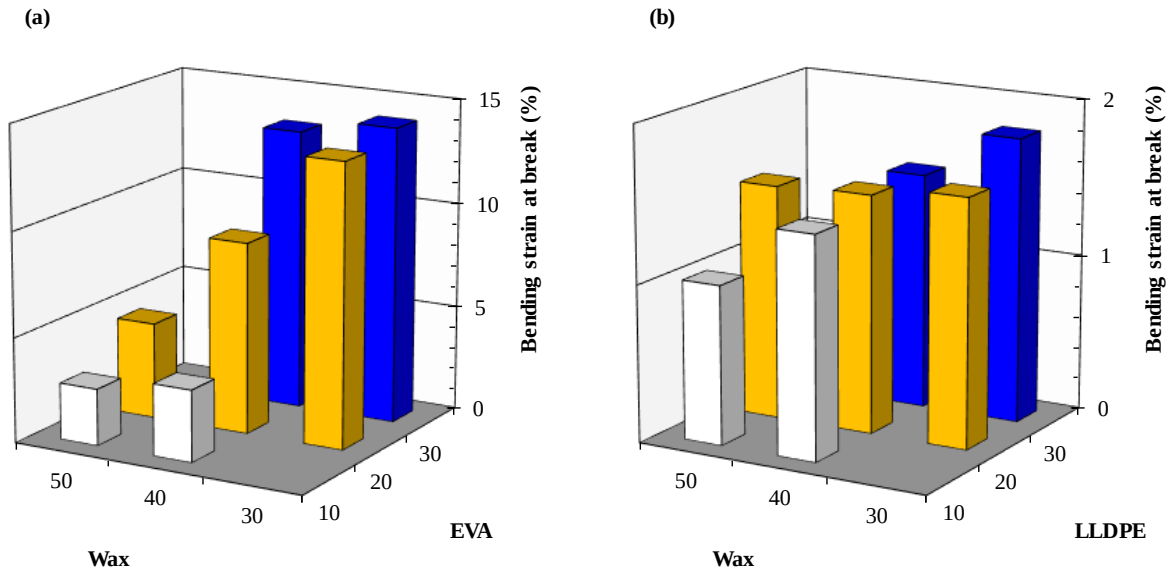

Figure 3.8: (a) Bending strain of wax/EVA blends (b) Bending strain of wax/LLDPE blends

As it can be seen in Figure 3.9 (a) and (b), the incorporation of EVA and LLDPE into paraffin wax has a significant influence on Young's modulus. This can be associated with the co-crystallization of wax EVA and LLDPE. It can be further be seen also that as the wax content increases, there was an increase in the Young modulus. Young Modulus is dependent on the interaction between the crystalline and the amorphous regions of the blends due to elongation energy transmitted from the amorphous to the crystalline phase. Hence, as the wax content increases the crystallinity increases and the Young modulus is expected to increase. In the case of LLDPE, the polyethylene chains have an effect on the energy transfer to the crystalline phase hence the increase in the stiffness as compared to wax/EVA based blends. Generally, in the case of wax/LLDPE blends, the

crystallinity does not increase with increasing wax content for hence as it can be seen in Figure 3.9 (b), the effect on Young modulus is small for all the blends.

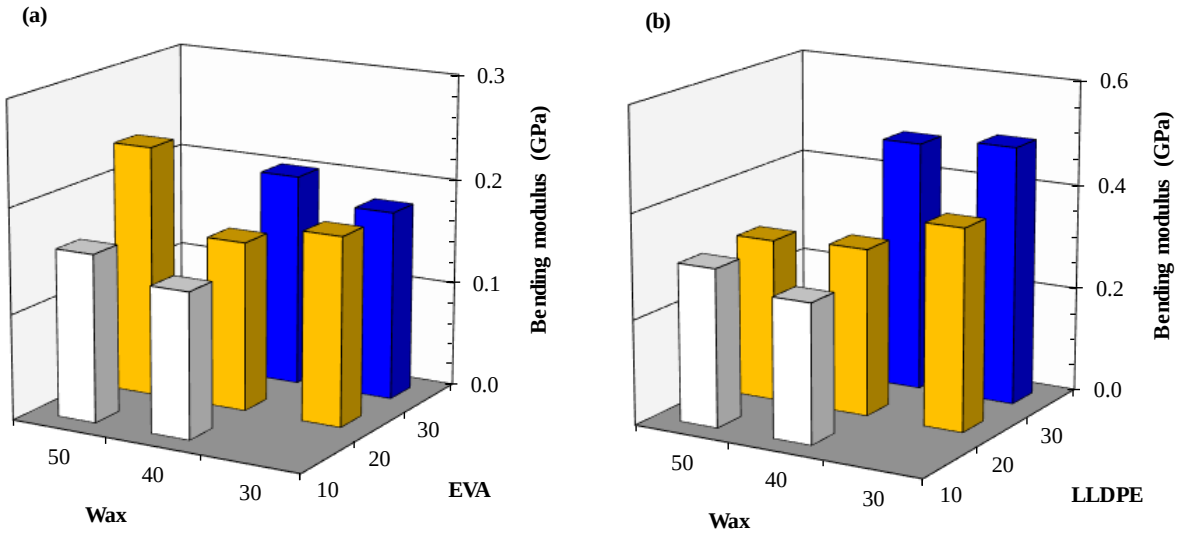

Figure 3.9: (a) Bending modulus of wax/EVA blends (b) Bending modulus of wax/LLDPE blends

3.3.5. Scanning electron microscopy (SEM)

Figure 3.10 (a), (b) and (c) shows the SEM micrograph of neat EVA, neat wax and neat LLDPE. From Figure 3.10 (a), it can be seen that EVA has a smooth surface with some interlinking of chains which can be attributed to the CH_2 interconnecting. Whereas in Figure 3.10 (b) it can be seen wax crystals are long and narrow chains of hydrocarbons which form in plates. Generally, wax is characterized by homogeneous constitution and distribution due to its refining process. Figure 3.10 (c) shows a less smooth surface of LLDPE. LLDPE tend to be amorphous in nature.

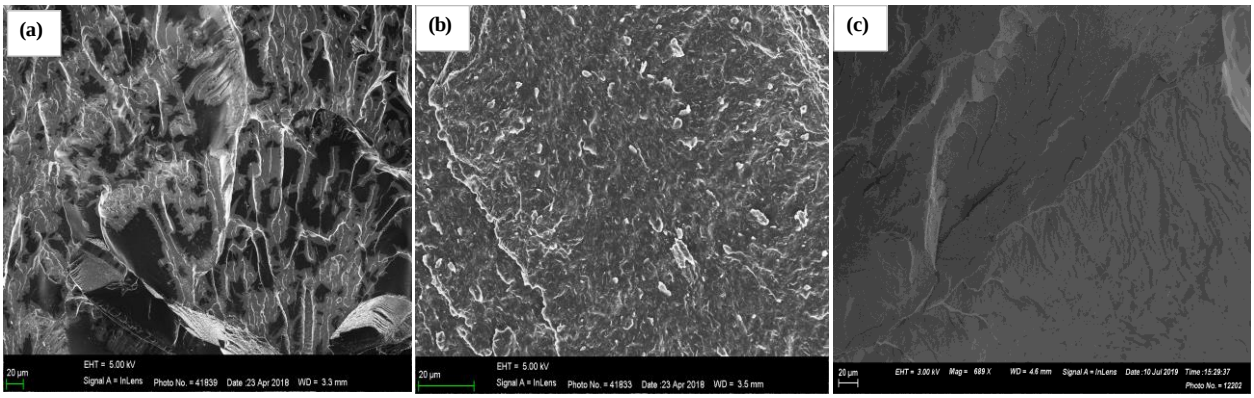

Figure 3.10: SEM micrographs (a) neat EVA, (b) neat wax and (c) neat LLDPE

Figure 3.11 (a), (b) and Figure 3.12 (a), (b) shows the morphologies of a low wax concentration in EVA and LLDPE as well a high wax concentration in EVA and LLDPE blends. It can be observed that there was a difference in morphologies in both the low and high concentration in EVA and LLDPE. At low wax content, in the case of wax/EVA blend and wax/LLDPE, a homogeneous surface and good dispersion of the wax. It can be concluded that, despite the fact that the EVA/wax blends were compounded under the same experimental conditions, the dispersion of wax in the EVA and wax in LLDPE matrix strongly depended on: (i) the wax percentage added to the polymer and (ii) the morphology structure of the polymer. Further, increasing the wax content in the blend causes an increase in phase separation and immiscibility hence a rough surface morphology was observed. Generally, EVA/wax shows less phase separation due to both EVA and wax consisting of a network of long CH_2 chains.

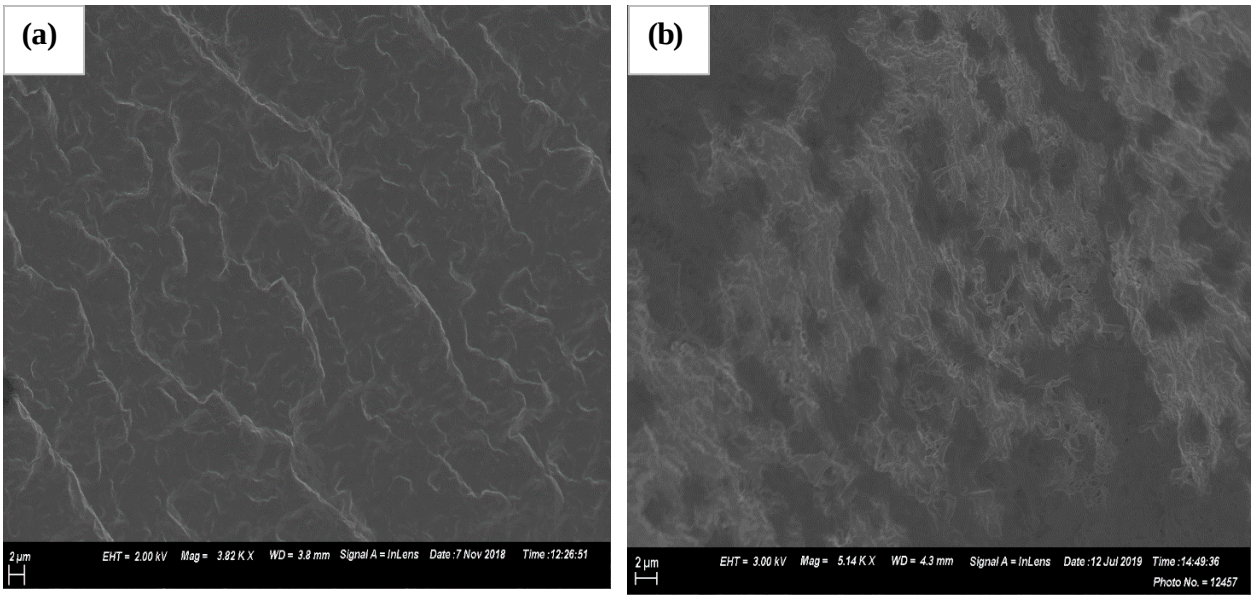

Figure 3.11: SEM micrographs (a) wax/EVA 1/1, (b) wax/LLDPE 1/1

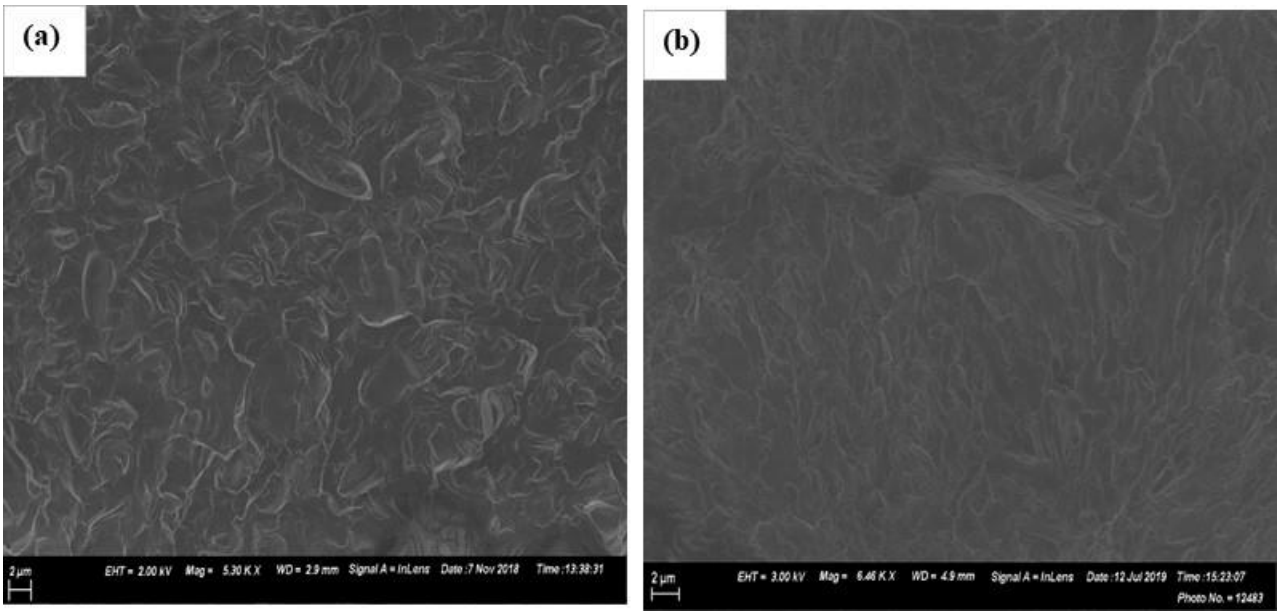

Figure 3.12: SEM micrographs (a) wax/EVA 5/1, (b) wax/LLDPE 5/1

3.3.6. Thermomechanical analysis (TMA)

Figure 3.13 shows the TMA penetration curves of (a) wax, EVA and wax/EVA binary blends and (b) wax, LLDPE and wax/LLDPE blends. As it can be seen in both Figure 3.13 (a) and (b), as low

force was applied, the needle penetrated slowly in all the blends. It can be seen that neat wax is softer than EVA and LLDPE. The rate of penetration in all the binary blends decreased when the applied force was applied during the full 2 min testing interval for all the blends. In both the EVA based and LLDPE based wax blends, the hardness of the binary blends formulated was higher than that of wax, EVA and LLDPE. EVA and LLDPE forms a polymer blend with improved mechanical properties though this all depends on the ratios of the polymers which has a great effect on its interaction with wax.

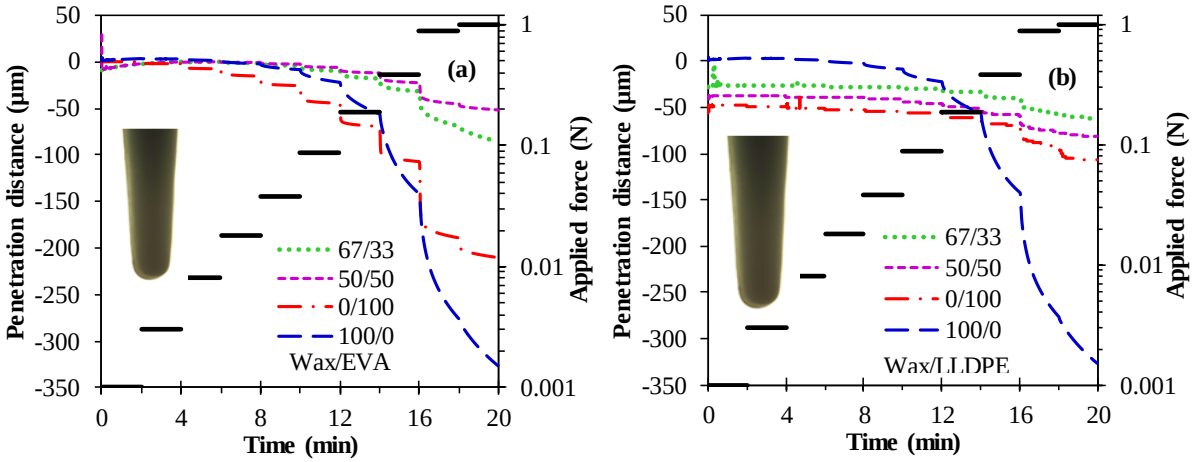

Figure 3.13: TMA curves (a) wax and wax/EVA (b) wax and wax/LLDPE. The inset shows the needle profile.

Table 3.4: TMA needle penetration results

Wax	EVA	Penetration (µm)	Wax	LLDPE	Penetration (µm)
100	0	327.0	100	0	327.0
57	43	63.1	30	20	47.6
67	33	97.6	30	30	62.4
5	2	97.4	40	10	120.0
50	50	51.7	40	20	81.6
60	40	85.8	40	30	42.2
80	20	240.7	50	10	162.7
83	17	293.7	50	20	215.1

*Needle penetration test. Depth measured after application of a final force of 1 N for 2 min.

3.3.7. Rheology of wax/ EVA blends and wax/LLDPE blends

The melt flow behaviour of wax/EVA blends and wax/LLDPE blends at a temperature of 90 °C was measured as a function of shear rate. From Figure 3.14 (a), it can be seen that the melt viscosity increases as the EVA and LLDPE content is increased and EVA-wax based blend have a slightly higher viscosity measurements than LLDPE wax based blends.

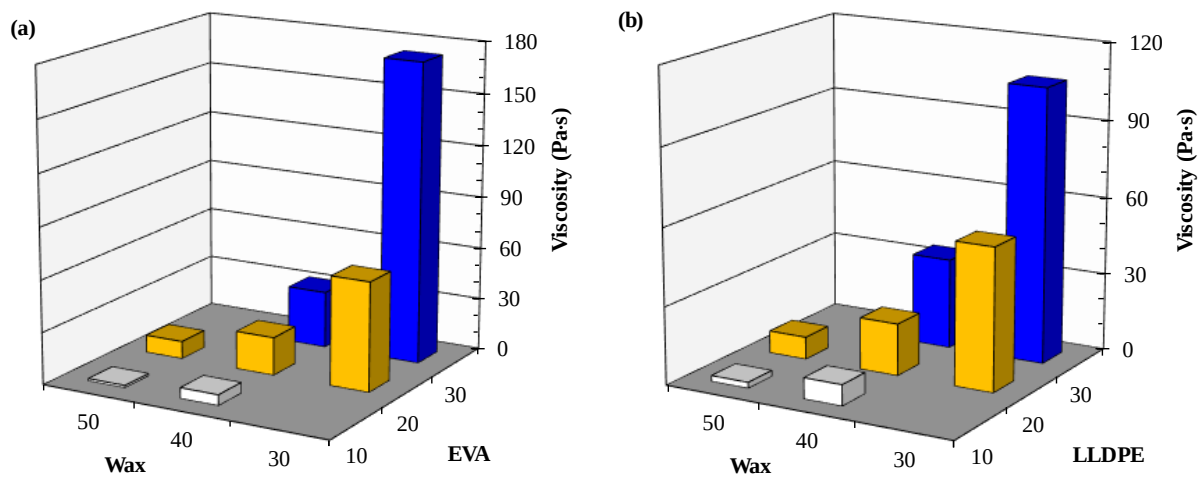

Figure 3.14: Viscosity of (a) wax/EVA and (b) wax/LLDPE blends measured at 90 °C

The viscosity of the blends follows a form of the composition dependence proposed by Arrhenius (Arrhenius, 1887) as modified by (Grunberg and Nissan, 1949) (Equation 3.4):

$$\eta_{mix} = \exp\left(w_{wax} ln\eta_{wax} + 2\, w_{wax} w_{EVA} ln\eta_{Int} + w_{EVA} ln\eta_{EVA}\right) \qquad (3.4)$$

Where η_{mix} is the viscosity of the binary mixture, and w_{wax} and $w_{EVA/LLDPE}$ are the mass fractions of the wax and EVA respectively. The parameters η_{wax} and $\eta_{EVA/LLDPE}$ represent the viscosities of the neat wax and EVA respectively.

The η_{Int} is an interaction term. It and $\eta_{EVA/LLDPE}$ were treated as adjustable parameters as it was not possible to accurately measure the viscosity of the EVA and LLDPE with the equipment available as it is not sufficiently fluid at 90 °C. Least squares regression yielded and $ln\eta_{Int}$ = –5.944 and $ln\eta_{EVA}$ = 16.98 on setting $ln\eta_{wax}$ = -2.615. The solid line in Figure 3.15 (a) and (b) shows the trend predicted by equation (1) with these values for the parameters.

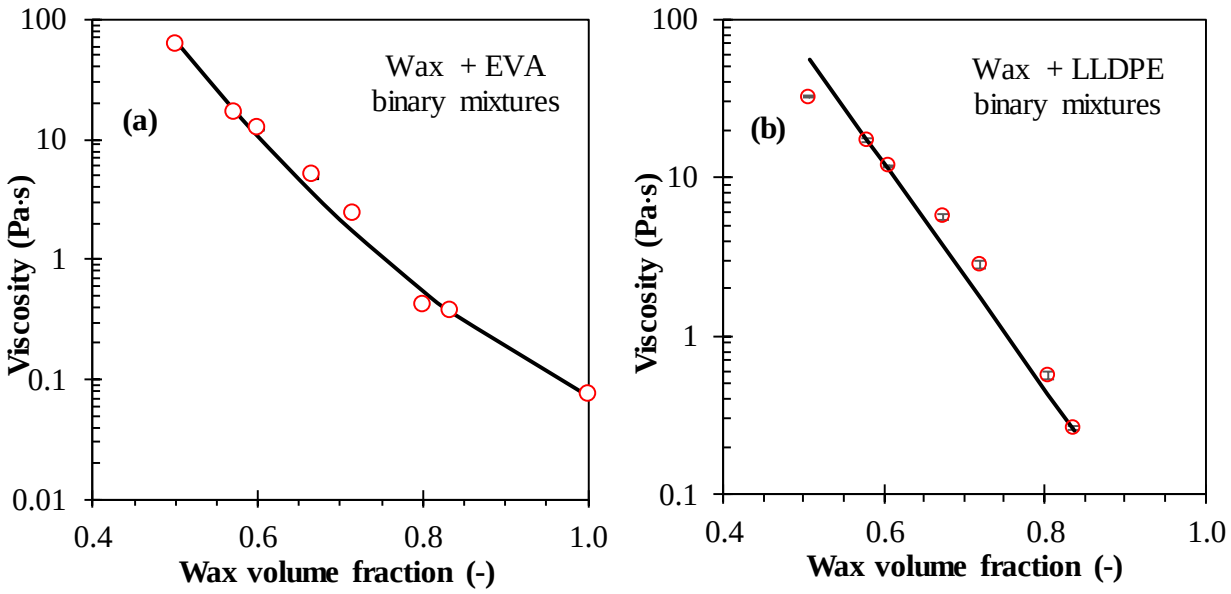

Figure 3.15: Viscosity of (a) wax/EVA binary blends and (b) wax/LLDPE binary blends

3.4. CONCLUSIONS

The following conclusions were made:

(i). The thermal stability of wax improved when both EVA and LLDPE was incorporated into the wax matrix. EVA content in wax/EVA binary blends causes an increase in the binary blend melting point during heating whereas, on cooling the low crystallinity in EVA-28 means the congealing point is almost identical to that of paraffin wax. In the case of wax/LLDPE, crystallization of the blend of LLDPE is strongly affected by the wax loading. Wax acts as a solvent for LLDPE hence its melting and crystallization depends on the amount of wax and LLDPE.

(ii). An increase in the EVA weight in the binary blend led to a retardation in the brittle fracture behaviour of the blend which resulted to a product having an increasing degree of plastic deformation before fracture. In the case of wax/LLDPE blends, The Young modulus, stress and

strain increased with an increase in the amount of LLDPE. This could be attributed to higher degree of crystallinity experienced.

(iii) The viscosity of neat paraffin wax increased when it was blended with EVA and LLDPE. At EVA and LLDPE weight loading of 30%, the viscosity was in magnitude of almost 100 for LLDPE and almost 200 in the case of EVA. Both EVA and LLDPE had low MFI hence, at higher weight ratios in the blends, the viscosities will increase by a higher margin. The Krieger Dougherty function (K-D) revealed that the experimental results in both EVA based and LLDPE wax based blends agrees with the correlation for the of volume fractions tested.

(iv). SEM spectra indicated that the smooth wax surface was affected by EVA and LLDPE.A rougher surface was witnessed in the case of LLDPE as compared to EVA.

Chapter 4 : THERMAL, MECHANICAL SURFACE CHARACTERIZATION AND RHEOLOGY OF WAX/EVA/PMMA FORMULATION.

ABSTRACT

Paraffin wax-based compounds are utilised as investment casting pattern materials. In this study, the thermal, mechanical, surface and flow properties of Fischer-Tropsch wax-EVA-polymethylmethacrylate (PMMA) ternary blend were characterized using thermogravimetric analysis (TGA), differential scanning calorimetry (DSC), thermomechanical analysis (TMA), three-point bending test, scanning electron microscope (SEM), Fourier transform infrared (FT-IR) and rheology. This study considered the effect of composition variations on the properties of paraffin wax-poly (ethylene-co-vinyl acetate) (EVA) blends filled with poly (methyl methacrylate) (PMMA) microbeads. The EVA addition significantly improved mechanical properties while the PMMA improved the needle penetration hardness. Both polymers increased the melt viscosity of the wax composition. Thermal gravimetric analysis of the pyrolysis behaviour showed that the compounds volatilise readily with virtually no residue remaining above 500 °C. The 40/20/40 wax/EVA/PMMA composition offers a balanced property profile with the bending stress approaching 6 MPa, the bending strain at break exceeding 4 % and a melt viscosity of about 12 Pa·s at 90 °C. The Krieger Dougherty function (K-D) revealed that the experimental results agrees with the correlation for the of volume fractions tested.

Key words*:* *Investment casting pattern, Fischer-Tropsch wax, EVA, Fischer-Tropsch wax-EVA blend, thermal stability.*

4.1. INTRODUCTION

Investment casting is a near-net shape fabrication process for metal components (Singh and Singh, 2016). It is capable of producing parts with complex shapes subject to tight dimensional tolerances and outstanding surface finishes (Bemblage and Karunakar, 2011). It is used to manufacture a myriad of products (Upadhya *et al*., 1995) including medical implants (Horáček *et al*., 2010) and aircraft components (Tomasik *et al*., 2009). The investment casting process utilises ceramic moulds into which a liquid metal alloy is poured and allowed to cool and solidify to yield the desired casting (Jones and Yuan, 2003).

The moulds are prepared by repeated dipping of a wax model in liquid suspensions of ceramic precursor powders. Each deposited coating is first air dried before the next immersion. In this way, successive layers, comprising particles of increasing coarseness, are built up to form the green shell. After drying, the wax is removed by melting in an autoclave. The finished ceramic mould is obtained by a careful heat treatment protocol. This includes a final firing at temperatures as high as 1000 °C (Jones and Yuan, 2003).

The wax models are manufactured by an injection moulding process. The pattern material should have good mechanical strength, to allow ease of handling and assembly, and excellent dimensional stability in order to achieve quality investment casting products (Pattnaik *et al*., 2012). A high fluidity in the molten state is necessary for assisting the dewaxing process. Therefore, the choice of the investment pattern material is critical. This justifies the drive towards further improvement of physical, thermal, mechanical and flow properties (Tewo *et al*., 2018). Possible routes towards fortifying the base wax include blending with polymers (Rutto and Focke, 2009) and incorporation of fillers to improve both thermal expansion and mechanical properties (Pattnaik *et al*., 2012).

Organic modifiers are preferred because combustion should leave little, if any, ash residues (Biernacki *et al*., 2015).

This communication explored the utility of a paraffin wax modified with poly (ethylene-co-vinyl acetate) (EVA) and filled with poly (methyl methacrylate) (PMMA) powder for application as an investment casting pattern material. This selection was informed by observations made by previous investigators. First, paraffin wax is used in investment casting pattern materials (Bemblage and Karunakar, 2011) and it has an important effect on surface roughness (Katiyar *et al*., 2012). Second, paraffin wax combines with EVA to form stable, homogeneous blends with near constant melting and solidification phase transition behaviours (Standring *et al*., 2016). The hardness of such paraffin/EVA blends increases with the copolymer concentration and decreases with decreasing VA content (Nebykov *et al*., 1985). The melt viscosity of paraffin wax/EVA blends increases markedly with increasing EVA content (Standring *et al*., 2016) but decreases with increasing polymer MFI and vinyl acetate (VA) content (Nebykov *et al*., 1985). The flexural modulus of the EVA/wax blends attains a maximum value at an intermediate EVA contents (about 30-40 wt-%) (Kim and Kim, 1999). As the EVA content is increased the brittle nature of the paraffin wax morphs into a more flexible material with plastic deformation properties (Standring *et al*., 2016).

Based on these observations, an EVA grade containing 28% VA was selected. Thirdly, poly(methyl methacrylate) (PMMA) and poly(ethylene-co-vinylacetate) (EVA) are immiscible blend components (Laurienzo *et al*., 1989). This implies that the PMMA filler powder should not dissolve in the wax/EVA matrix at the low processing temperatures employed in investment casting, i.e. it would be a stable organic filler. Lastly, all these components vaporise on pyrolysis leaving virtually no residue.

4.2. MATERIALS AND METHODS

4.2.1 Materials

Hydrocarbon wax M3B (Congealing point = 62 °C, mean molecular mass = 785 $g \cdot mol^{-1}$, density 0.900 $g \cdot cm^{-3}$ at 25 °C) was obtained from Sasol Performance Chemicals. The poly (ethylene-co-vinyl acetate) grade used was Elvax 250 (28 % vinyl acetate, melting point = 70 °C, density 0.95 $g \cdot cm^{-3}$ at 25 °C and melt flow index (MFI) 25 g/10 min@190 °C, 2.16 kg). Advanced Polymers supplied PMMA microbeads. All the materials were used as received.

4.2.2 Method

The wax formulations indicated in the experimental design shown in Figure 4.1 were prepared as follows. The required components amounts were weighed out into a container, sealed and thoroughly mixed by vigorous shaking. The formulations were compounded on a TX28P 28 mm co-rotating twin-screw extruder with an L/D ratio of 18. The screw design comprised intermeshing kneader elements with a forward transport action.

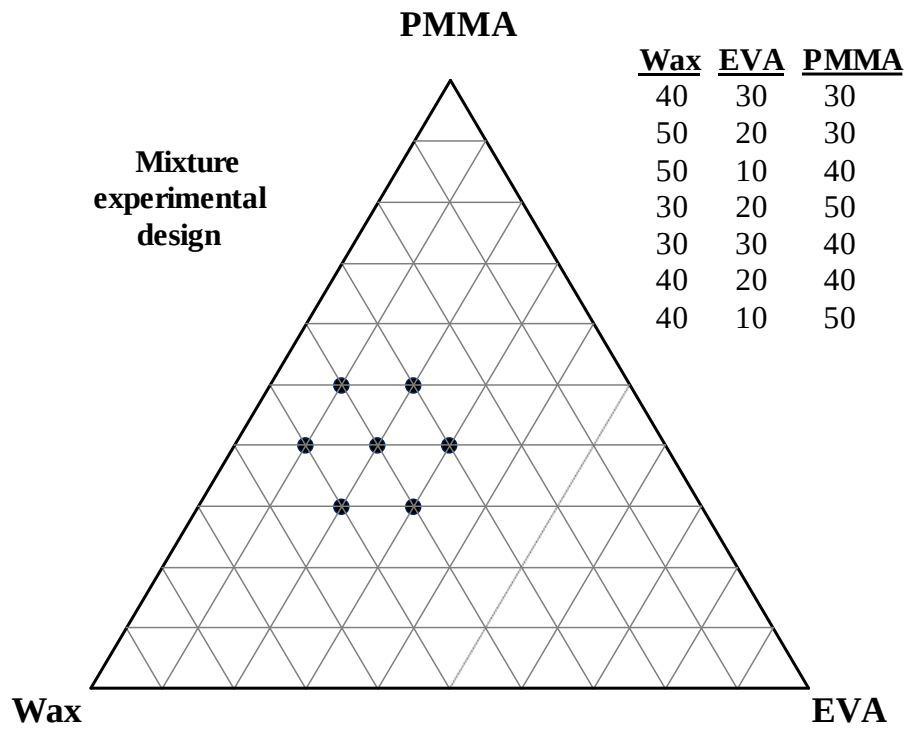

Figure 4.1: Experimental design for the wax/EVA/PMMA blend formulations

The processing temperature profile, from hopper to die, was 40/80/90/100 °C. The melt was extruded directly into a water bath. The extrudate was granulated and allowed to dry under ambient conditions. Test bars for three-point bending (10 × 10 × 80 mm) were cast from the melt using a silicone rubber (Appendix I).

4.2.3 Characterization techniques

4.2.3.1 Particle size distribution

The particle size distribution of the PMMA powder was determined with a Mastersizer Hydrosizer 2000. The shape of the filler powder particles, and the fracture surface morphology of the wax blends, were imaged with a Zeiss Ultra 55 FESEM field emission scanning electron microscope.

Samples were mounted on a double-sided tape fixed on a metallic plate and coated with a thin layer of gold before viewing.

4.2.3.2 Thermal studies

Thermogravimetric analysis (TGA) was performed on a TA Instruments SDT Q 600 TGA analyser. Samples weighing ca. 8 ± 2 mg were placed in a 70 µL alumina pan and heated from 30 °C to 900 °C at a scan rate of 10 $K \cdot min^{-1}$. The purge gas (nitrogen) flow rate was 50 $mL \cdot min^{-1}$. Differential scanning calorimetry (DSC) was conducted on a Perkin Elmer DSC 4000 analyser. Sample masses weighing 15 ± 2 mg were placed in sealed aluminium pans and heated at 20 $K \cdot min^{-1}$ from at 20 °C and 200 °C, held at this temperature for one minute and then cooled back to 20 °C at the same rate. The reported response curves correspond to data obtained during the second heating-cooling cycle.

4.2.3.3 Fourier transform infrared (FTIR)

FTIR spectra were recorded on a Perkin Elmer spectrum 100 FTIR spectrometer fitted with an ATR cell. The spectra represent the average of 16 scans obtained at a resolution of 4 cm^{-1} over the wavenumber range 4000 - 600 cm^{-1}.

4.2.3.4 Thermomechanical analysis (TMA)

Needle penetration tests are used to judge the hardness of wax compositions (Nebykov *et al*., 1985). The present measurements were conducted at 30 °C on a TA Instruments Q400 Thermo Mechanical Analyzer fitted with a needle with a tip radius of 1.4 mm (Appendix II). A wax sample was cast in a 90 µL alumina pan. The test protocol was as follows. At the start, the applied force was set at 0.001 N. Thereafter it was increased after two-minute intervals using the following

successive force increments: 0.002, 0.005, 0.01, 0.02, 0.05, 0.1, 0.2 and 0.5 N. Lastly, the force was increased to 1 N and applied for a further two minutes after which the final needle penetration was recorded. During the experiment, the penetration depth of the needle was tracked as a function of time.

4.2.3.5 Three-point bending tests

Three-point flexural testing, executed according to ASTM 790, was performed on an Instron 5564 twin column tensile tester fitted with a 5 kN load cell. The crosshead speed was set at 1.8 $mm \cdot min^{-1}$ and the sample support span was 64 mm. Five test specimens were prepared and average values are reported.

4.2.3.6 Rheology

Viscosity was determined at a shear rate of 1 s^{-1}. An Anton Paar MCR301 rheometer was employed using the parallel plate configuration with a 25 mm ϕ spindle. The temperature was controlled at 90 °C. All the measurement were done under a nitrogen blanket in order to avoid thermal oxidation.

4.2.3.7 Morphological studies

The surface morphology of wax, EVA and EVA/wax/PMMA formulations was observed using Zeiss Ultra PLUS FESEM (high resolution micrograph) scanning electron microscope. The wax/EVA/PMMA blends were placed on a double-sided tape fixed on a metallic plate and then coated with a thin layer (50 Å thickness) of gold powder sputter module in a vacuum evaporator in an argon atmosphere.

4.3. RESULTS AND DISCUSSION

4.3.1. Thermogravimetric analysis (TGA)

TGA mass loss and DTG derivative mass loss curves for the wax, EVA, PMMA and 40/20/40 wax/EVA/PMMA blend are presented in Figure 4.2 (a) and (b). The mass loss is effectively complete for all samples by the time the temperature reaches 500 °C. The PMMA featured the lowest thermal stability. It started losing minor amounts of mass just above 100 °C with rapid mass loss commencing above 250 °C. This polymer has a ceiling temperature of 198 °C. Above this temperature PMMA depolymerises according to an unzipping mechanism that yields the constituent monomer in the gaseous form. However, the multiple peaks in the DTG curve shown in Figure 4.2 (b) suggest that additional degradation mechanisms play a role. The DTG curve for the wax suggests that the apparent mass loss occurred, for the most part, as a one-step process. However, it happened over a large temperature interval from about 200 to 450 °C. This means that the mass loss of the wax is most likely dominated by concurrent evaporation and thermal degradation events. The EVA featured the highest thermal stability. Its mechanism of thermal degradation involves two major steps (Troitskii *et al*., 1973) attributed to (Zanetti *et al*., 2001) (a) the loss of vinyl acetate units via a de-acylation process resulting in the formation of double bonds, and (b) to the degradation of resulting partially unsaturated polyethylene material polymer. The wax blends considered all showed apparent two-step mass loss profiles with thermal stabilities intermediate to those of the PMMA and EVA behaviours. The 40/20/40 wax/EVA/PMMA composition was thermally the most stable blend considered. However, all the blends showed higher-than-expected thermal stability as is illustrated in Figure 4.2 (a). It compares an actual mass loss curve with one generated based on a mass fraction weighted linear combination of the TGA

curves for the constituents. The actual measured mass loss was significantly less that predicted. The reasons for this behaviour are currently unknown.

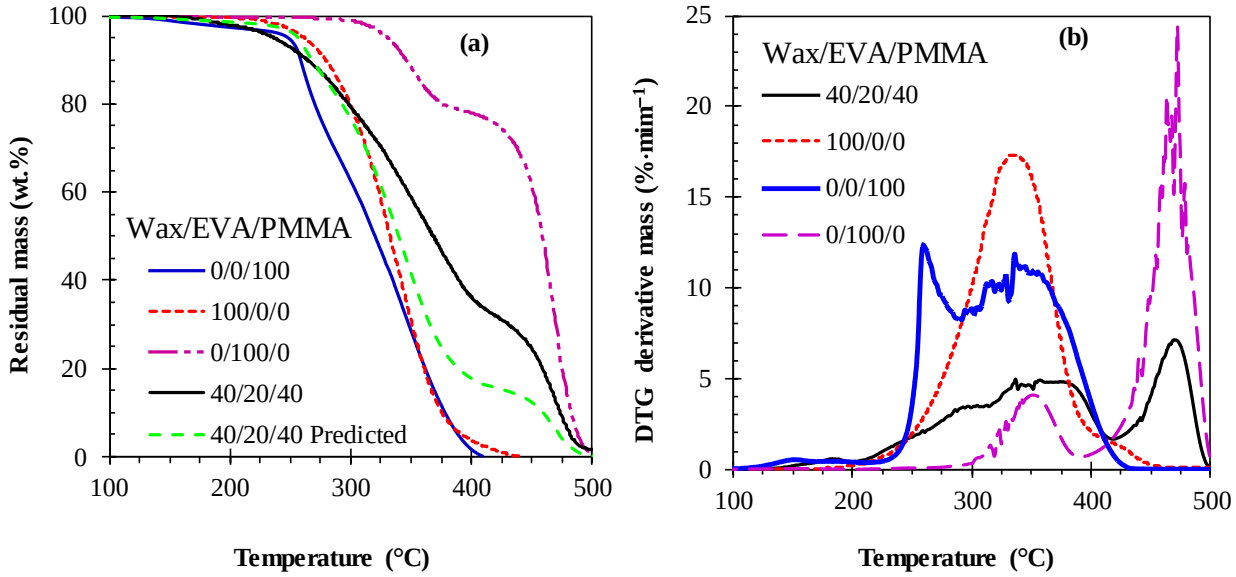

Figure 4.2: (a) TGA curve for the wax, EVA, PMMA and 40/20/40 wax/ EVA/ PMMA blend (b) DTG curve for the wax, EVA, PMMA and 40/20/40 wax/ EVA/ PMMA blend. The curve predicted for the latter is based on the assumption of a mass fraction weighted linear combination of the TGA curves for the constituents.

4.3.2. Differential scanning calorimetry (DSC)

The differential scanning calorimetry (DSC) results are summarized in Table 4.1. Representative heating and cooling curves are shown in Figure 4.3 (a) and (b). The EVA features a very broad melting range and, based on the endotherm peak, is not yet fully molten at 90 °C. The crystallisation onset temperature is ca. 58 °C. The wax shows two endothermic events in the heating curve while the cooling curve also features two exothermic events. The wax is completely

molten above 70 °C. The lower temperature peaks are due to a solid–solid phase transformation. The other peaks are due to the solid–liquid melting or crystallization transitions. Before melting, the phase transformation of the solid–solid transition changes from an ordered to a more disordered phase. The enthalpy of fusion of the wax is much higher than that of the EVA. The heating and cooling curves for the wax blends have shapes similar to that of the neat wax except that the enthalpies are significantly lower. Obviously, this is caused by the presence of the amorphous filler and the EVA. The specific enthalpies of melting and of crystallization increased with an increase in the wax content.

Table 4.1: DSC parameters obtained for the wax, EVA and wax/EVA/PMMA blend

Sample (EVA/wax/PMMA)	T_{om} (°C)	T_{oc} (°C)	T_{pm} (°C)	T_{pc} (°C)	$\Delta H_{(pm)}$ (J/g)	$\Delta H_{(pc)}$ (J/g)
0/100/0	42.74	60.22	60.98	50.26	195.20	-156.62
100/0/0	38.40	72.43	71.82	72.43	11.28	-36.36
30/40/30	41.70	63.80	57.05	51.65	79.26	-78.02
20/40/40	42.24	63.97	66.92	57.76	73.10	-66.22
20/50/30	42.86	63.17	58.01	50.56	77.69	-74.53
30/30/40	43.02	63.28	59.50	51.39	68.40	-66.77
20/30/50	45.47	62.58	59.34	51.05	63.74	-62.97
10/40/50	42.03	63.83	57.23	51.97	58.88	-59.47
10/50/40	44.31	61.80	59.15	50.59	76.72	-76.96

Further from Figure 4.3, it can be seen that wax /EVA/PMMA 10/50/40 formulation, one exothermic peak was observed. This can be attributed to the blend being miscible at molten state

and exhibiting macroscopic homogeneity. Generally, most wax components solidify in a planar zigzag form, hence, this can explain the macroscopic homogeneity in the blend.

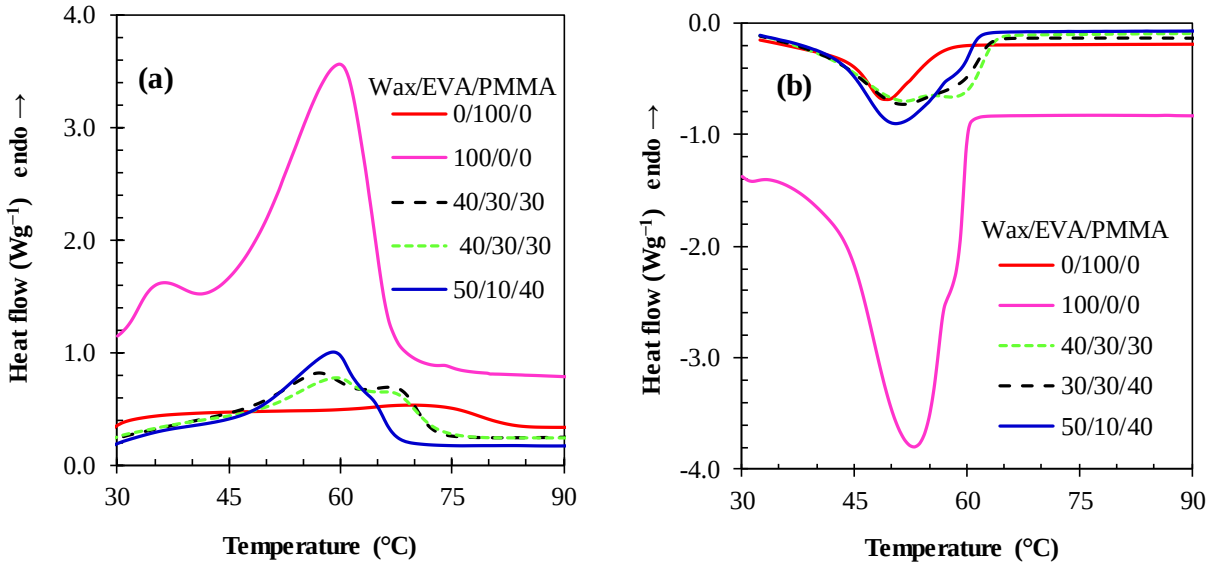

Figure 4.3: (a) DSC heating and (b) DSC cooling curves obtained for the wax, EVA, PMMA and the 50/10/40 wax/ EVA/ PMMA blend.

4.3.3. Fourier transform infrared (FTIR)

The FTIR spectra of the formulation components and one of the wax blends are reported in Figure 4.4. The absorption bands present in the wax spectrum are typical for long-chain aliphatic hydrocarbons, i.e. C–H stretch at 2957, 2917 and 2847 cm^{-1}; C–H bending at 1464 cm^{-1} and 1368 cm^{-1}, and in-phase rocking of CH_2 chains at 720 cm^{-1}. The spectra for the EVA and the PMMA feature similar bands. Prominent, and additional, are the ester carbonyl C=O stretching bands located at 1736 cm^{-1} and 1717 cm^{-1} in the EVA and PMMA spectra respectively. Close inspection of the spectra revealed that the peak positions of the carbonyl absorption bands in the 40/30/30

wax/EVA/PMMA blend are the same as that for the EVA, i.e. 1736 cm^{-1}. Since the spectra correspond to ATR data collection, this suggests that the EVA covered the PMMA particles. Alternatively, it signifies the absence of strong molecular interactions between the two species. This behaviour confirms the formation of a physical wax/EVA PMMA blend.

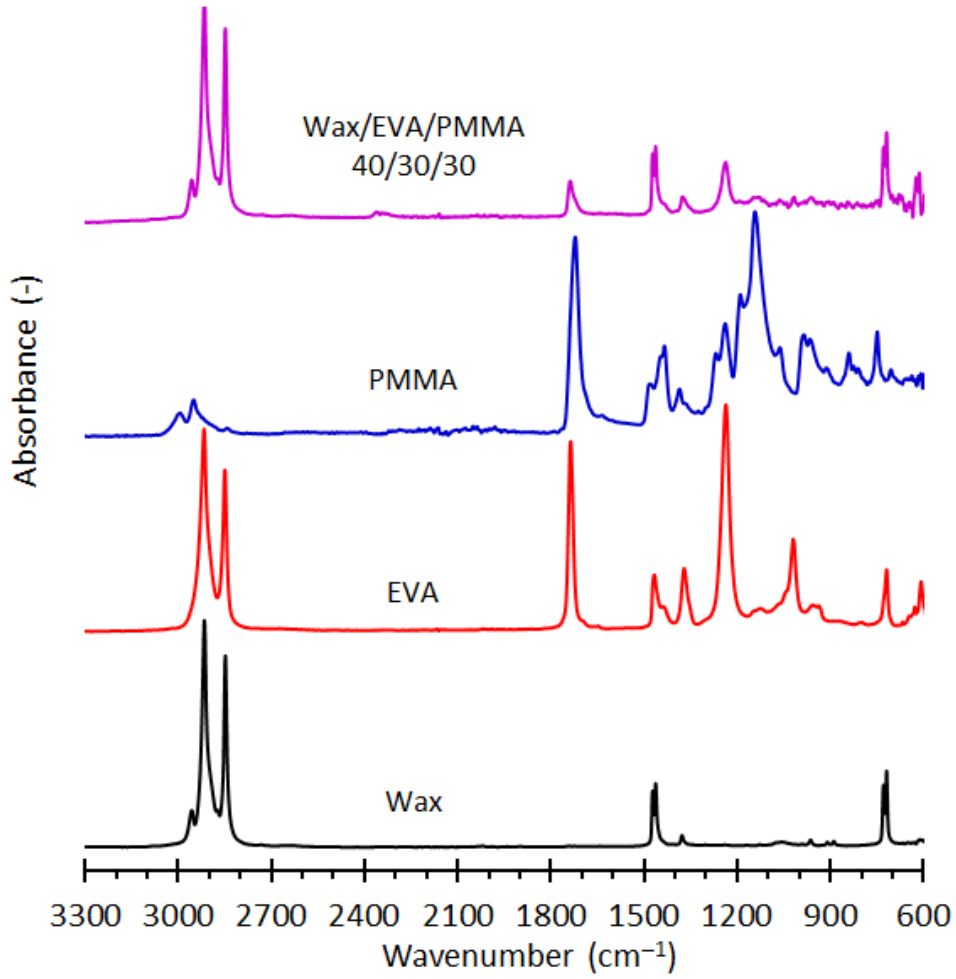

Figure 4.4: FTIR absorbance spectrum for the 40/30/30 wax/EVA/PMMA formulations compared to those of the formulation components

4.3.4. Particle size distribution (PSD)

Figure 4.5 shows the particle size distribution of the PMMA powder. The D_{10}, D_{50} and D_{90} particle sizes were 43.2, 82.0 and 141 µm respectively. From Figure 4.5, the insert on the graph shows the SEM micrograph of PMMA. As it can be seen in Figure 4.5, it can be observed that PMMA is composed of spherical beads spread on its matrix.

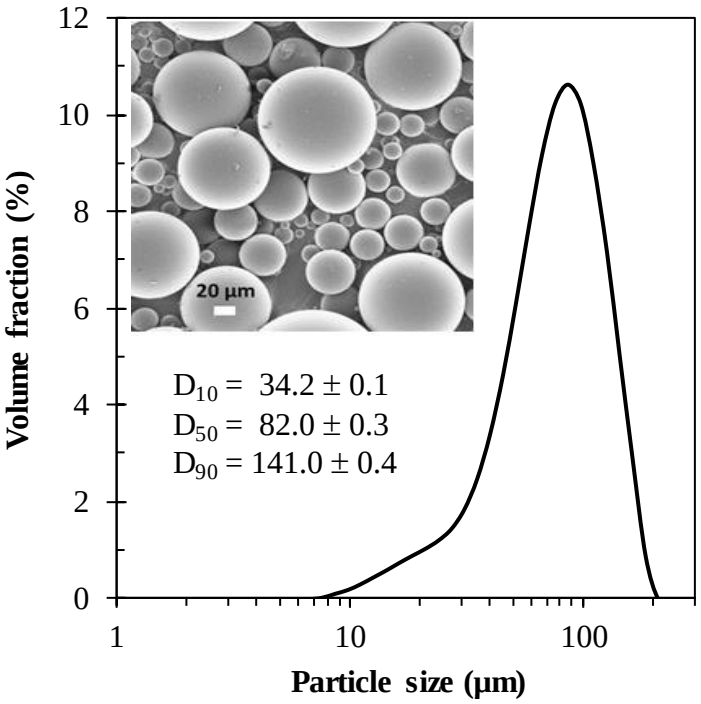

Figure 4.5: PMMA particle size distribution. The insert shows a SEM micrograph of the PMMA

4.3.5. Three-point bending

Figure 4.6 (a) and (b), Figure 4.7 and Figure 4.8 shows typical load versus deflection curves for the wax and wax/EVA/PMMA blends. Table 4.2 report on the mechanical properties of the wax and the formulated blends. The neat wax is very brittle with an average strain at break of just 1.7 ± 0.5 %. Most samples showed similar brittle failure behaviour with an abrupt fracture observed

when the maximum load is reached. Adding the PMMA filler increases the modulus but reduces the strain at break. Addition of EVA clearly inproves the bending strength in addition to increasing the deformation at break. Samples containing 30 wt-% EVA even failed in a ductile fashion. This is exemplified by the behavior of the 30/30/40 wax/EVA/PMMA blend shown in Figure 4.6. The highest bending strength (σ_B = 7.1 MPa) was obtained with the 40/30/30 wax/EVA/PMMA blend.

Table 4.2: Three-point bending results and needle penetration results

Wax	EVA	PMMA	Stress (MPa)	Strain (%)	Modulus (MPa)	Penetration* (μm)
100	0	0	1.3±0.1	1.7±0.5	38±20	327
30	20	50	4.4±1.0	3.8±1.2	255±44	54
30	30	40	5.0±1.1	5.8±0.8	209±34	85
40	10	50	4.9±0.8	1.4±0.3	624±96	69
40	20	40	5.7±0.3	7.2±0.6	225±21	50
40	30	30	7.1±0.7	6.6±1.6	290±57	90
50	10	40	2.8±0.1	1.5±0.3	369±95	245
50	20	30	3.9±0.1	1.3±0.1	416±88	65

*Needle penetration test. Depth measured after application of a final force of 1 N for 2 min.

Table 1V (a) – (c) gives the results of first a parametric analysis of variance (ANOVA) statistical analysis of the three-point bending results of wax/EVA/PMMA blends. supplementary material (see Appendix IV). This was performed to detect significant factors that might have an influence on the mechanical properties of the extruded wax/EVA/PMMA blends. The important conclusions

of the statistical analysis were that, at the 95% level of confidence, wax, EVA, and PMMA had significant effect on the mechanical properties of the blends.

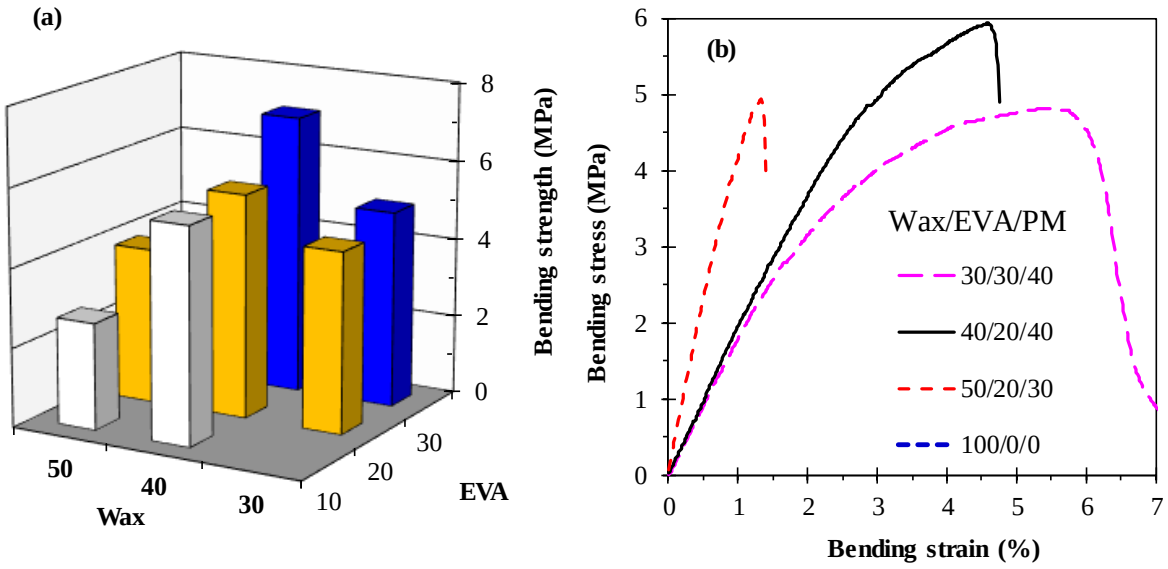

Figure 4.6: (a) Effect of varying wax and EVA on the bending stress properties obtained from three-point bending test; (b) Typical stress- strain curve

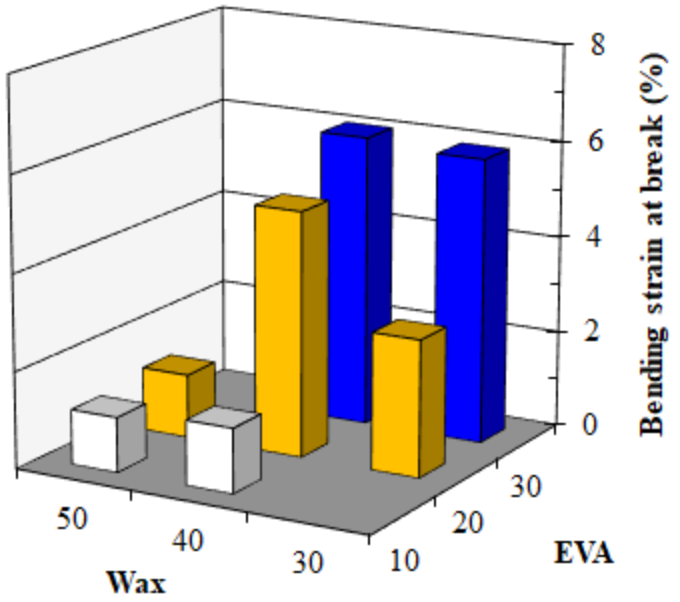

Figure 4.7: Bending strain at break properties obtained from three-point bending test

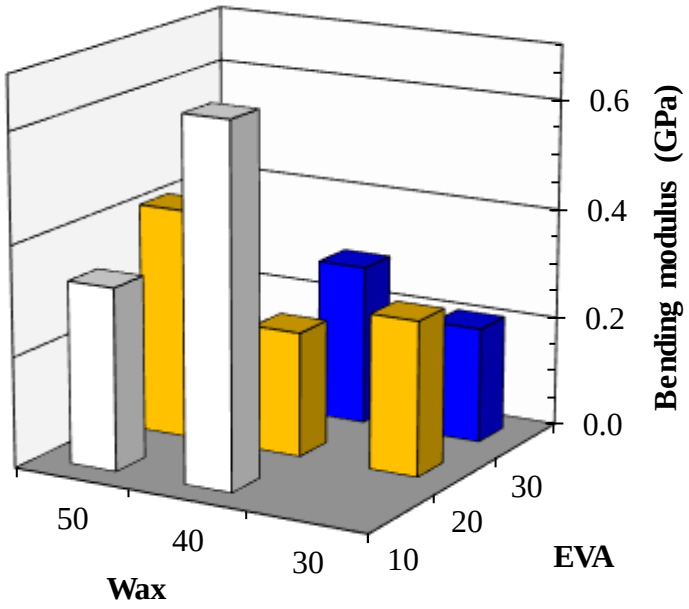

Figure 4.8: Bending modulus properties obtained from three-point bending test

4.3.6. Thermomechanical analysis (TMA)

Figure 4.9 shows representative force-time penetration curves recorded for the wax, the EVA and selected wax blends. The needle easily penetrated the neat wax but there was more resistance from the neat EVA. Note that, for very low applied forces, the needle penetrates but, eventually, its advance is arrested. When larger forced are applied, the needle penetration continues during the full 2 min testing interval but the rate of penetration decreases over time. This is exemplified for the curve obtained with the neat wax. The needle penetration was significantly less for the wax blends and this is attributable to the presence of the rigid PMMA filler particles.

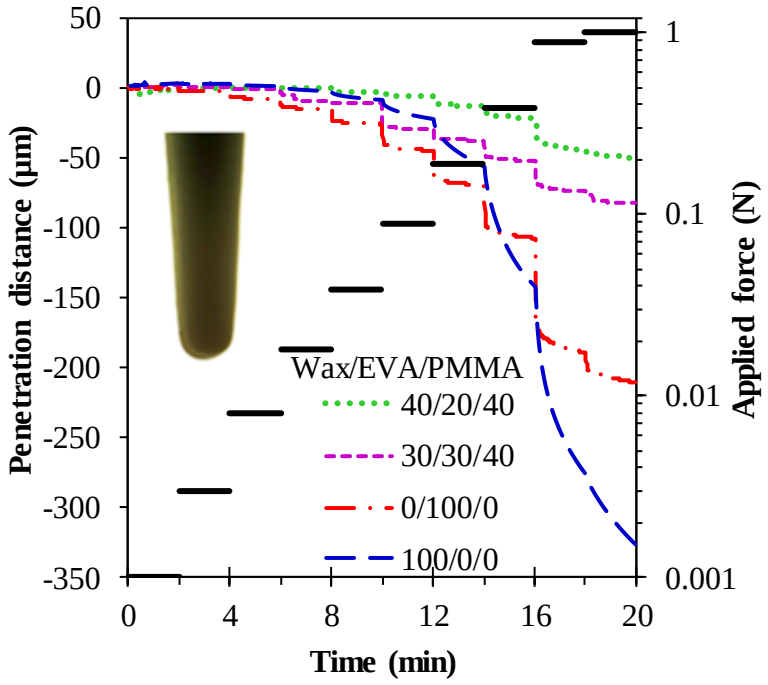

Figure 4.9: Needle penetration curves showing the time sequencing of the applied force and the response obtained with selected wax/EVA/PMMA blends. The inset shows the needle profile.

4.3.7. Rheology

Figure 4.10 summarizes the effect of blend composition on the melt viscosity measured at 90 °C. The melt viscosity increases as the EVA and/or the PMMA content is increased. The effect of the composition of the melt and the filler content of the viscosity can be considered separately. Figure 4.11 shows the variation of the viscosity measured at 90 °C for (a) binary blends of wax with EVA, and (b) the effect of adding the spherical PMMA filler to such blends. The viscosity of the blends follows a form of the composition dependence proposed by Arrhenius (Arrhenius, 1887) as modified by (Grunberg and Nissan, 1949):

$$\eta_{mix} = \exp\left(w_{wax} ln\,\eta_{wax} + 2\,w_{wax} w_{EVA} ln\,\eta_{Int} + w_{EVA} ln\,\eta_{EVA}\right) \quad (4.1)$$

Where η_{mix} is the viscosity of the binary mixture, and w_{wax} and w_{EVA} are the mass fractions of the wax and EVA respectively.

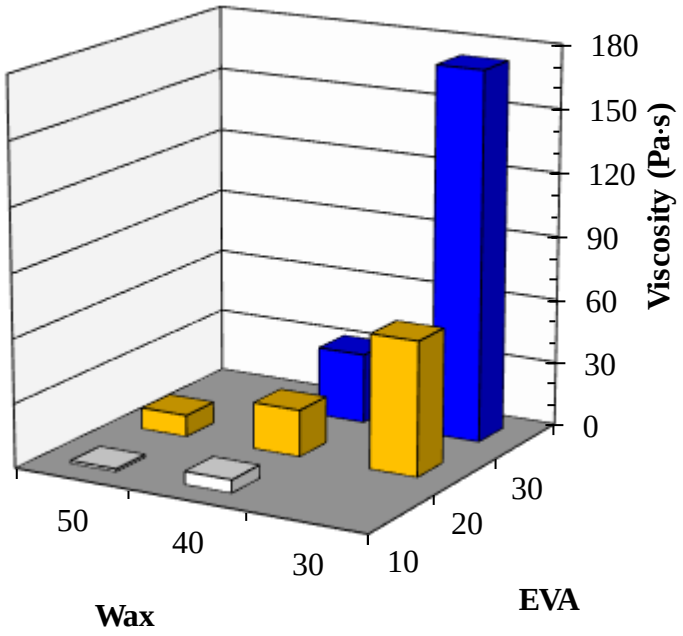

Figure 4.10: Viscosity of the wax blends measured at 90 °C

The parameters η_{wax} and η_{EVA} represent the viscosities of the neat wax and EVA respectively. The η_{Int} is an interaction term. It and η_{EVA} were treated as adjustable parameters as it was not possible to accurately measure the viscosity of the EVA with the equipment available as it is not sufficiently fluid at 90 °C. Least squares regression yielded and $ln\,\eta_{Int}$ = –5.944 and $ln\,\eta_{EVA}$ = 16.98 on setting $ln\,\eta_{wax}$ = -2.615. The solid line in Figure 4.14 shows the trend predicted by equation (4.1) with these values for the parameters.

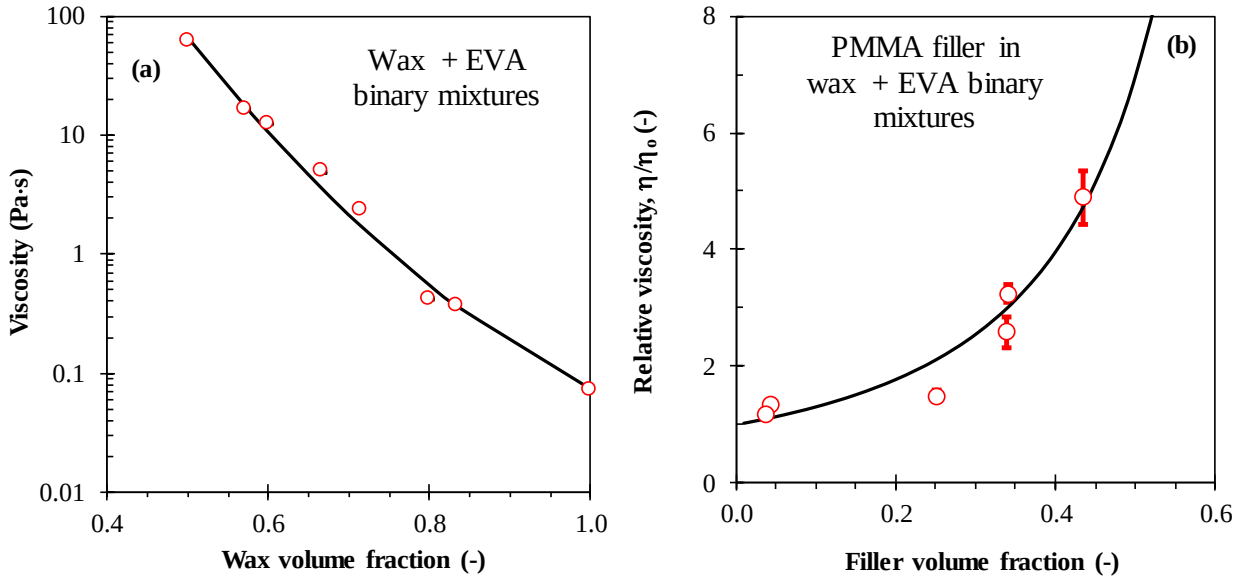

Figure 4.11: Viscosity of (a) unfilled, and (b) PMMA filled wax/EVA binary mixtures measured at 90 °C at a shear rate of 10 s^{-1}.The solid line in (a) represents the predictions of the Grunberg and Nissan (1949) model, equation (1) in the text. The line in (b) represents the predictions of the Krieger-Dougherty mechanistic model (Krieger, 1972), equation (2) in the text, with φ_{max} = 0.81.

The presence of solid filler particles in a liquid melt increases the apparent viscosity. The modified Krieger and Dougherty expression (Krieger, 1972) is a practically useful mechanistic model for the viscosity of a suspension of non-interacting particles suspended in a Newtonian liquid (Focke *et al*., 2009):

$$\frac{\eta}{\eta_o} = \left(1 - \frac{\varphi}{\varphi_{max}}\right)^{-2.5k\varphi_{max}} \qquad (4.2)$$

Here η and η_o represent the viscosity of the suspension and that of the pure fluid respectively; k is a particle shape factor that assumes the value unity for a suspension of spheres (Focke *et al*., 2009);

φ is the volume fraction of suspended particles; φ_{max} is the maximum attainable volume fraction of suspended particles. At this level, an abrupt transition to elastic solid-like behaviour is observed (Jones *et al*., 1991). Figure 4.11 indicates fair agreement of the experimental results with the predictions of equation (2) with $\varphi_{max} = 0.81$.

4.3.8. Scanning electron microscopy (SEM)

The SEM micrograph of wax/EVA/PMMA as shown in in Figure 4.12 also reveals a near perfect spherical nature for the filler particles. Figure 4.12 shows the fracture surface of the 40/20/40 wax/EVA/PMMA blend. It shows that the filler was well distributed in the wax/EVA matrix. It appears that the PMMA particles were only weakly bonded to the matrix material. The black striations were a feature observed in all the wax blends. It is speculated that they represent a dispersed EVA-rich phase in the matrix.

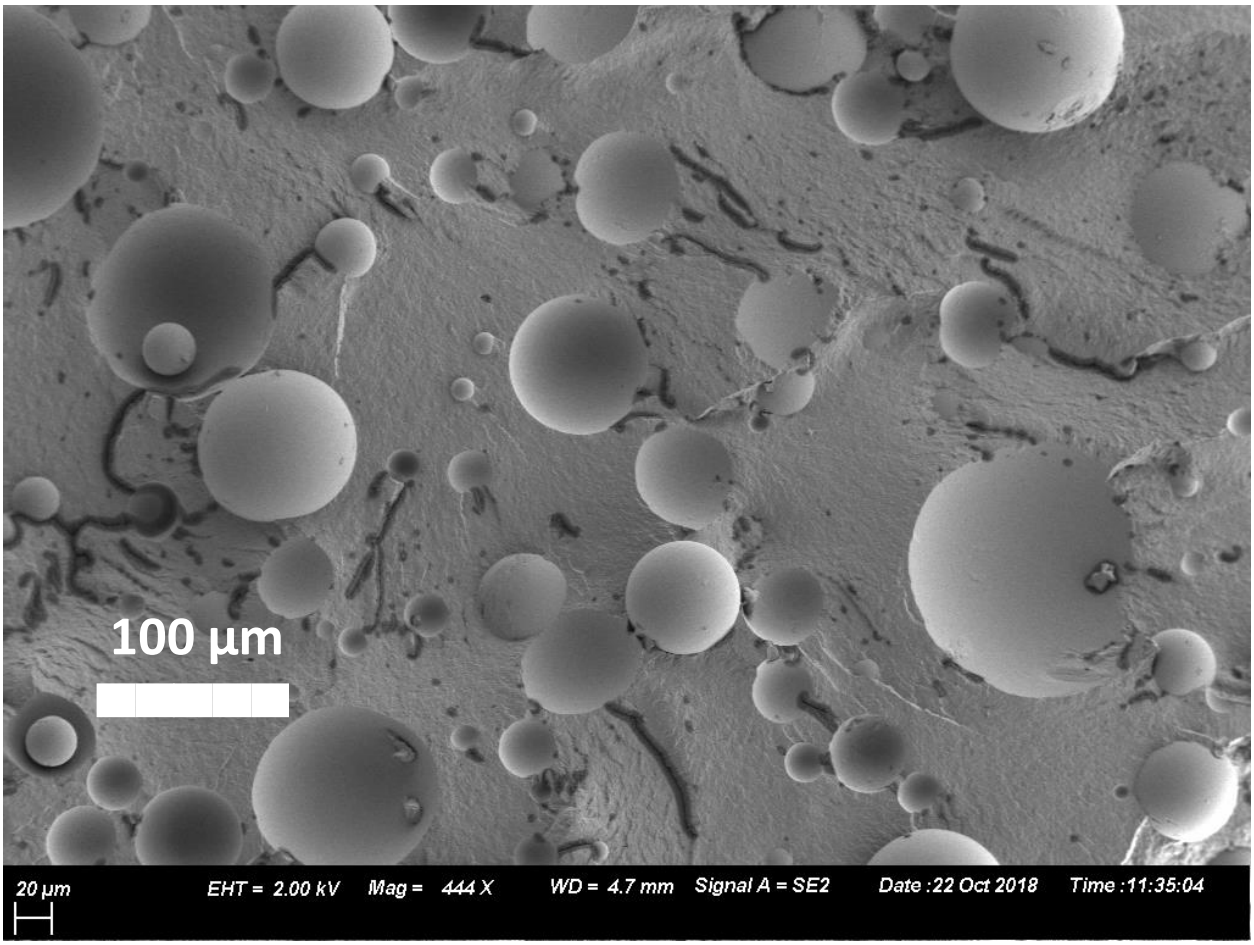

Figure 4.12: SEM micrograph of the fracture surface of the 40/30/40 wax/EVA/PMMA blend.

4.4. CONCLUSION

Modified paraffin wax, fortified by blending with poly (ethylene-co-vinyl acetate) (EVA) and filled with PMMA microbeads, holds promise as investment casting pattern material. A 40/20/40 wt-% wax/EVA/PMMA blend showed a good balance of properties. Compared to the neat wax, it offered significantly improved flexural strength (5.7 ± 0.3 vs. 1.3 ± 0.1 MPa), greater strain at break (7.2 ± 0.6 vs. 1.7 ± 0.5 %) and increased needle penetration hardness at the cost of an

increased melt viscosity. On pyrolysis above 500 °C, this blend volatilizes leaving almost no residue

Chapter 5 : THERMAL, MECHANICAL, SURFACE AND RHEOLOGICAL CHARACTERIZATION OF WAX/LLDPE/PMMA FORMULATION.

ABSTRACT

The thermal and mechanical properties of paraffin wax, linear low-density polyethylene (LLDPE) and poly (methyl methacrylate) (PMMA) microbeads formulations were prepared via extrusion process. The blends were characterized by thermogravimetric analysis (TGA), differential scanning calorimetry (DSC) and its tensile properties (stress at break, strain at break and modulus of elasticity). The results indicated that both LLDPE and PMMA had an influence on the thermal properties and the tensile properties of the blends. The TGA analysis showed that the thermal stabilities of the developed polymer increased and also at temperatures above 600 °C, there was no residue. DSC curves of the blends indicated two main exothermic peaks at 60 °C and 120 °C. This could be probably due to the wax structure and the LLDPE peak structure. DSC curves further suggested that the compatibility of the paraffin wax/LLDPE two phases increased with an increase in the filler content. The bending stress at break and the Young's modulus increased with increasing LLDPE content whereas the PMMA beads increased modulus there was no gradual strain increment. Both LLDPE and PMMA increased the melt viscosity of the wax composition. The Krieger Dougherty function (K-D) revealed that the experimental results agrees with the correlation for the of volume fractions tested.

Key words: Investment casting pattern, paraffin wax, LLDPE, PMMA, thermal stability, tensile testing

5.1. INTRODUCTION

For the past few decades, the use of polymer blends for many industrial applications such as pattern material for investment casting has been popular (Borah, 2013). In the investment casting industries, modification of wax properties has been done by blending wax with other materials such as polymers, fillers and resins in order to develop a wax pattern which can have the functional properties for complex patterns (Rutto & Focke, 2009; Tewo *et al*., 2018).

Polyolefins are generally characterized by good processability, high flexibility, dimensional stability and excellent resistance to acids, bases and alcohols (Micic *et al*., 1996; Chen & Wolcott, 2013). Linear low density polyethylene is characterized by low-temperature properties which is a crucial functional property in investment casting process, heat tolerance and better tensile strength as compared to low density polyethylene (LDPE) (Micic *et al*., 1996; Kim & Lee, 2017). Paraffin waxes (Fischer–Tropsch synthesis) aliphatic hydrocarbons are characterized by straight or branched carbon chains (Mpanza & Luyt, 2006; Krupa *et al*., 2014). Some of the properties associated with paraffin wax include: (a) smooth texture; (b) water repellency; (d) good dielectric properties and (e) low toxicity levels (Lewis, 2007).

Polymer blending depends largely depends the miscibility or immiscibility of the two components polymers. Immiscibility of polymers allows to keep the good features of each of the base polymer components of the blend (Mpanza & Luyt, 2006). An example of the feature improved by immiscible polymers is the impact test. Blending paraffin wax with polyethylene such as LLDPE duces a polymer blend with valuable properties such as good processability, low cost and light weight which gives the right compromise of the properties of the finished products (Kim & Lee, 2017). Several researchers have conducted lots of studies on the preparation of paraffin wax and polyethylene-based polymer blends via extrusion, injection molding, mechanical mixing and melt-

mixing methods. Krupa & Luyt (2001b) studied how the effects of blending LLDPE with oxidized wax affects its physical properties. The authors concluded that the stability of wax is improved by blending it with LLDPE. Hato & Luyt (2006) researched on blending different types of polyethylene's and waxes together. The authors concluded that the miscibility of polyethylene and wax depends on the co-crystallization of the individual polymers. Mhike *et al.* (2012) investigated the melt blending of wax, LDPE and graphite to develop a phase change material. The authors found out that graphite had a huge influence on the thermal conductivity of the blend. Chen & Wolcott (2013) researched on the crystallization and co-crystallization behavior of polyethylene and paraffin wax blends. The authors summarized that crystallization and co-crystallization depended largely on the blend concentrations.

The present study explores the utilization of a paraffin wax modified with linear low-density polyethylene and filled with poly (methyl methacrylate) (PMMA) as polymer-based blend for investment casting process pattern. Paraffin wax, LLDPE and PMMA were developed by the extrusion process. The produced blend was characterized in terms of its thermal properties, mechanical properties, surface morphology and the rheological properties.

5.2. MATERIALS AND METHODS

5.2.1 Materials

Hydrocarbon wax M3B (Congealing point = 62 °C, mean molecular mass = 785 $g \cdot mol^{-1}$, density 0.900 $g \cdot cm^{-3}$ at 25 °C) was obtained from Sasol Performance Chemicals. The linear low-density polyethylene (melting point = 70 °C, density 0.926 $g \cdot cm^{-3}$ at 25 °C and melt flow index (MFI) 50 g/10 min@190 °C, 2.16 kg) was supplied by Sabric, SA Pty. Advanced Polymers supplied PMMA microbeads. All the materials were used as received.

5.2.2 Method

The experimental design used for the wax/LLDPE/PMMA formulations followed Figure 3.1. Wax, LLDPE and PMMA weight ratios were weighed out into a container, sealed and thoroughly mixed. The formulations were compounded using a TX28P 28 mm co-rotating twin-screw extruder with an L/D ratio of 18. The screw design comprised intermeshing kneader elements with a forward transport action. The temperature profile used for processing of the wax/LLDPE/PMMA formulations from hopper to die was 65/120/150/160 °C. The melt was extruded directly into a water bath.

5.2.3 Characterization techniques

5.2.3.1. Thermal studies

Thermal behaviour of the blends was studied by thermogravimetric analysis (TGA) and differential scanning calorimetry (DSC). TGA was carried out using a TA Instruments SDT Q 600 TGA analyser. The sample weighing ca. 8 ± 2 mg were placed in a 70 µL alumina pan and scanned from 25 to 900 °C at a scan rate of 10 $K \cdot min^{-1}$ under a nitrogen atmosphere at a flow rate of 50 $mL \cdot min^{-1}$. DSC was carried out using a Perkin Elmer DSC 4000 analyser. Sample masses weighing 15 ± 2 mg were placed in sealed aluminium pans and heated at 20 $K \cdot min^{-1}$ from at 20 °C and 200 °C, held at this temperature for one minute and then cooled back to 20 °C at the same rate. The reported response curves correspond to data obtained during the second heating-cooling cycle.

5.2.3.2. Fourier transform infrared (FTIR)

FTIR spectroscopic analyses of the extruded wax/LLDPE/PMMA formulations were conducted in ATR mode using a Perkin Elmer spectrum 100 FTIR spectrometer fitted with an ATR cell. The spectra represent the average of 16 scans obtained at a resolution of 4 cm^{-1} over the wavenumber range 4000 - 600 cm^{-1}.

5.2.3.3. Thermomechanical analysis (TMA)

Needle penetration tests were conducted to determine the hardness of wax/LLDPE/PMMA formulations (Nebykov *et al*., 1985). The penetration measurements were conducted at 30 °C on a TA Instruments Q400 Thermo Mechanical Analyzer fitted with a needle with a tip radius of 1.4 mm. A wax/LLDPE/PMMA sample was cast in a 90 µL alumina pan. The test protocol was as follows. At the start, the applied force was set at 0.001 N. Thereafter it was increased after two-minute intervals using the following successive force increments: 0.002, 0.005, 0.01, 0.02, 0.05, 0.1, 0.2 and 0.5 N. Lastly, the force was increased to 1 N and applied for a further two minutes after which the final needle penetration was recorded. During the experiment, the penetration depth of the needle was tracked as a function of time.

5.2.3.4. Three-point bending tests

The mechanical properties of the extruded wax/LLDPE/PMMA blends were assessed using three-point flexural testing, executed according to ASTM 790. The testing was performed on an Instron 5564 twin column tensile tester fitted with a 5 kN load cell at room temperature. The mould used for the specimen preparation was also fabricated using silicon according to ASTM 790. Test bars for three-point bending (10 x 10 x 80 mm) were cast from the melt using a silicone rubber (Appendix I). The crosshead speed was set at 1.8 $mm \cdot min^{-1}$ and the sample support span was 64 mm. An average of five specimens were taken in reporting the yield stress and strain at break.

5.2.3.5. Rheology

The rheological properties of the blends were investigated using an Anton Paar MCR301 rheometer at a shear rate of 1 s^{-1}. All the rheological experiments were performed in oscillation mode in the parallel plate geometry with a plate diameter of 25 mm ϕ spindle. The temperature was controlled at 125 °C. All the measurements were done under a nitrogen blanket in order to avoid thermal oxidation.

5.2.3.6. Morphological studies

The surface morphology of wax/LLDPE/PMMA formulations were observed using Zeiss Ultra PLUS FESEM (high resolution micrograph) scanning electron microscope. The wax/LLDPE/PMMA blends fractured at liquid-nitrogen temperature and were placed on a double-sided tape fixed on a metallic plate and then coated with a thin layer (50 Å thickness) of gold powder sputter module in a vacuum evaporator in an argon atmosphere.

5.3. RESULTS AND DISCUSSION

5.3.1. Thermogravimetric analysis (TGA)

TGA and DTG curves were used to determine the thermal stability of wax, LLDPE, PMMA and wax/LLDPE/PMMA blends. Figure 5.1 (a) and (b) shows the TGA and DTG curves of wax, LLDPE, PMMA and wax/LLDPE/PMMA blends respectively. As it can be seen in Figure 5.1 (a), LLDPE is more thermally stable than both wax and PMMA and its degradation occurred in one step at a temperature of about 360 °C to 530 °C. This can be attributed to the decomposition of C-C bonds present in the main LLDPE chain. Wax has two distinct degradation peaks at around 210 °C and 396 °C associated with concurrent evaporation and thermal degradation events. The DTG

curve as shown in Figure 5.1 (b) for the wax suggests that the apparent mass loss occurred, for the most part, as a one-step process. The blends had three peaks associated with the peaks of the individual components incorporated. PMMA has three distinct degradation peaks. In the case of wax, the peaks could be attributed to the melting of hydrocarbons whereas in the case of PMMA, the first degradation step at a temperature of around 150 °C can be ascribed to the degradation of weak head to head bonds. The second degradation peak at around 230 – 300 °C can be attributed to degradation of unsaturated chains of PMMA and the third degradation peak at around 320 °C can be related to random scission of polymer chains (Valandro *et al*., 2014). The wax/LLDPE/PMMA blends showed three degradation peaks corresponding to wax, LLDPE and PMMA phases.

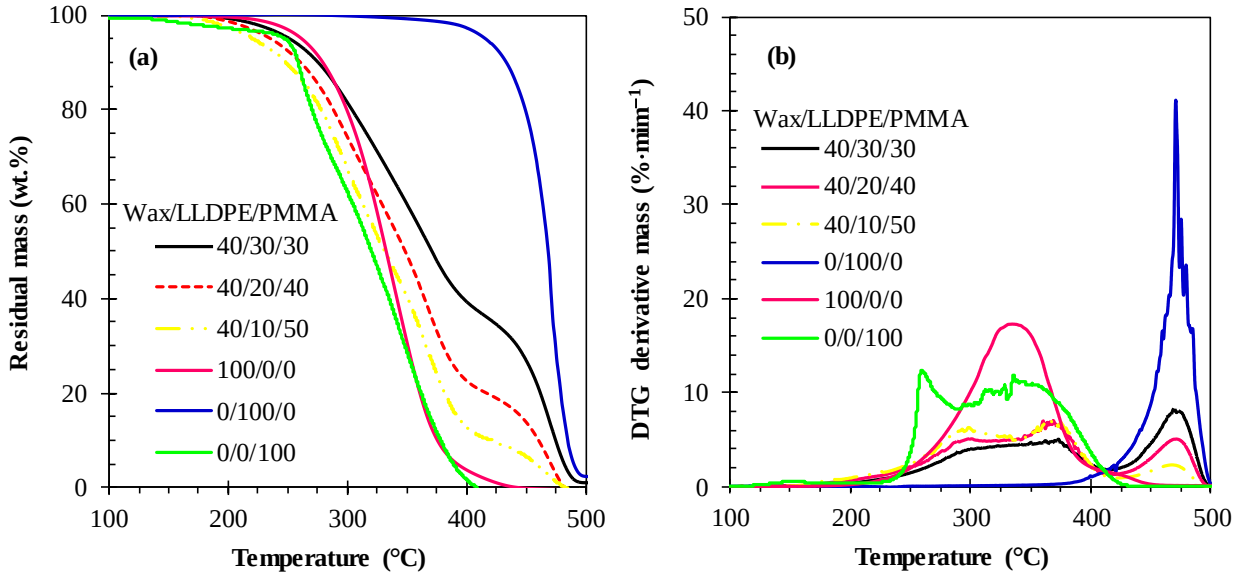

Figure 5.1: (a)TGA curve and (b) DTG curve for the wax, LLDPE, PMMA and 40/20/40, 40/30/30 and 40/10/50 wax/ LLDPE/ PMMA blend.

5.3.2. Differential scanning calorimetry (DSC)

Figure 5.2 (a) and (b) shows the DSC curves of wax, LLDPE and wax/LLDPE/PMMA during heating and cooling respectively.

Table 5.***1*** shows the melting onset temperatures, crystallisation onset temperature and enthalpies of melting and crystallization. The blends have two melting and crystallization peaks in the range of 50 -70 °C and 105 -120 °C. As it can be seen in Figure 5.2 (a), wax has a sharp distinct main peak at a temperature of 60 °C which represents the solid–liquid phase change of the wax. The minor peak at a temperature of 38 °C corresponds to the solid–solid phase transition of wax. (Rao & Zhang, 2011; Mhike *et al*., 2012) reported similar peaks match of pure paraffin wax. During cooling, a broad crystallization peak was observed. LLDPE has one endothermic peak at a temperature around 125 °C as it can be seen in Figure 5.2 (a). This can be associated with the melting of the LLDPE matrix. During cooling as shown in Figure 5.2 (b), LLDPE has a main exothermic peak at around 105 °C. This peak corresponds to the crystallization of LLDPE chains. In the case of heating and cooling of wax/LLDE/PMMA blends as shown in Figure 5.2 (a) and (b), the melting and solidification temperatures did not change significantly, There was also a small shift in the melting and solidification points and thus can be attributed to co-crystallization of the lower molecular weight fractions of the LLDPE with wax. The specific enthalpies reduced to a great margin.

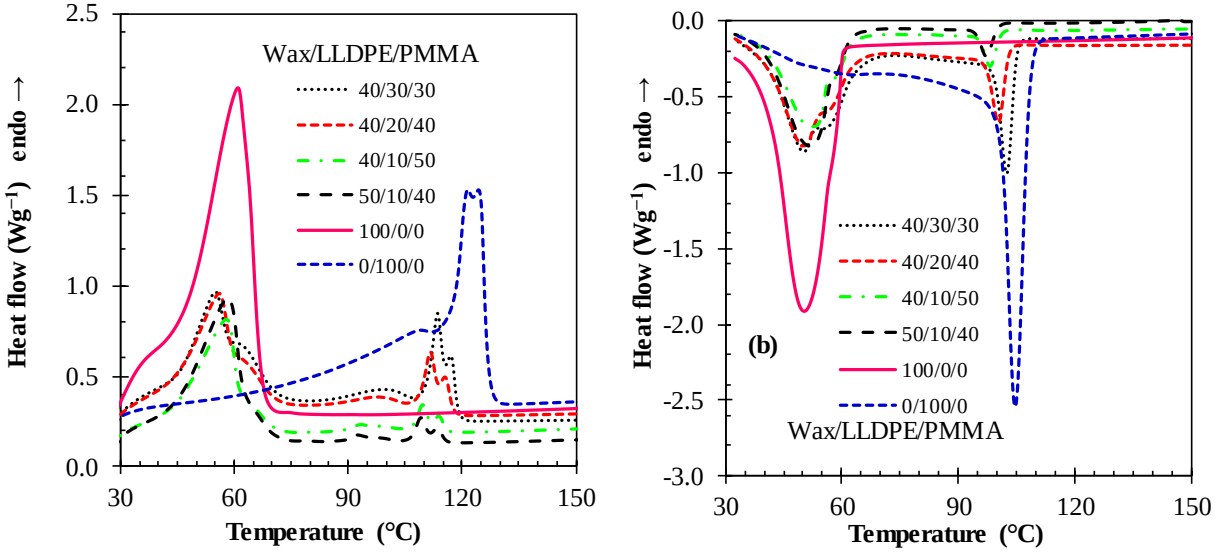

Figure 5.2: (a) DSC heating and (b) DSC cooling curves obtained for the wax, LLDPE, PMMA and the 50/10/40 wax/ LLDPE/ PMMA blend.

Table 5.1: DSC parameters obtained for the wax, LLDPE and wax/LLDPE/PMMA blend

Sample Wax/LLDPE/PMMA	T_{om} (°C)	T_{oc} (°C)	T_{pm} (°C)	T_{pc} (°C)	$\Delta H_{(pm)}$ (J/g)	$\Delta H_{(pc)}$ (J/g)
100/0	42.74	60.22	60.98	50.26	195.20	-156.62
0/100	109.12	119.32	115.97	113.97	56.24	-96.36
40/30/30	43.35	58.94	55.22	50.21	56.872	-66.651
	110.63	105.04	113.58	102.45	15.590	-28.861
40/20/40	42.67	58.31	56.18	49.77	55.722	-65.893
	108.81	103.01	111.74	100.43	9.566	-11.041
50/20/30	44.05	58.60	56.87	51.18	66.912	-73.983
	108.19	102.22	110.95	99.72	9.542	-10.461
30/30/40	42.55	64.86	53.74	48.80	32.755	-42.379
	111.72	105.19	114.72	102.63	12.717	-17.082
30/20/50	42.75	58.95	55.10	49.69	34.668	-42.253
	109.40	103.70	112.45	101.05	8.688	-11.020
40/10/50	43.47	57.90	58.04	52.49	47.882	-57.528
	107.20	100.91	109.63	98.20	3.857	-4.794
50/10/40	43.82	59.09	58.33	52.03	65.611	-68.397
	106.59	100.17	109.14	97.35	11.239	-4.391

5.3.3. Fourier transform infrared (FTIR)

Figure 5.3 shows the FTIR absorbance spectra of wax, LLDPE, PMMA and wax/LLDPE/PMMA formulations. Wax has C- H stretching vibrations of saturated hydrocarbons at 2947 cm^{-1} and -CH_3 and C-H deformations observed at around 1460 cm^{-1} and 1380 cm^{-1}. Also, at 720cm^{-1} rocking and wagging clear peak of -CH_2- is observed as it can be seen in Figure 5.3. In the case of LLDPE, the first peak was observed at 2850–2920 cm^{-1} due to C-H stretching, another peak at 1472 cm^{-1} caused by C-H bending, another peak at1366 cm^{-1} caused by C-H bending and at 720 cm^{-1} attributed to C-H rocking. PMMA spectra featured similar bands to LLDPE spectra except a distinct and additional peak at 1736 cm^{-1} and 1717 cm^{-1} due to the ester carbonyl C=O stretching bands. Close review of wax/LLDPE/PMMA blend spectra shows absence of strong molecular interactions wax, LLDPE and wax species. With this development, a physical wax/LLDPE PMMA blend formed since in all the wax/LLDPE formulation, a weak peak at a wavelength of around 1730 cm^{-1} can be observed and this can be due to the incorporation of PMMA into the blend.

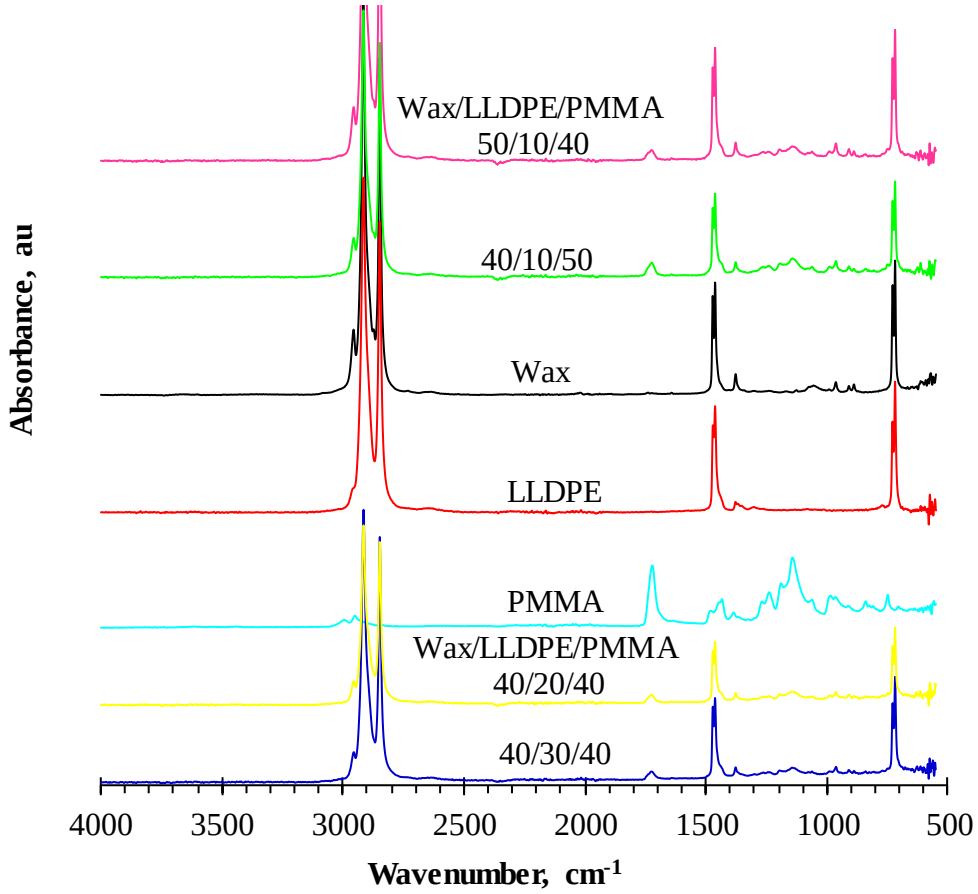

Figure 5.3: FTIR absorbance spectrum for the wax, LLDPE, PMMA and wax/LLDPE/PMMA formulations

5.3.4. Thermomechanical analysis (TMA)

Figure 5.4 shows the TMA needle penetration of wax, LLDPE and sample formulation of wax/LLDPE/PMMA blends. As it can be seen in Figure 5.4, the needle easily penetrated in neat wax but there was some resistance from the neat LLDPE. It can also be seen that when the force applied is increased, the needle penetration continues during the full 2 min testing interval but the rate of penetration decreases over time. The blends have more resistance than both neat wax and LLDPE as it can be seen in Appendix VI.

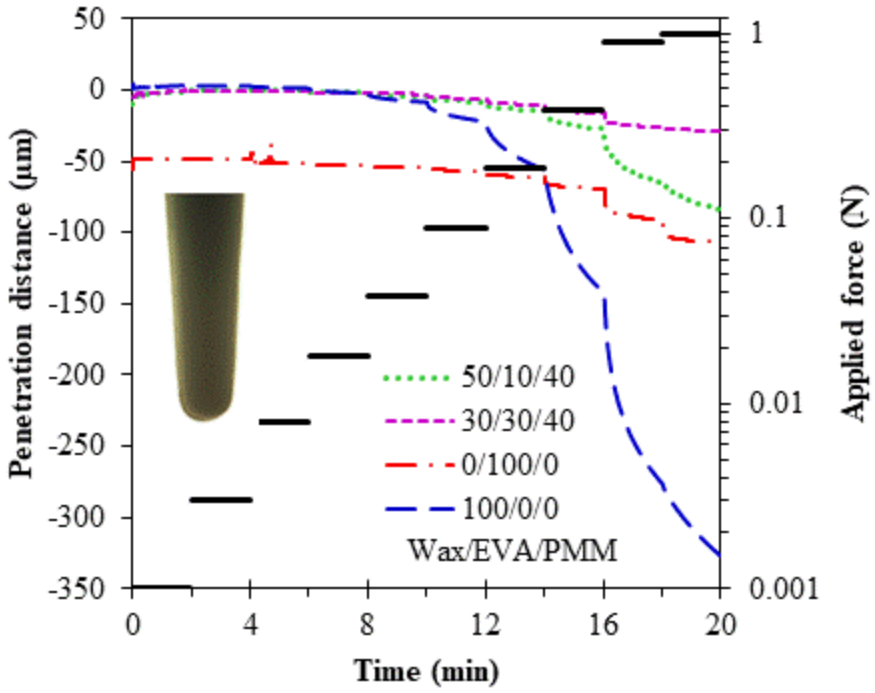

Figure 5.4: Needle penetration curves showing the time sequencing of the applied force and the response obtained with selected wax/LLDPE/PMMA blends. The inset shows the needle profile.

5.3.5. Three-point bending tests

Figure 5.5 (a) and (b), Figure 5.6, Figure 5.7 and Table 5.2 represent the bending strength, the bending strain at break and the Young modulus of elasticity for wax, wax/LLDPE/PMMA blends. As it can be observed in Table 5.2 and Figure 5.5 (a) and (b) the bending strength increased with an increase in LLDPE amount, whereas the stain at break decreased in all the formulations except the formulations with a higher LLDPE content. Wax/LLDPE/PMMA blends containing the highest amount of LLDPE (30% -weight) failed in a ductile faction when load was applied. This is exemplified by the behavior of the 30/30/40 and 40/30/30 wax/LLDPE/PMMA blend shown in Figure 5.5 (a). The highest bending strength (σ_B = 7.8 MPa) was obtained with the 30/40/30 wax/LLDPE/PMMA blend. The bending strength properties are mainly depending on polymer

crystallinity. Generally, interfacial adhesion between the polymer have a great influence on its mechanical properties. It can also be seen in Table 5.2 that as the ratio of wax in increased in the blend, there is a decrease in the strain. LLDPE is a bit branched, hence it has a lower bonding forces between chains and lower degree of crystallinity. The hardness of the blend was impoved by blending wax with LLDPE as it can be seen in Table 5.2.

Table 5.2: Three-point bending results

Wax	LLDPE	PMMA	Stress (MPa)	Strain (%)	Modulus (MPa)	Penetration (μm)
100	0	0	1.3±0.1	1.7±0.5	38±20	327
30	20	50	5.0±0.3	1.3±0.2	676±61	122
30	30	40	7.8±0.7	2.2±0.4	671±74	29
40	10	50	2.8±0.3	1.0±0.2	417±80	83
40	20	40	4.8±0.4	1.3±0.2	708±197	45
40	30	30	6.2±0.2	1.8±0.1	607±70	50
50	10	40	3.2±0.4	0.8±0.1	541±101	84
50	20	30	3.8±0.8	1.3±0.2	515±121	44

*Needle penetration test. Depth measured after application of a final force of 1 N for 2 min.

Table 1V (e) – (f) gives the results of first a parametric analysis of variance (ANOVA) statistical analysis of the three-point bending results of wax/LLDPE/PMMA blends. supplementary material (see Appendix IV). This was performed to detect significant factors that might have an influence on the mechanical properties of the extruded wax/LLDPE/PMMA blends. The important

conclusions of the statistical analysis were that, at the 95% level of confidence, wax, LLDPE, and PMMA had significant effect on the mechanical properties of the blends.

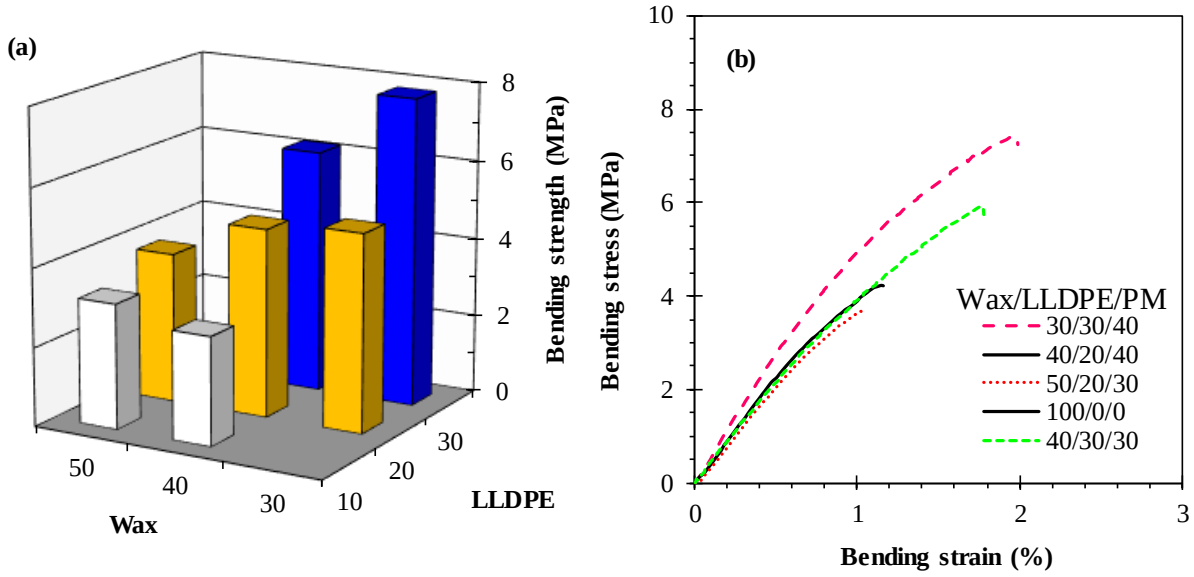

Figure 5.5: (a) Effect of varying wax and EVA on the bending stress properties obtained from three-point bending test; (b) Typical stress- strain curve

It can also be seen in Figure 5.6 that as the ratio of wax in increased in the blend, there is a decrease in the strain. This can be attributed to the branched nature of LLDPE, which is characterized by a lower bonding forces between chains and lower degree of crystallinity. An increase in wax and LLDPE could have led to a reduction in crystallinity of the blend which in turn affects the elongation at break of the wax/LLDPE/PMMA blends.

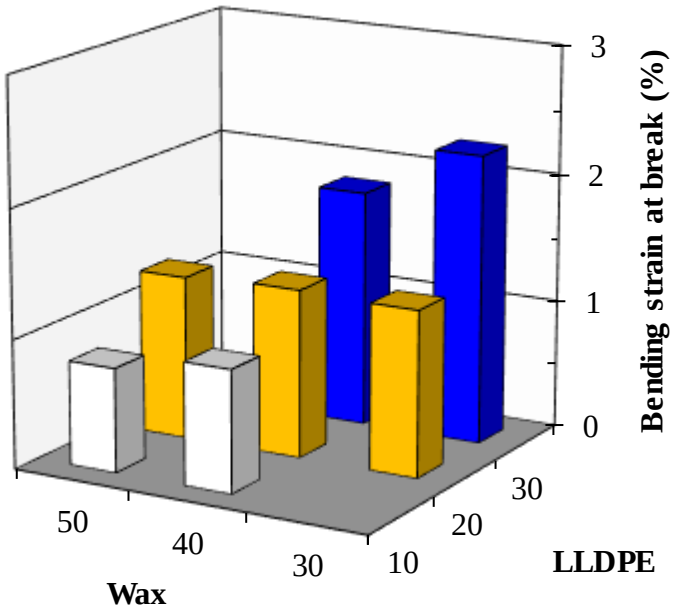

Figure 5.6: Bending strain at break properties obtained from three-point bending test

Further, as it can be seen in Figure 5.7, an increase in the percentage composition of LLDPE in the wax/LLDPE/PMMA blends was responsible for an enhancement of the elastic modulus and of a decrease in the strain at break. Studies by (Marsilla *et al*., 2016) indicated that fillers have an effect on the modulus of polymer blends due to polymer chain disruptions. The authors further concluded that the Young modulus is not affected by poor adhesion as in the case of tensile strength.

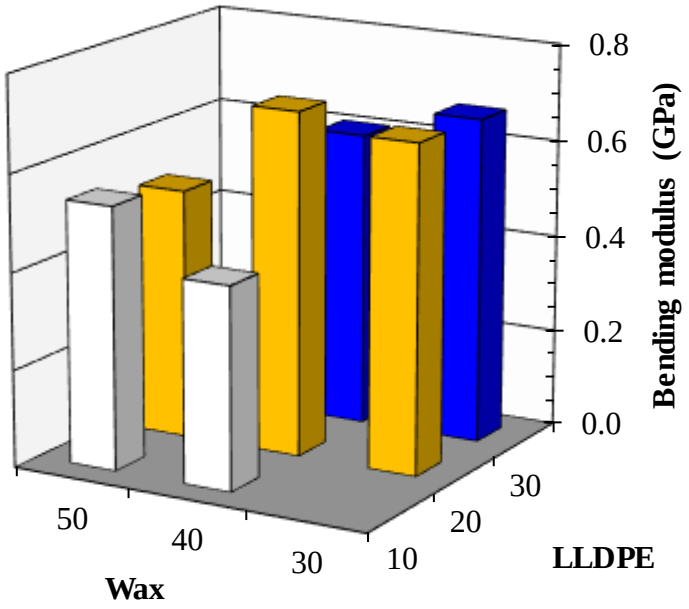

Figure 5.7: Bending modulus properties obtained from three-point bending test

5.3.6. Rheology

Figure 5.8 shows the variation of the viscosity measured at 125 °C for (a) binary blends of wax with EVA, and (b) the effect of adding the spherical PMMA filler to such blends. Figure 5.7 shows the viscosity of wax/LLDPE/PMMA blends with variation in wax and LLDPE content considered. As it can be seen in *Figure 5.8*, there is a gradual increase in the viscosity of the blends with as increase in the amount of LLDPE content. The viscosity of the blends follows a form of the composition dependence proposed by Arrhenius (Arrhenius, 1887) as modified by (Grunberg and Nissan, 1949) as shown in Equation 4.1 and the modified Krieger and Dougherty expression (Krieger, 1972) Equation 4.2 when a solid spherical material is incorporated into polymer blends.

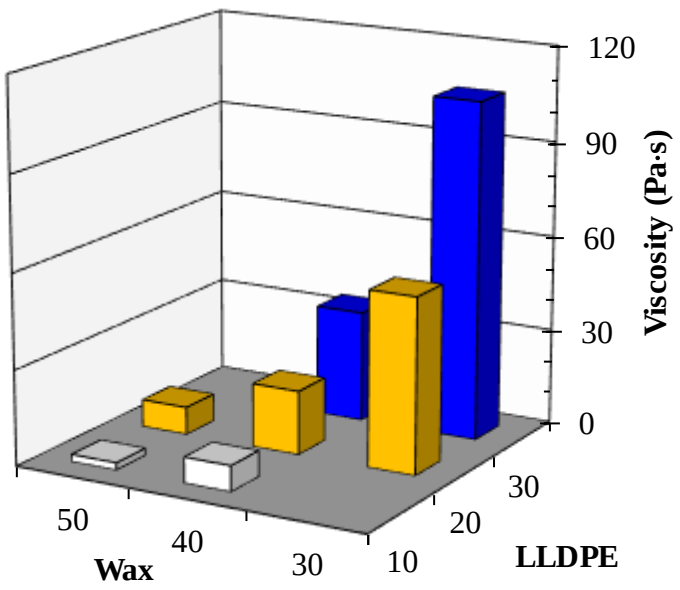

Figure 5.8: Viscosity of the wax/LLDPE blends measured at 125 °C

Figure 5.9 (a) and (b) shows the experimental wax/LLDPE data and fitted with Grunberg and Nissan model equation and the wax/LLDPE/PMMA experimental results fitted with Krieger-Dougherty mechanistic model respectively. As it can be seen in Figure 5.9 (b) PMMA particles incorporation into wax/LLDPE blends liquid melt increased its apparent viscosity. It can also be seen that the experimental results indicate fair agreement of the predicted results developed using equation (4.2) with φ_{max} = 0.74. Generally, when solid filler materials are added into polymer blends, the blend rheological properties are directly related to the degree of dispersion of the spherical filler material in the polymer blend matrix and the degree of interfacial interactions between the filler and polymer blends. It can be further stated that the increase in apparent viscosity can be attributed to the molecular mobility restriction and free volume reduction caused by the dispersion and interaction of the fillers in the polymer blend matrix. Similar observations were made by (Chafidz *et al*., 2014).

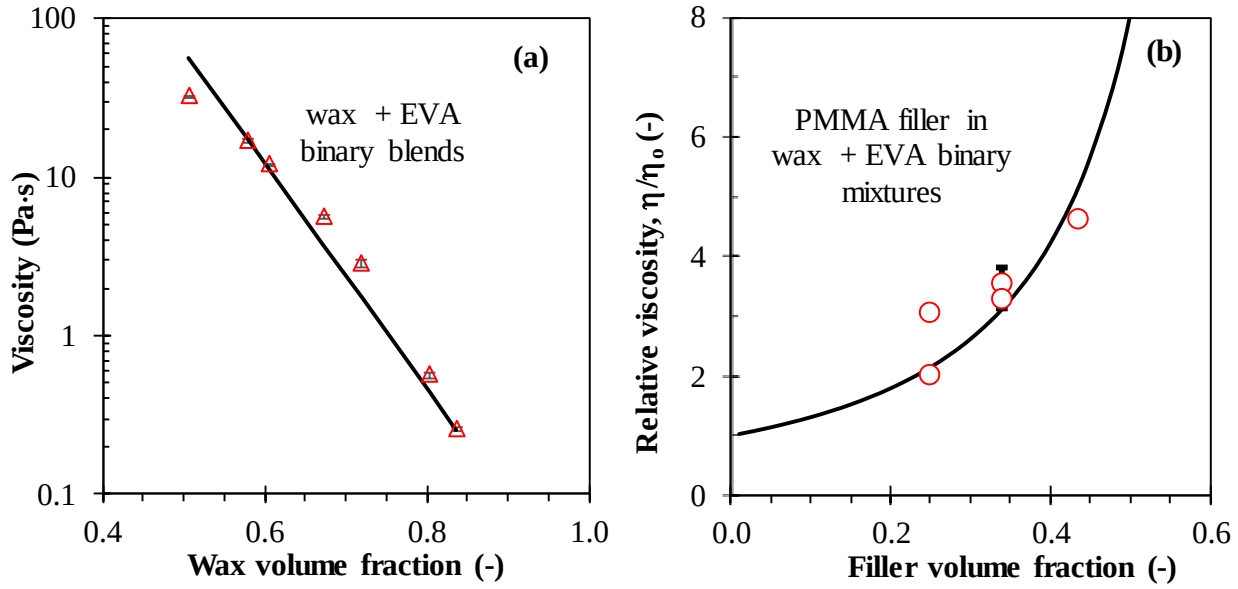

Figure 5.9: Viscosity of (a) unfilled, and (b) PMMA filled wax/LLDPE binary mixtures measured at 125 °C at a shear rate of 10 s^{-1}. The solid line in (a) represents the predictions of the Grunberg and Nissan (1949) model, equation (4.1) in the text. The line in (b) represents the predictions of the Krieger-Dougherty mechanistic model (Krieger, 1972), equation (4.2) in the text, with φ_{max} = 0.74.

5.3.7. Scanning electron microscopy (SEM)

Figure 5.10 shows the SEM spectra of wax/LLDPE/PMMA. The study on the surface phase morphology of wax/LLDPE/PPMA blends was investigated by SEM. Due to lack of strong structure interaction, it is expected that a two-phase morphology will be observed as it can be seen in Figure 5.10. As the filler content of the blend is increased, the size and complexity of the dispersed phase increases as expected also. As it can also be seen in Figure 5.10 (a), the PMMA

particles were evenly distributed in the wax/LLDPE matrix and no observable agglomeration was witnessed. Generally, solid fillers incorporated into a polymer blend matrix in most cases improves the interfacial adhesion between the two-phase polymers and also has a positive effect on the dispersed phase domain size. At low filler loading, as it can be seen in Figure 5.10 (a), the improvement in phase morphology of the wax/LLDPE blends can be attributed to filler particles interfacial activity and it can be also due to rheological behaviour change of the polymer blends during mixing process. At high filler loading as seen in Figure 5.10 (b), a coarser morphology was formed. High solid filler contents affect the interfacial adhesion between the polymer blends. Studies by (Paul & Tiwari, 2014; Valandro *et al*., 2014; Liu *et al*., 2018) had similar findings.

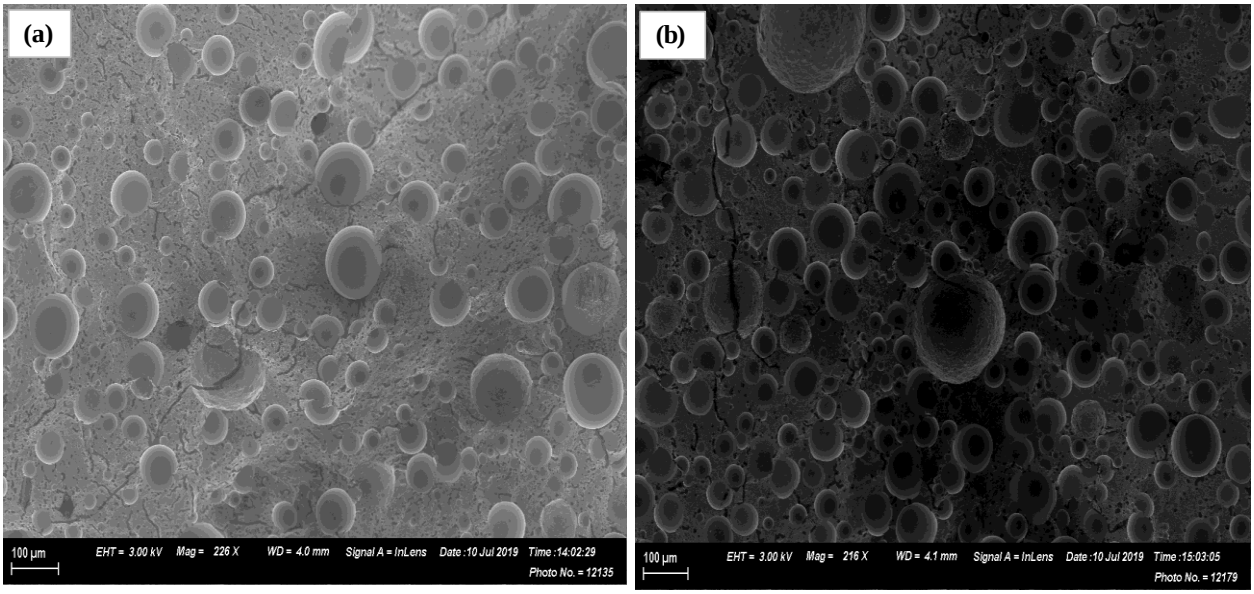

Figure 5.10: SEM pictures (a) wax/LLDPE/PMMA with low filler loading (b) wax/LLDPE/PMMA with high filler loading

5.4. CONCLUSION

In summary, the following conclusions were drawn:

1. LLDPE and PMMA incorporation into melt on wax has an influence in wax thermal properties. The TGA showed that thermal stability of paraffin wax was improved with blending with LLDPE and PMMA;
2. The DSC curves showed that multiple endothermic and exothermic peaks during heating and cooling were obtained. The first distinct peak is associated with the Fischer–Tropsch paraffin wax solid-solid transition as well as its melting and the second distinct peak was due to LLDPE lower content, miscibility of the blend can be possible;
3. Higher tensile strength and Young modulus was seen in the blends as compared to the neat paraffin wax. These are of great importance when determining the stiffness and allowable load in materials;
4. The melt rheology of the blends was higher than that of neat paraffin wax. This is caused by molecular mobility restriction due to the interaction of PMMA particles in the wax/LLDPE polymer blend matrix. Additionally, Krieger-Dougherty mechanistic model fitted with the experimental data was obtained;
5. Filler loadings has an effect on the refinement of the phase morphology of the wax/LLDPE polymer binary blend matrix.

Chapter 6 . CONCLUSIONS AND RECOMMENDATIONS

6.1. CONCLUSIONS

The broad objective of this work was to critically examine the development of an improved pattern material for investment casting process using EVA and LLDPE precursor materials and incorporating spherical PMMA as a filler material. PMMA was obtained as a waste material from an additive manufacturing plant. The literature review discussed the challenges associated with unfilled wax as a pattern material for investment casting process as well as the previous studies done on blending wax with other compounds to produce a functional pattern material which can be used for complex shapes produced by investment casting process. Limitations of the new patterns was also highlighted.

The capability of incorporating EVA, LLDPE and PMMA into wax to form strong polymer blend with good thermal stabilities was investigated. The polymer blends were produced by an extrusion-compounding process in which the polymer melt, containing PMMA as a filler material up to 50% weight loading was quenched in a water bath. Before compounding, it was ascertained that the PMMA filler could not be degraded when exposed to the high polymer blends processing temperatures of 160 °C in the case of LLDPE based polymer blends and 100 °C in the case of EVA based polymer blends. The TGA was used to understand the degradation behaviour of the developed polymer blends. The TGA curves gave an indication that wax is less thermally stable as compared to EVA, LLDPE and PMMA. The thermal stabilities of the blends improved with an increase in EVA, LLDPE and addition of PMMA. This can be probably attributed to the reduction in interaction between the wax and EVA or LLDPE chains due to reduced chain mobility hence slowing down the degradation process. DSC curves indicated that wax and EVA are homogeneous

at the macro scale level though there was a slight clear phase separation between wax and EVA at a higher EVA loading as it can be seen in the melting temperatures as well as the endotherms. With an increase in wax content, the T_{oc}, T_{om} slightly decreased. The specific enthalpies of melting in the blends increased with an increase in the wax content. The dispersion of wax in a polymer matrix depends on the wax loading and the molecular structure of the polymer blended with wax.

In the case of wax/LLDPE and wax/LLDPE/PMMA blends, the thermal stability of both blends decreased with increasing wax content. This can be attributed to the crystalline polymer blends being formed with less wax content. DSC curves shows that two peaks at around 112 °C and 120 °C were observed in the case of neat LLDPE. The first peak can be ascribed to distribution of the short chain branches along the main chains in the polymer. This is due to the short chains in LLDPE not being distributed equally along the main chains. In the case of wax/LLDPE and wax/LLDPE/PMMA blends, the first LLDPE melting point is slightly affected by wax incorporation. This can be attributed to the side chains of LLDPE co-crystallizing with wax. Generally, in polymer blends, the melting temperature depends on to the size and perfection of the crystalline regions of the polymers. The specific enthalpies of the blends are affected by wax purity which has an effect on the crystalline effect of the blend formed.

The mechanical properties of paraffin wax at ambient temperatures were found to be modified by the incorporation of EVA, LLDPE and PMMA. Addition of EVA and LLDPE into wax increased the tensile strength, Young modulus and strain though with LLDPE, there was no significant difference in the strain percent. EVA and LLDPE increased wax rigidity hence having an effect on the tensile strength of the polymer blend formed. This may be attributed to the low molecular weight of wax as compared to both EVA and LLDPE hence, it improves the stress cracking and weak points during deformation. The increase in Young modulus in both the blends can be due to

the high modulus of EVA and LLDPE as compared to that of wax hence increasing the modulus of the blends. Young's modulus generally depends on the transformation of energy between the amorphous and crystalline regions of the polymer blends. The hardness of the blends by TMA penetration technique was also improved by addition of EVA and LLDPE. The interaction between the CH_2 polymer chains in both the polymers improved the strength of the developed products.

Paraffin wax (Sasol fischer M3B) has a low viscosity. Blending wax with EVA and LLDPE increased the viscosity of the blend gradually. EVA and LLDPE increased the viscosity of wax. This may in turn have an effect on the processability of wax. The increase in the melt viscosity of wax/EVA and wax/LLDPE could be attributed to an increase in the interaction between the wax chains and the EVA and LLDPE long polymer chains. As the EVA and LLDPE mass loading increased in the binary polymer blends, the viscosity of the blend formed increased. This could be ascribed to the longer chains in EVA and LLDPE causing increased interlinking hence more resistance to flow is experienced. At higher EVA mass loading, a shear thinning behaviour was observed at lower shear rates. In the case of spherical filler material being incorporated into both wax/EVA and wax/LLDPE, solid loading in polymer blends brings the formation of a suspension. The presence of PMMA resulted in higher viscosity of both EVA and LLDPE wax based blends. Variation in spherical filler loading (high solid loading especially) has a pronounced effect on the viscosity of the binary blends. The increase in viscosity of the suspension is attributed to the existence of local structures in the wax/LLDPE and wax/EVA that bring about the immobilization of the media hence preventing it from taking part in the hydrodynamic flow. The use of modified Krieger-Dougherty mechanistic empirical models fitted with the rheology experimental results and the maximum packing factor for EVA based polymer blend was $\varphi_{max} = 0.74$ whereas in the case of LLDPE based polymer blend the maximum packing factor was $\varphi_{max} = 0.81$.

Scanning electron microscopy (SEM) of PMMA showed that complete smooth uniform microspheres with solid surface morphology was witnessed in its polymeric matrix. In the case of both wax/EVA/PMMA and wax/LLDPE/PMMA polymer blends, the PPMA microspheres were uniformly distributed in the polymer matrix though poor affinity was witnessed with high PMMA loading polymer blends which caused the PMMA to be weakly bonded to the wax/EVA and wax/LLDPE polymer matrix.

6.2. RECOMMENDATIONS

As in any research work, there are certain areas for continuous improvement and, expansion. Several recommendations were identified for extending the results of this research to improve the integrated system are listed as follows:

(i) More work needs to be done in creating a pattern which best fits the needs for mold development. Complexity of geometry may not pose difficulties, therefore there is a need to make several patterns in order to develop consistent data hence superior patterns from the developed polymer blends prior to its use in investment casting process.

(ii). The prediction of melt flow behaviour of the polymer blends developed can be further predicted more accurately using the developed simulation models. This will particularly broaden the understanding on the flow characteristics which is an important factor in dewaxing of pattern materials hence a better understanding of the injection process of the developed pattern material thereby ultimately increasing it’s need of usage by investment casting industry.

(iii). Investigating the applicability of the developed polymer blends in making particular metal products/parts depending on the part geometry. This will help in giving a better representation with

regards to the shrinkage tendencies of pattern material for investment casting which is one of the technological requirements of investment casting process industry.

(iv). The influence of post treatment application and reuse of the developed material after dewaxing process need to studied and the properties of the dewaxed material analysed and compared with the developed pattern and the conventional pattern material. Its reuse is an important factor in the cost aspect of the process in totality.

REFERENCES

Abu-Bakar, A. & Moinuddin, K.A.M. 2012. Effects of Variation in Heating Rate , Sample Mass and Nitrogen Flow on Chemical Kinetics for Pyrolysis. In *18th Australasian Fluid Mechanics Conference Launceston, Australia, December (3-7)*. 18–21.

Al-Shemmeri, T. 2012. *Engineering Fluid Mechanics*. Al-Shemmeri & Ventus Publishing ApS, London, UK.

Aldin, S. & Christian, F. 2015. A generalized equation for rheology of emulsions and suspensions of deformable particles subjected to simple shear at low Reynolds number. *Rheological Acta*. 2015:85–108. DOI: 10.1007/s00397-014-0825-8.

Alshamari, A.K. & Sayed, W.M. 2016. Synthesis and Structure of Poly (methyl methacrylate) (PMMA) Nanoparticles in the Presence of Various Surfactants. *Chemical Science Review and Letters*. 5(17):161–169.

Anjo, V. 2012. Numerical simulation of steady state conduction heat transfer during the solidification of aluminum casting in green sand mould. *Leonardo Electronic Journal of Practices and Technologies*. 11(20):15–24.

Ansarifar, A. & Saeed, F. 2012. Effect of Different Paraffin Waxes and Antiozonant on the Processing and Mechanical Properties of Natural Rubber. *Journal of Rubber Research*. 15(1):35–45.

Azimi, H.R., Rezaei, M., Abbasi, F., Charchi, A. & Bahluli, Y. 2009. Non-isothermal degradation kinetics of MMA-St copolymer and EPS lost foams. *Journal of Macromolecular Science*. 49:25–63. DOI: 10.1080/15583720802656237.

Azzam, A. & Li, W. 2014. An experimental investigation on the three-point bending behavior of composite laminate. In *2014 Global Conference on Polymer and Composite Materials (PCM 2014), May (27-29)*. Ningbo, China. 1–9. DOI: 10.1088/1757-899X/62/1/012016.

Bala, K.C. & Khan, R.H. 2014. Rate of solidification of aluminium casting in varying wall thickness of cylindrical metallic moulds. *Leonardo Journal of Sciences*. (25):19–30.

Bala, K.C., Khan, R.H., Abolarin, M.S. & Abubakre, O. 2013. Investigation on the Rate of Solidification and Mould Heating in \nthe Casting of Commercially Pure Aluminium in Permanent Moulds of varying Thicknesses \n. *IOSR Journal of Mechanical and Civil Engineering (IOSR-JMCE)*. 6(1):33–37. Available: http://www.iosrjournals.org/iosr-jmce/papers/vol6-issue1/E0613337.pdf.

Bemblage, O. & Karunakar, D.B. 2011. A Study on the Blended Wax Patterns in Investment Casting Process. In *Proceeding of the World Congress on Engineering , July (6 - 8), 2011, London, U.K.* V. I.

Bhardwaj, A., Rawlani, M. V & Mukherjee, C.K. 2014. " Permanent Mold Casting " Excellent Casting Method for Manufacture of Automotive Components. *International Journal on Recent and Innovation Trends in Computing and Communication*. 2(8):2254–2255.

Bonilla, W., Masood, S.H. & Iovenitti, P. 2001. An investigation of wax patterns for accuracy improvement in investment cast parts. *International Journal of Advanced Manufacturing Technology*. 18(5):348–356. DOI: 10.1007/s001700170058.

Borah, J. 2013. Study on the Compatibility and Mechanical Properties of BR-LDPE-PVC Blends. In *4th International Conference on Biology, Environment and Chemistry November (21-23)*. V.

58. Phuket, Thailand. 37–40. DOI: 10.7763/IPCBEE.

Borcherding, A. & Luck, T. 1998. Application of Plant Proteins as Thermoplastics. *Plant Proteins from European Crops*. 313–314.

Breitenbach, J. 2002. Melt extrusion : from process to drug delivery technology. *European Journal of Pharmaceutics and Biopharmaceutics*. 54(2002):107–117.

Brennen, C. 2005. *Fundamentals of Multiphase Flows*. V. 128. London, UK: Cambridge University Press. DOI: 10.1007/s11214-006-9083-0.

Brown, M.E. 1988. *Handbook of thermal analysis and calorimetry: Principles and Practice*. Dordrecht, Netherlands: Kluwer Academic Publishers.

Butler, W.A. 2001. Die Casting (Permanent Mold). *Encyclopedia of Materials - Science and Technology*. (July 2015):2147–2152. DOI: 10.1016/B0-08-043152-6/00387-9.

Campbell, J. 2015. *Complete Casting Handbook- Metal Casting Processes, Metallurgy, Techniques and Design*. 1st ed. Oxford, UK: Butterworth-Heinemann Inc. DOI: 10.1016/B978-0-444-63509-9.00009-1.

Cassagnau, P. 2008. Melt rheology of organoclay and fumed silica nanocomposites. *Polymer,* vol. 49, no. 9, pp. 2183-2196.

Chafidz, A., Kaavessina, M., Al-zahrani, S. & Al-otaibi, M.N. 2014. Rheological and mechanical properties of polypropylene / calcium carbonate nanocomposites prepared from masterbatch. *Journal of Thermoplastic Composite Materials*. 1–30. DOI: 10.1177/0892705714530747.

Chen, F. & Wolcott, M.P. 2013. Miscibility studies of paraffin/polyethylene blends as form-stable phase change materials. *European Polymer Journal*. 4(September):1–27. DOI:

10.1016/j.eurpolymj.2013.09.027.

Christy, A., Ozaki, Y. & Gregoriou, V. 2001. *Modern Fourier Transform Infrared Spectroscopy: Comprehensive Analytical Chemistry*. London,UK: John Wiley & Sons, Ltd.

Conti, M. & Marconi, U.M.B. 2000. Interfacial dynamics in rapid solidification processes. *Physica A: Statistical Mechanics and its Applications*. 280(1):148–154. DOI: 10.1016/S0378-4371(99)00631-7.

Crawford, B. 2017. Casting status in South Africa. *Casting SA*. 18(4):1-12.

Czaniková, K., Špitalský, Z. & Krupa, I. 2012. Electrical and Mechanical Properties of Ethylene Vinyl Acetate Based Electrical and Mechanical Properties of Ethylene Vinyl Acetate Based Composites. *Materials Science Forum*. 714(March):4–11. DOI: 10.4028/www.scientific.net/MSF.714.193.

Dai, H. 2009. A Study of Solidification Structure Evolution during Investment Casting of Ni-based Superalloy for Aero-Engine Turbine Blades. A Thesis submitted for the degree of Doctor of Philosophy (Department of Mechanical Engineering) at the University of Leicester. Available: http://hdl.handle.net/2381/4551.

Dargusch, M.S., Dour, G., Schauer, N., Dinnis, C.M. & Savage, G. 2006. The influence of pressure during solidification of high pressure die cast aluminium telecommunications components. *Journal of Materials Processing Technology*. 180(1–3):37–43. DOI: 10.1016/j.jmatprotec.2006.05.001.

Das, S. & Himte, R.L. 2013. Design &Analysis of Pure Iron Casting with Different Moulds. *International Journal of Modern Engineering Research (IJMER)*. 3(5):2875–2887. Available:

http://www.ijmer.com/papers/Vol3_Issue5/BS3528752887.pdf.

Doli Rani & D.B. Karunakar. 2013. Recycling of Pattern Wax In The Investment Casting Process Using Microwave Dewaxing. *IOSR Journal of Engineering (IOSRJEN)*. 3(5):5–10.

Dombe, G., Maurya, M., Organisation, D. & Bhongale, C. 2015. Application of Twin Screw Extrusion for Continuous Processing of Energetic Materials. *Central European Journal of Energetic Materials*. 12(3):507–522.

Ferreira, A.C., Diniz, M.F. & Mattos, C. 2018. FT-IR methodology (transmission and UATR) to quantify automotive systems. *Polymers*. 28(1):6–14.

Fifield, F.W. & Kealey, D. 2000. *Principles and Practice of Analytical Chemistry*. 5th ed. London, UK B:Lackie Academic Professional.

Frank, M.C., Petrzelka, J.E., Yang, Z., Wysk, R.A. & Joshi, S. 2009. Conventional machining methods for rapid prototyping and direct manufacturing. *International Journal*. 10(October 2014):1–22. DOI: 10.1504/IJRAPIDM.2009.028931.

Gebelin, J.-C., Cendrowicz, A.M. & Jolly, M.R. 2003. Modelling of the wax injection process for the investment casting process: prediction of defects. In *Third International Conference on CFD in the Minerals and Process Industries CSIRO, December (10-12)*. Melbourne, Australia. 415–420.

Gonzalez-leon, J.A. & Mayes, A.M. 2003. Phase Behavior Prediction of Ternary Polymer Mixtures. *Macromolecules*. 2003(36):2508–2515. DOI: 10.1021/ma0209803.

Groover, M.P. 2010. *Fundamentals-of-Modern-Manufacturing- Materials, Processes, and Systems*. Hoboken, USA: John Wiley & Sons, Inc.

Guinn, P. 2002. *Patent No. US Patent 6,485,553 B1*. USA. DOI: 10.1074/JBC.274.42.30033.(51).

Güner, A., Arıkan, M. & Nebioglu, M. 2015. New Approaches to Aluminum Integral Foam Production with Casting Methods. *Metals*. 5(3):1553–1565. DOI: 10.3390/met5031553.

Haines, P.J. 1995. *Thermal methods of analysis principles, applications and problems*. London, UK: Blackie Academic & Professional, London, UK.

Hallquits, M. 2011. Heat Transfer and Pressure Drop Characteristics of Smooth Tubes At a Constant Heat Flux in the Transitional Flow Regime. *Heat Transfer Journal*. 4(December):1–145.

Hamilton, E. 1989. *Pattern Making Handbook*. 5 th ed. Crosby Lockwood and Son Inc: London, UK.

Hassankiadeh, M.N., Khajehfard, A. & Golmohammadi, M. 2012. Kinetic and Product Distribution Modeling of Fischer-Tropsch Synthesis in a Fluidized Bed Reactor. *International Journal of Chemical Engineering and Applications*. 3(6):400–403. DOI: 10.7763/IJCEA.2012.V3.227.

Hato, M.J. & Luyt, A.S. 2006. Thermal Fractionation and Properties of Different Polyethylene /Wax Blends. *Journal of Applied Polymer Science*. 104(September):2225–2236. DOI: 10.1002/app.

Higgins, J.S., Lipson, J.E.G. & White, R.P. 2010. A simple approach to polymer mixture miscibility. *Philosophical transactions of Royal Society A*. 2010(368):1009–1025. DOI: 10.1098/rsta.2009.0215.

Holman, J.P. & Lloyd, J. 2010. *Fluid Mechanics S1.2*. 4th ed. V. 6. New York, USA: McGraw-Hill. DOI: http://dx.doi.org/10.1016/j.rser.2004.09.010.

Horton, R.A. & Tetlow, A.R. 2005. *Patent No. US Patent No 2005/0182195 A1*. USA.

Hu, J., Yu, F. & Lu, Y. 2012. Application of Fischer–Tropsch Synthesis in Biomass to Liquid Conversion. *Catalysts*. 2:303–326. DOI: 10.3390/catal2020303.

Huang, B.C., Jian, G., Delisio, J.B., Wang, H., Zachariah, M.R. & Wang, H. 2014. Electrospray Deposition of Energetic Polymer Nanocomposites with High Mass Particle Loadings : A Prelude to 3D Printing of Rocket Motors. *Advanced Engineering Material*. 17(1):95–101. DOI: 10.1002/adem.201400151.

Huang, C., Leu, M.C. & Richards, V.L. 2007. Investment Casting With Ice Patterns and Comparison with other types of rapid protying patterns. In *NSF Design and Manufacturing Grantees Conference May (1-3)*. London, UK. 1–7.

Ilangovan, S. 2014. Effects of Solidification Time on Mechanical Properties and Wear Behaviour of Sand Cast Aluminium Alloy. *International Journal of Research in Engineering and Technology*. 3(2):71–75.

Jang, J. & Lee, D.K. 2003. Plasticizer effect on the melting and crystallization behavior of polyvinyl alcohol. *Polymer*. 44(26):8139–8146. DOI: 10.1016/j.polymer.2003.10.015.

Januszewicz, K., Klein, M. & Klugmann-radziemska, E. 2017. Thermogravimetric analysis / pyrolysis of used tyres and waste rubber. *Physicochemical Problems and Mineral processing*. 53(2):802–811.

Jesiotr, M. & Myszka, D. 2013. Thermal Analysis of Selected Polymer Materials for Precision Casting Models. *Archives of Foundry Engineering*. 13(2):61–64.

Jones, S. & Yuan, C. 2003. Advances in shell moulding for investment casting. *Journal of*

Materials Processing Technology. 135(2003):258–265. DOI: 10.1016/S0924-0136(02)00907-X.

Kannan, M., Bhagawan, S., Thomas, S. & Joseph, K. 2012. Thermogravimetric analysis and differential scanning calorimetric studies on nanoclay-filled TPU / PP blends. *Journal of thermal analysis and calorimetry*. 2010(2):78–90. DOI: 10.1007/s10973-012-2693-8.

Karwiński, A., Młodnicki, S., Pabiś, R., Robak, I. & Kubosz, G. 2011. New generation of pattern materials for investment casting. *Archives of Foundry Engineering*. 11(1):53–56.

Kim, J.W. & Lee, J.S. 2017. Effect of Heat Drawing Process on Mechanical Properties of Dry-Jet Wet Spun Fiber of Linear Low Density Polyethylene / Carbon Nanotube Composites. *International Journal of Polymer Science*. 2017:1–9.

Kim, K.D., Yang, D.Y. & Jeong, J.H. 2006. Plaster casting process for prototyping of die casting based on rapid tooling. *International Journal of Advanced Manufacturing Technology*. 28(9):923–929. DOI: 10.1007/s00170-004-2291-4.

Klancnik, G., Medved, J. & Mrvar, P. 2010. Differential thermal analysis (DTA) and differential scanning calorimetry (DSC) as a method of material investigation. *Materials and Geoenvironmentent*. 57(1):127–142.

Kochan, D., Kai, C.C. & Zhaohui, D. 1999. Rapid prototyping issues in the 21st century. *Computers in Industry*. 39(1999):3–10.

Kodre, K.., Attarde, S.., Yendhe, P.., Patil, R.. & Barge, V.. 2014. Differential scanning calorimetry: A review. *Research and Reviews: Journal of Phamaceutical Analysis*. 3(3):11–22.

Koenig, M. 1979. *Patent No. US Patent 4,144,075*. USA. DOI: 10.1016/j.scriptamat.2005.10.045.

Krupa, I. & Luyt, A.S. 2000. Mechanical Properties of Uncrosslinked and Crosslinked Linear Low-Density Polyethylene / Wax Blends. *Journal of Applied Polymer Science*. 4(1):973–980.

Krupa, I. & Luyt, A.S. 2001a. Thermal and mechanical properties of extruded LLDPE / wax blends. *Polymer Degradation and Stability*. 73:157–161.

Krupa, I. & Luyt, A.S. 2001b. Physical properties of blends of LLDPE and an oxidized paraffin wax. *Polymer*. 42(2001):7285–7289.

Krupa, I., Nógellová, Z., Špitalsky, Z., Janigová, I., Boh, B., Sumiga, B., Kleinová, A., Karkri, M., et al. 2014. Phase change materials based on high-density polyethylene filled with microencapsulated paraffin wax Phase change materials based on high-density polyethylene filled with microencapsulated paraffin wax. *Energy Conversion and Management*. 87(2014):400–409. DOI: 10.1016/j.enconman.2014.06.061.

Kumar, S. 2014. Experimental characterization of physical and thermal behaviour of blended wax pattern in investment casting. In *Proceedings of 8th IRF International Conference, 28th December (12-14). Goa, India.* 17–21.

Kumar, S., Kumar, P. & Shan, H. 2009. Characterization of the refractory coating material used in vacuum assisted evaporative pattern casting process. *Journal of Materials Processing Technology*. 4:1–8. DOI: 10.1016/j.jmatprotec.2008.06.010.

Kumar, S., Gandotra, S., Kumar, S. & Tripathi, H. 2016. Investigate the effect of additives on mechanical properties during casting of 6351 aluminium. In *MATEC Web of Conferences*. V. 3008. 1–5.

Lee, H.S. 2008. Computational and Rheological Study of Wax Deposition and Gelation in Subsea

Pipelines. A Thesis submitted for the degree of Doctor of Philosophy (Department of Chemical Engineering), The University of Michigan.

Leviness, S., Tonkovich, A.L., Jarosch, K., Fitzgerald, S., Yang, B. & Mcdaniel, J. 2011. Improved Fischer-Tropsch Economics Enabled by Microchannel Technology. *Velocys*. 1:1–7.

Lewis, R.J. 2007. *Condensed Chemical Dictionary*. New York, USA: JohnWiley&Sons,Inc.

Li, H. & Zhang, J. 2003. A generalized model for predicting non-Newtonian viscosity of waxy crudes as a function of temperature and precipitated wax. *Fuel*. 82(11):1387–1397. DOI: 10.1016/S0016-2361(03)00035-8.

Liu, Z., Cai, X., Ke, X. & You, F. 2018. Influence of CaCO 3 / glass fiber hybrid fillers on the mechanical and thermal properties of polytetrafluoroethylene. *Advanced Polymer Technology*. 3(February 2017):1–9. DOI: 10.1002/adv.21953.

Magampa, P.P., Manyala, N. & Focke, W.W. 2013. Properties of graphite composites based on natural and synthetic graphite powders and a phenolic novolac binder. *Journal of Nuclear Materials*. 436(1–3):76–83. DOI: 10.1016/j.jnucmat.2013.01.315.

Marsilla, K., Ishak, K. & Verbeek, C.J. 2016. Mechanical Properties of Protein-Based Polymer Blends. *Journal of Engineering Science*. 12(2016):77–86.

McLaren, R.A, Alcott, C.A, Nasser, W.. 1975. *Patent No. US Patent 3,880,790*. USA. DOI: 10.1074/JBC.274.42.30033.(51).

Medell, H.I. & Potos, S.L. 2016. Rapid Prototyping and Manufacturing : A Review of Current Technologies IMECE2009-11750. In *Proceedings of the ASME 2009 International Mechanical Engineering Congress & Exposition, November (13-19)*. Lake Buena Vista, Florida, USA. 1–13.

DOI: 10.1115/IMECE2009-11750.

Menard, K. 1999. *Dynamic Mechanical Analysis: a practical introduction*. New York, USA: CRC Press.

Mendes, R. 2015. Rheological behavior and modeling of waxy crude oils in transient flows. A Thesis submitted for the degree of Doctor of Philosophy (Department of Chemical Engineering), University of Paris.

Merges, J., Mills, G. & Ware, R. 1972. Investment Casting wax. US Patent 3,667,979. USA.

Mhike, W., Focke, W.W., Mofokeng, J.P. & Luyt, A.S. 2012. Thermochimica Acta Thermally conductive phase-change materials for energy storage based on low-density polyethylene , soft Fischer – Tropsch wax and graphite. *Thermochimica Acta*. 527(2012):75–82. DOI: 10.1016/j.tca.2011.10.008.

Micic, P., Bhattacharya, S.N. & Field, G. 1996. Melt Strength and Elastic Behaviour of LLDPE / LDPE Blends. *International polymer processing*. 1:14–20.

Molaba, M.P., Dudi, D. & Luyt, A.S. 2015. Influence of the presence of medium-soft paraffin wax on the morphology and properties of iPP / silver nanocomposites. *Express Polymer Letters*. 9(10):901–915. DOI: 10.3144/expresspolymlett.2015.82.

Mpanza, H.S. & Luyt, A.S. 2006. Influence of Different Waxes on the Physical Properties of Linear Low-density Polyethylene. *South African Journal of Chemistry*. 59:48–54.

Mueller, B.S., Llewellin, E.W. & Mader, H.M. 2010. The rheology of suspensions of solid particles. *Proceedings of the Royal Society Academy*. 2010(466):1201–1228. DOI: 10.1007/BF01432034.

Muller, H. & Sladojevik, J. 2001. Rapid tooling approaches for small lot production of sheet-metal parts. *Journal of Material Processing Technology*. 115(2001):97–103.

Muschio, H.. I. 1996. *Patent No. US Patent 5,518,537*. USA.

Muthuraman, V., Arunkumar, S. & Baskarlal, V.P.M. 2017. Modelling and simulation analysis of metal castings. *ARPN Journal of Engineering and Applied Sciences*. 12(6):1876–1879.

Nascimento, I., Bruns, R.E., Siqueira, D.F. & Nunes, S.P. 1997. Application of Statistical Mixture Models for Ternary Polymer Blends. *Journal of Brazilian Chemical Society*. 8(6):587–595.

Nebykov, V., Kazakova, L., Anisimov, I. & Druzhina, E. 1985. Properties of compounds of paraffin and ceresins with copolymer of ethylene and vinyl acetate. *Chemistry and Technology of Fuels and Oils*. 4:40–43.

Nordqvist, D., Hedenqvist, M.S., Lagaron, J.M. & Sanchez-garcı, M.D. 2009. Incorporating Amylopectin in Poly (lactic Acid) by Melt Blending Using Poly (ethylene -co- vinyl Alcohol) as a Thermoplastic Carrier . (I) Morphological Characterization. *Journal of Applied Polymer Science*. 115(I). DOI: 10.1002/app.

Novais, V.R., Versluis, A. & Soares, C.J. 2011. Three-point bending testing of fibre posts : critical analysis by finite element analysis. *International Endodontic Journal*. 1–6. DOI: 10.1111/j.1365-2591.2011.01856.x.

Nyembwe, K.D. 2007. Technologies for the base metal casting industry in southern Africa: The impact of rapid prototyping. *The Southern African Institute of Mining and Metallurgy*. 305–312.

Ochowiak, M. & Rozanski, J. 2012. Rheology and Structure of Emulsions and Suspensions. *Journal of Dispersion Science and Technology*. 33:174–184. DOI:

10.1080/01932691.2010.548694.

Ogunwole, O.A., Olugboji, O.A. & Abolarin, M.S. 2007. Casting of Brake Disc and Impeller from Aluminium Scrap Using Silica Sand. *Leonardo Journal of Practices and Technologies*. (10):145–150. Available: http://lejpt.academicdirect.org/A10/145_150.pdf.

Osswald, T.A. 2011. *Understanding Polymer Processing: Porcesses and Governing Equations*. Munich, Germany: Hanser Publishers.

Pachamuthu, P. & Hatna, S. 2005. Studies on Poly(Methyl Methacrylate) (PMMA) and Thermoplastic Polyurethane (TPU) Blends. *Journal of Macromolecular Science*. 42(October):1399–1407. DOI: 10.1080/10601320500205764.

Pankaj Sharma, Doli Kasana, Vijay Kumar & Charat Goel. 2013. Analysis the Properties of Lost Wax Process and Its Use ability Exploring Possibilities. *International Journal of Engineering Science Invention*. 2(2):32–35.

Pastirčák, R., Sládek, A. & Kucharčíková, E. 2015. The Production of Plaster Molds with Patternless Process Technology. *Archives of Foundry Engineering*. 15(2):91–94. DOI: 10.1515/afe-2015-0045.

Patel, B. 2016. Evaluation of physical and mechanical properties for various wax blend patterns. *International Journal of Scientific and Research Publications*. 6(4):285–288.

Pattnaik, S., Karunakar, D.B. & Jha, P.K. 2012. Developments in investment casting process - A review. *Journal of Materials Processing Technology*. 212(11):2332–2348. DOI: 10.1016/j.jmatprotec.2012.06.003.

Paul, D.R. & Tiwari, R.R. 2014. *Polymer Blends Containing "Nanoparticles"*. DOI: 10.1007/978-

94-007-6064-6.

Pawlak, M. & Władysiak, R. 2009. Plaster mould casting process of AlSi11 alloy. *Archives of Foundry Engineering*. 9(4):225–232.

Pham, C.B., Leong, K.F., Lim, T.C. & Chian, K.S. 2008. Rapid freeze prototyping technique in bio-plotters for tissue scaffold fabrication. *Rapid Prototyping Journal*. 14(4):246–253. DOI: 10.1108/13552540810896193.

Prasad, R. 2012. Progress in Investment Castings. *Science and Technology of Casting Process*. 25–72. DOI: 10.5772/50550.

Pu, G., Wang, J., Severtson, S.J., Ave, F., Paul, S., Company, N. & Naperville, W.D.R. 2007. Properties of Paraffin Wax / Montmorillonite Nanocomposite Coatings. A report submitted to Department of Bioproducts and Biosystems Engineering , University of Minnesota , 2004. 2:112–115.

Rafat, F. 2014. Effect of different heating rate on the thermal decomposition of urea in an open reaction vessel. *Archives of Applied Science Research*. 6(5):75–78.

Rafique, M.M. a. 2015. Modeling and simulation of heat transfer phenomena. *Heat Transfer Studies and Applications*. 225–257. DOI: 10.5772/61029.

Rajagopal, P., Chitre, V. & Aras, M.A. 2012. A comparison of the accuracy of patterns processed from an inlay casting wax , an auto-polymerized resin and a light-cured resin pattern material. *Indian Journal of Dental Research*. 23(2):152–156. DOI: 10.4103/0970-9290.100418.

Rajendran, S., Prabhu, M.R. & Rani, M.U. 2008. Characterization of PVC / PEMA Based Polymer Blend Electrolytes. *International Journal of Electrochemical Science*. 3:282–290.

Rao, Z.H. & Zhang, G.Q. 2011. Thermal Properties of Paraffin Wax-based Composites Containing Graphite. *Energy Sources, Part A*. 7036(33):587–593. DOI: 10.1080/15567030903117679.

Ray, I., Roy, S., Chaki, T.K. & Khastgir, D. 1994. Studies on thermal degradation behaviour of EVA / LDPE blend. *Journal of elastomers and plastics*. 26(April):168–182.

Raza, M. 2015. Process Development for Investment Casting of Thin-Walled Components. A Thesis submitted for the degree of Doctor of Philosophy (School of Innovation, Design and Engineering), Malardalen University, Sweden.

Reddy, B.P., Gunasekar, C., Mhaske, A.S. & Krishna, V.N. 2018. Enhancement of thermal conductivity of PCM using filler graphite powder materials. In *2nd International conference on Advances in Mechanical Engineering (ICAME 2018), March (22-24), Chennai, India.* 1–10. DOI: 10.1088/1757-899X/402/1/012173.

Rides, M. 2005. *NPL REPORT Rheological characterisation Of filled materials : A review*. Middlesex, United Kingdom. DOI: NPL Report DEPC-MPR 013.

Ridge, O. 2004. Tests for determining viscoelastic properties of investment casting waxes. In *Investment Casting Institute 52-nd Technical Meeting, November (23-25).* Oak Ridge, USA. 1–11.

Róz, A.L. Da, Ferreira, A.M., Yamaji, F.M. & Carvalho, A.J.F. 2012. Compatible blends of thermoplastic starch and hydrolyzed ethylene-vinyl acetate copolymers. *Carbohydrate Polymers*. 90(1):34–40. DOI: 10.1016/j.carbpol.2012.04.055.

Rutto, H. & Focke, W.W. 2009. Thermo-mechanical properties of urea-based pattern molding compounds for investment casting. *International Polymer Processing*. 25(1):15–22. DOI:

10.3139/217.2256.

Sabau, A.S. 2005. Numerical Simulation of the Investment Casting Process. *AFS Transactions*. 160(4):1–11.

Sabau, A.S. & Viswanathan, S. 2003. Material properties for predicting wax pattern dimensions in investment casting. *Materials Science and Engineering A*. 362(1–2):125–134. DOI: 10.1016/S0921-5093(03)00569-0.

Saikaew, C. & Wiengwiset, S. 2012. Optimization of molding sand composition for quality improvement of iron castings. *Applied Clay Science*. 67–68:26–31. DOI: 10.1016/j.clay.2012.07.005.

Schramm, G. 1994. A Practical Approach to Rheology and Rheometry. *Rheology*. 291. DOI: 10.1017/CBO9781107415324.004.

Sęk, J.P., Błaszczyk, M.M. & Przybysz, Ł. 2019. A rheological model to predict viscosity of dispersions as a function of the modified Peclet number. *Korea-Australia Rheology Journal*. 31(May):81–88. DOI: 10.1007/s13367-019-0009-2.

Selvakumar, R.D. & Dhinakaran, S. 2016. Effective viscosity of nanofluids-A modified Krieger-Dougherty model based on particle size distribution (PSD) analysis Effective viscosity of nanofluids — A modified Krieger – Dougherty model based on particle size distribution (PSD) analysis. *Journal of Molecular Liquids*. 225(October 2018):20–27. DOI: 10.1016/j.molliq.2016.10.137.

Shekhawat, M.S. 2013. Thermo Gravimetric and Differential Thermal Analysis of Clay of Western Rajasthan (India). *International Journal of Modern Physics: Conference Series*. 22:458–465. DOI:

10.1142/S2010194513010519.

Shivappa, D.N., Prasad, A.J.K., Harisha, K. & Manjunath, R. 2014. Studies on Recyclability of Investment Casting Wax Formulation – An Experimental Study. *Recent Advances in Mechanical Engineering and Mechanics*. 60(6):37–41.

Siaotong, B.A.C., Tabil, L.G., Panigrahi, S.A. & Crerar, W.J. 2005. Effect of Extrusion Parameters on the Physical Characteristics of Extruded Flax Fiber- Reinforced Polyethylene Composites. *The Canadian Society for Engineering in agricultural, food, and biological systems*. 2(5): 23-35.

Sin, S.L. & Dube, D. 2004. Influence of process parameters on fluidity of investment-cast AZ91D magnesium alloy. *Materials Science and Engineering A*. 386(1–2):34–42. DOI: 10.1016/j.msea.2004.07.028.

Singh, R., Singh, S. & Singh, G. 2014. Cast Component Hardness Comparison for Investment Casting Prepared with Wax and ABS Patterns. *Transactions of the Indian Institute of Metals*. 68(1):17–21. DOI: 10.1007/s12666-014-0432-5.

Smith, C. 2011. *Fundamentals of Fourier Transform Infrared*. 2nd ed. New York, USA: CRC Press.

Sorn, S. 2011. Examination of proper span/depth ratio range in measuring the bending strength of wood based on the elementary bending theory. In *15th International Research/Expert Conference: Trends in the Development of Machinery and Associated Technology, April (2-4)*. Prague, Czech Republic. 761–764.

Stuart, B. 2004. *Infrared Spectroscopy: Fundamentals and Applications*. London,UK: John Wiley & Sons, Ltd.

Stubsjøen, M. 2013. Analytical and Numerical Modeling of Paraffin Wax in Pipelines. Studies on Recyclability of Investment Casting Wax Formulation – An Experimental Study. A Thesis submitted to the (Department of Petroleum Engineering and Applied Geophysics), Norwegian University of Science and Technology.

Sturgis, D.., Yasrebi, M., Taft, M. & Sorbel, M.. 2001. *Patent No. US Patent 6,326,429 B1*. USA.

Su, B., Zhou, Y. & Wu, H. 2017. Influence of mechanical properties of polypropylene / low-density polyethylene nanocomposites : Compatibility and crystallization. *Nanomaterials and nanotechnology*. 7:1–11. DOI: 10.1177/1847980417715929.

Taşcıoğlu, S. & Akar, N. 2003. Conversion of an Investment Casting Sprue Wax to a Pattern Wax by Chemical Agents. *Materials and Manufacturing Processes*. 18(5):753–768. DOI: 10.1081/AMP-120024973.

Teng, H. & Zhang, J. 2013. Modeling the viscoelasto-plastic behavior of waxy crude. *Petroleum Science*. 10(3):395–401. DOI: 10.1007/s12182-013-0287-0.

Tewo, R.K., Rutto, H.L., Focke, W., Seodigeng, T. & Koech, L.K. 2018. Formulations , development and characterization techniques of investment casting patterns. *Reviews in Chemical Engineering*. 7(2):1–15.

Tham, D.Q., Tuan, V.M., Thi, D., Thanh, M. & Chinh, N.T. 2015. Preparation and Properties of Ethylene Vinyl Acetate Copolymer / Silica Nanocomposites in Presence of EVA-g-Acrylic Acid. *Journal of Nanoscience and Nanotechnology*. 15(April):2777–2784. DOI: 10.1166/jnn.2015.9209.

Throne, J. 1998. Processing Thermoplastic Composites. *Handbook of Composites*. 1–9. DOI:

10.1007/978-1-4615-6389-1_25.

Tiaden, J. 1999. Phase field simulations of the peritectic solidification of Fe-C. *Journal of Crystal Growth*. 198–199(pt 2):1275–1280. DOI: 10.1016/S0022-0248(98)01009-4.

Tiwari, A. & Hihara, L.H. 2012. Deciphering the inert atmosphere degradation patterns in hybrid silicones. *Polymer Degradation and Stability*. 97(9):1633–1643. DOI: 10.1016/j.polymdegradstab.2012.06.021.

Tomasik, J., Haratym, R. & Biernacki, R. 2009. Investment casting or powder metallurgy – the ecological aspect. *Archives of Foundry Engineering*. 9(2):165–168.

Tyler, D., Aluminum, G., Co, M., Pischel, R. & Metallurgical, F. 2008. Permanent Mold Casting. In *Metal Casting Theory and Design*. V. 15. 689–699. DOI: 10.1361/asmhba0005260.

Upadhya, G.K., Das, S., Chandra, U. & Paul, A.J. 1995. Modelling the investment casting process: a novel approach for view factor calculations and defect prediction. *Applied Mathematical Modelling*. 19(6):354–362. DOI: 10.1016/0307-904X(95)90001-O.

Uygunoglu, T., Gunes, I., Brostow, W. & Faculty, E. 2015. Physical and Mechanical Properties of Polymer Composites with High Content of Wastes Including Boron. *Materials Research*. 18(6):1188–1196.

Valandro, S.R., Lombardo, P.C., Poli, A.L., Antonio, M., Jr, H., Neumann, M.G., Cristina, C. & Cavalheiro, S. 2014. Thermal Properties of Poly (Methyl Methacrylate)/ Organomodified Montmorillonite Nanocomposites Obtained by in situ Photopolymerization. *Materials Research*. 17(1):265–270.

Vihtelic, J., Graham, A., McCormick, R. & Carpenter, L. 1999. *Patent No. US Patent 5,983,982*.

USA. DOI: 10.1016/j.scriptamat.2005.10.045.

Wang, W. & Kaufman, M. 2001. Characterization of Distributive Mixing in Polymer Processing Equipment using Renyi Entropies. *International polymer processing*. 2001(1):315–322.

Wang, S., Miranda, a. G. & Shih, C. 2010. A Study of Investment Casting with Plastic Patterns. *Materials and Manufacturing Processes*. 25(12):1482–1488. DOI: 10.1080/10426914.2010.529585.

Wang, X., Wang, R., Peng, C. & Li, H. 2012. Progress in Natural Science : Materials International Rheology of aqueous BeO suspension with NH 4 PAA as a dispersant. *Progress in Natural Science: Materials International*. 22(4):347–353. DOI: 10.1016/j.pnsc.2012.07.003.

Ware, R.E. & Merges, J.C. 1972. *Patent No. US Patent No 3 704 145*. USA.

Wawulska-marek, P., Sitek, P.W.R., Bolek, T., Zdunek, J., Mizera, J. & Kurzydlowski, K.J. 2015. A Study on Technological Properties of Investment Casting Waxes. *Advances in Applied Plasma Science*. 10(2):3–7.

Welty, J.R., Wicks, C.E., Wilson, R.E. & Rorrer, G.L. 2008. *Fundamentals of Momentum, Heat, and Mass Transfer 5th eds*. Rosewood Drive, Danvers, USA: John Wiley & Sons, Inc. DOI: 10.1016/0017-9310(70)90063-3.

Williams, J. 1989. Characterization of dispersive and distributive mixing in a co-rotating trwin-screw compounding extruder. A Thesis submitted for the degree of Doctor of Philosophy (Department of Chemical Engineering), Brunel University, UK.

Xu, M. 2015. Characterization of investment shell thermal properties. A Thesis submitted for the degree of Doctor of Philosophy (Department of Materials Science and Engineering), Missouri

University of Science of Technology.

Xu, X., Yu, J., Xue, L., Zhang, C., Zha, Y. & Gu, Y. 2017. Investigation of Molecular Structure and Thermal Properties of Thermo-Oxidative Aged SBS in Blends. *Materials*. 10:2–11. DOI: 10.3390/ma10070768.

Yang, C., Liu, L., Zhao, X., Zhang, J., Sun, D. & Fu, H. 2014. Formation of stray grains during directional solidification of a superalloy AM3. *Applied Physics A: Materials Science and Processing*. 114(3):979–983. DOI: 10.1007/s00339-013-8046-z.

Yazmin, A., Delgado, C., Alonso, D. & Molina, R. 2016. Thermal and thermodynamic characterization of a dye powder from liquid turmeric extracts by spray drying. *Journal of the National Faculty of Agronomy*. 69(1):7845–7854. DOI: 10.15446/rfna.v69n1.54752.

Zapata, A.M.O., Rodríguez-Barona, S. and Gómez, G.I.G. 2015. Rheological characterization and stability study of an emulsion made with a dairy by-product enriched with omega-3 fatty acids. Brazilian Journal of Food Technology, vol. 18, no. 1, pp. 23-30.

Zanetti, M., Camino, G., Thomann, R. & Mu, R. 2001. Synthesis and thermal behaviour of layered silicate ± EVA nanocomposites. *Polymer*. 42(2001):4501–4507.

Zhang, N. and Gilchrist, M. 2012. Characterization of thermo-rheological behavior of polymer melts during the micro injection moulding process. Polymer Testing, vol. 31, no. 6, pp. 748-758.

Zhang, X., Chen, T., Qin, H. & Wang, C. 2016. A comparative study on permanent mold cast and powder thixoforming 6061 aluminum alloy and Sicp/6061Al composite: Microstructures and mechanical properties. *Materials*. 9(6). DOI: 10.3390/ma9060407.

Zloczower, M.I., Nir, A. & Tadmor, Z. 1983. Dispersive mixing in rubber and plastics. In *The*

Rubber Division, American Chemical Society. *May (12-15)*, Houston, Texas, USA.

CONTRIBUTIONS

The following publication is as a result of this work.

Tewo, R.K., Rutto, H.L., Focke, W., Seodigeng, T., & Koech, L.K. 2018. Formulations , development and characterization techniques of investment casting patterns. *Reviews in Chemical Engineering*. 7(2):1–15.

https://www.degruyter.com/view/j/revce.ahead-of-print/revce-2017-0068/revce-2017-0068.xml

Tewo, R. K., Rutto, H. L., Focke, W., Ramjee, S., Seodigeng, T. 2019. Investment casting pattern material based on paraffin wax fortified with EVA and filled with PMMA. *Journal of Applied Polymer Science. DOI: 10.1002/app.48774.*

https://onlinelibrary.wiley.com/doi/epdf/10.1002/app.48774

Tewo, R. K., Rutto, H. L., Focke, W., Ramjee, S., Seodigeng, T. 2019. Thermal, mechanical, surface characterization and rheology of EVA/wax and wax/LLDPE blends as a carrier vehicle for investment casting pattern. *Under Review, Journal of Polymer Engineering.*

Tewo, R. K., Rutto, H. L., Focke, W., Ramjee, S., Seodigeng, T. 2019. Thermal and mechanical properties of investment casting pattern material based on paraffin wax fortified with LLDPE and filled with PMMA. *Polymer Processing Europe-Africa 2019 regional conference,* November (18 – 21), Pretoria, South Africa.

Tewo, R. K., Rutto, H. L., Seodigeng, T. 2019. Rheological and morphological properties of investment casting pattern material based on paraffin wax fortified with LLDPE and filled with PMMA. *22nd International Conference on Chemical Engineering and Process Technology*, April (22 – 24), New York, USA.

APPENDICES

APPENDIX 1: Mould design development for three-point bending test analysis and a picture of the designed part

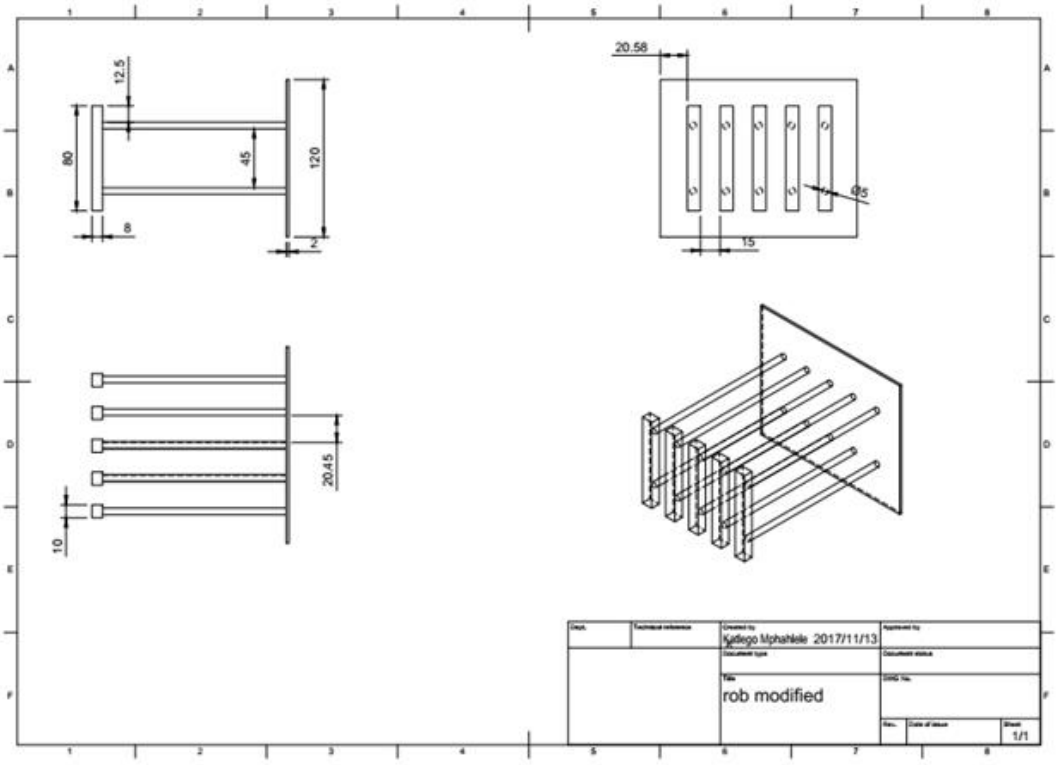

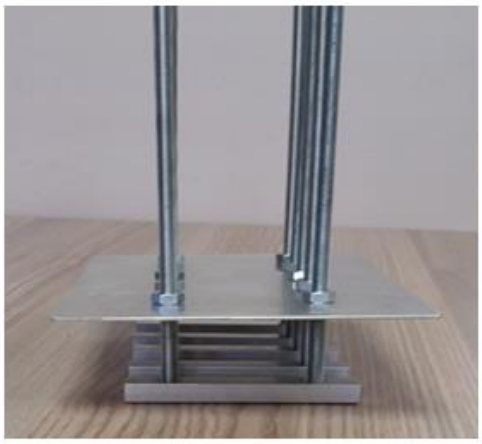

APPENDIX II: Needle used for TMA penetration measurements

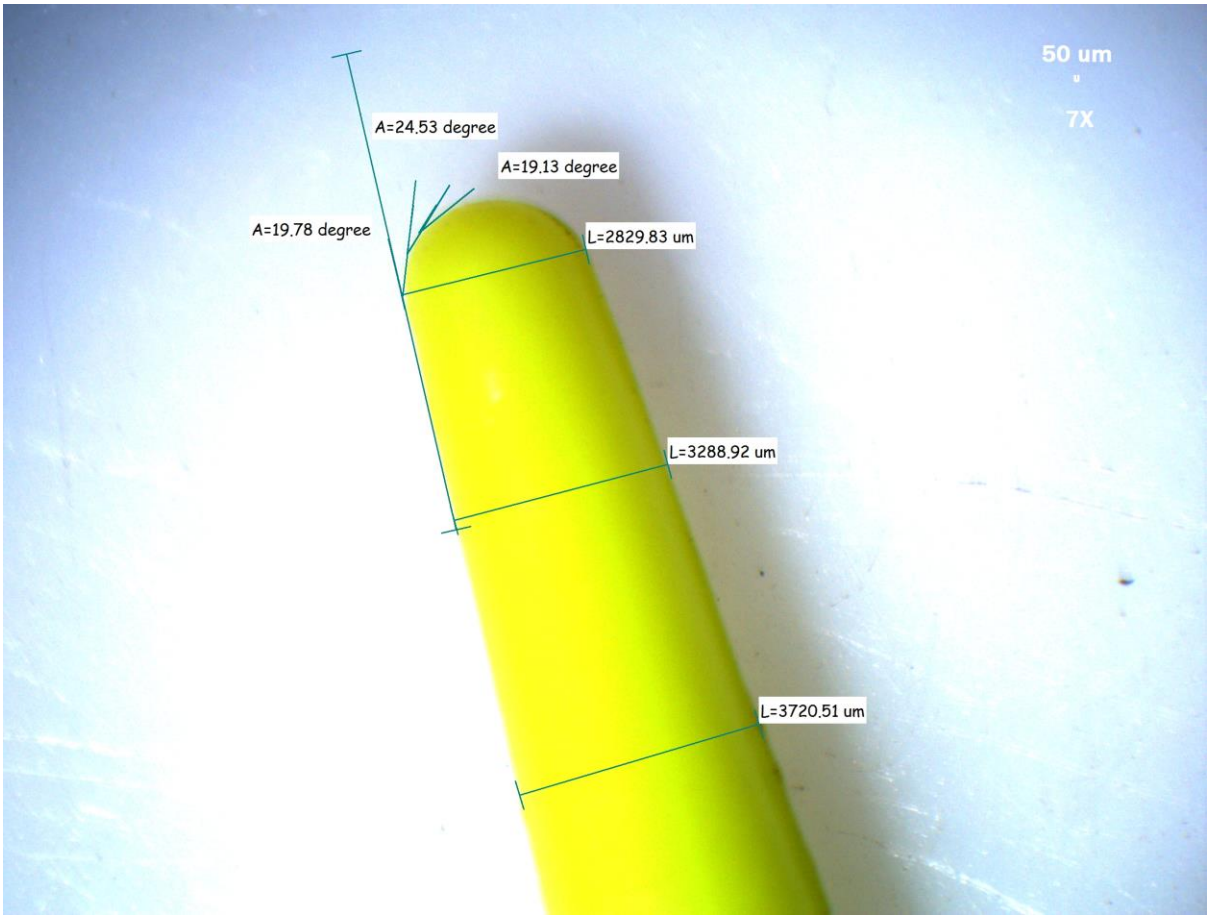

APPENDIX III: Properties of filled and non-filled industrial pattern wax for investment casting process

(i). (a) TGA and (b) DSC curves

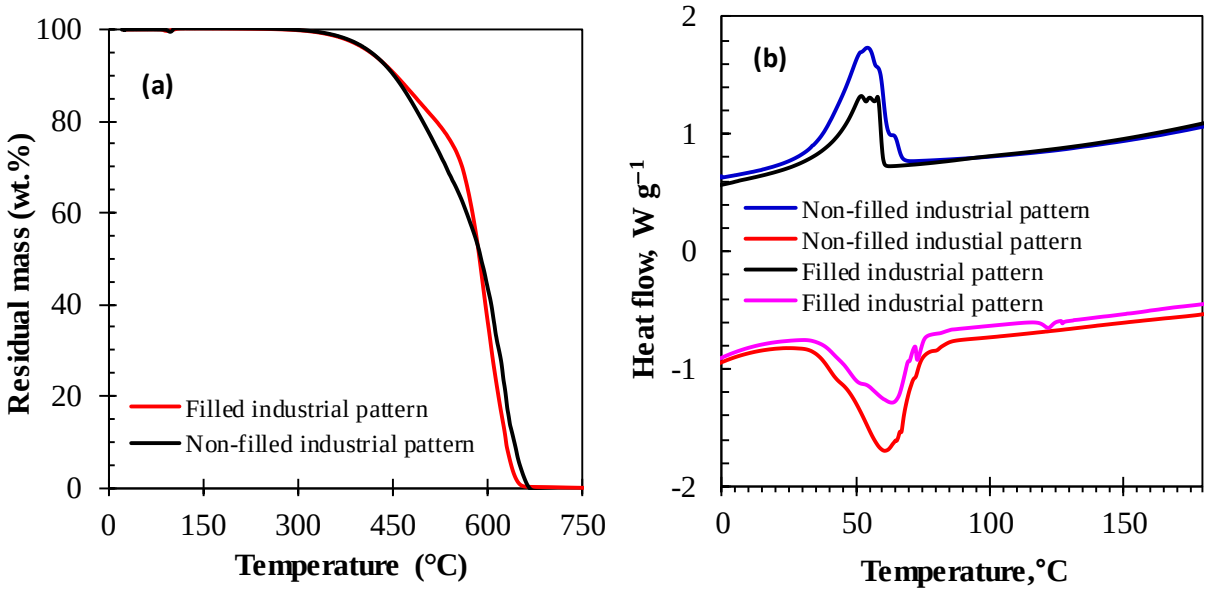

(ii). FTIR Spectra

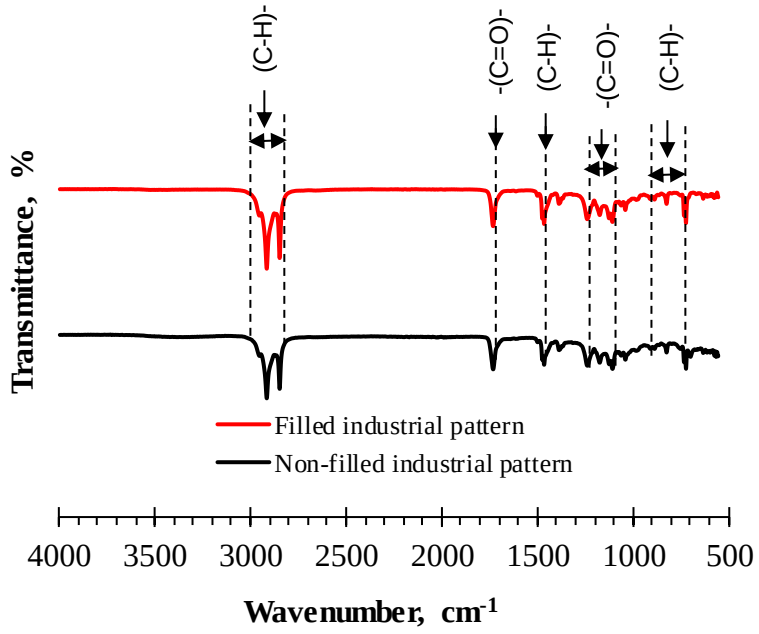

(iii). (a) Three-point bending (Load versus deflection curve); (b) TMA curves

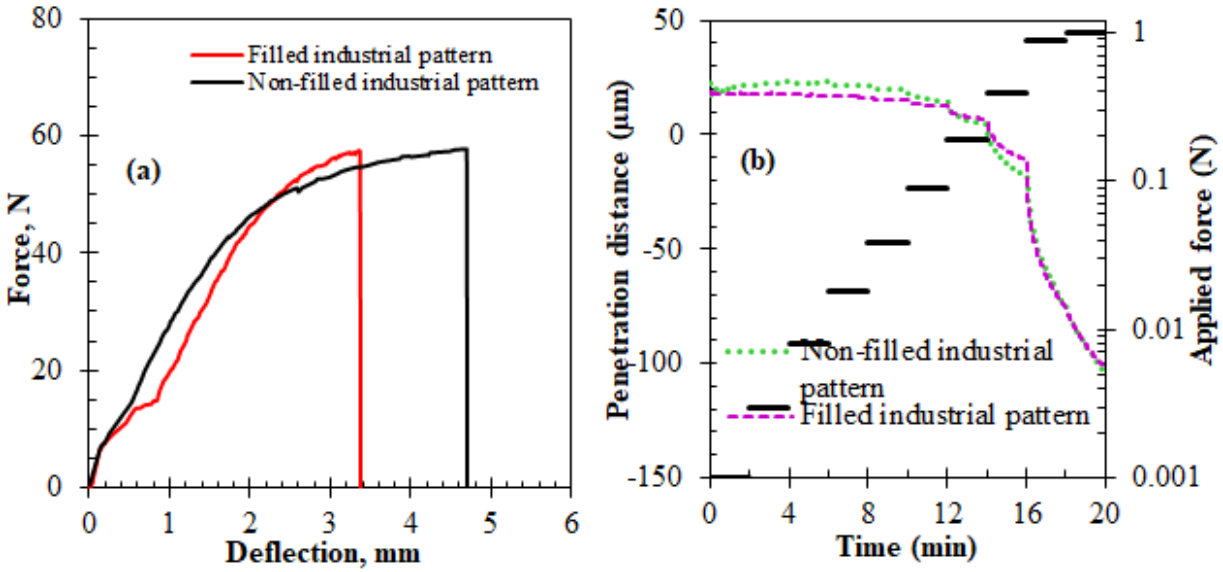

(iii). (a) SEM Micrographs (a) Filled industrial pattern; (b) Non-filled industrial pattern

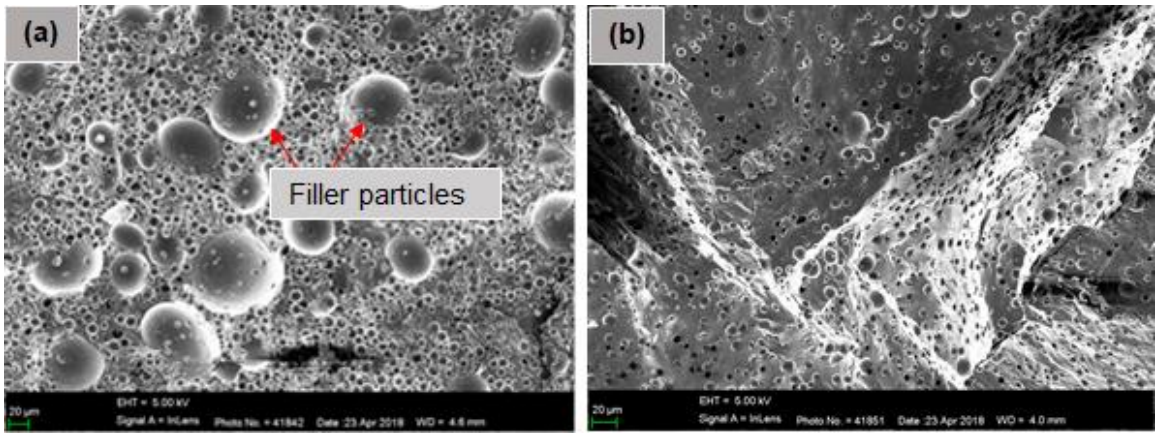

(iv). Viscosity curve of filled and non-filled industrial pattern

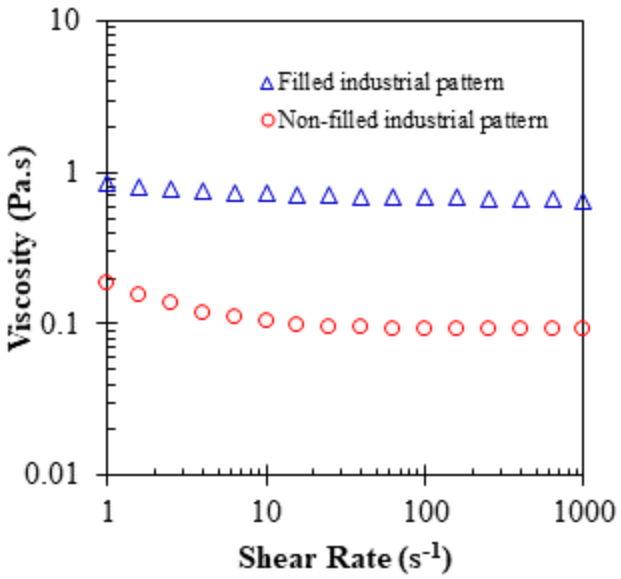

(v). solvent extraction of filler materials from filled and non-filled industrial pattern

	Filler content			
	Run 1	Run 2	Run 3	Average
Filled industrial pattern	38.08	37.17	37.89	37.71
Non-filled industrial pattern	5.38	6.49	5.63	5.83

APPENDIX IV: Two-way ANOVA for flexural stress data for the Wax/EVA/PMMA and Wax/LLDPE/PMMA blends

Table IV(a): Two-way ANOVA for flexural stress data for the Wax/EVA/PMMA

Source	Sum of Squares	Degree of freedom	Mean Square	F-value	Probability
Wax	15.79	2	7.90	189.53	0.0513
Wax*EVA	2.63	1	2.63	63.17	0.0797
Wax*PMMA	4.15	1	4.15	99.68	0.0636
EVA*PMMA	5.06	1	5.06	121.42	0.0576
Wax*EVA*PMMA	3.16	1	3.16	75.95	0.0727
Error	0.0417	1	0.0417		
Total	22.01	7			

$Y_{Stress} = 1.30X_{wax} + 150.86X_{EVA} + 44.97X_{PMMA} - 318.61X_{wax.}X_{EVA} - 94.31X_{wax}X_{PMMA} - 528.61 X_{EVA}X_{.PMMA} + 1246.53X_{wax.}X_{EVA.}X_{PMMA}$ $(r^2 = 0.9981)$

Table IV(b): Two-way ANOVA for flexural strain data for the Wax/EVA/PMMA

Source	Sum of Squares	Degree of freedom	Mean Square	F-value	Probability
Wax*EVA	14.16	1	14.16	7.35	0.2250
Wax*PMMA	3.14	1	3.14	1.63	0.4232
EVA*PMMA	10.84	1	10.84	5.63	0.2540
Wax*EVA*PMMA	15.23	1	15.23	7.91	0.2175
Error	1.93	1	1.93		
Total	44.96	7			

$Y_{Strain} = 1.70X_{wax} + 234.64X_{EVA} + 15.53X_{PMMA} - 738.89X_{wax}X_{.EVA} - 81.94X_{wax}X_{.PMMA} - 773.89X_{EVA}X_{PMMA} + 2734.72X_{wax.}X_{EVA.}X_{PMMA}$ $(r^2 = 0.9571)$

Table IV(c): Two-way ANOVA for Young modulus data for the Wax/EVA/PMMA

Source	Sum of Squares	Degree of freedom	Mean Square	F-value	Probability
Wax*EVA	3298.04	1	3298.04	0.1763	0.7469
Wax*PMMA	2283.30	1	2283.30	0.1221	0.7860
EVA*PMMA	552.13	1	552.13	0.0295	0.8917
Wax*EVA*PMMA	3977.66	1	3977.66	0.2127	0.7249
Error	18704.17	1	18704.17		
Total	2.078E+05	7			

$Y_{Modulus} = 38X_{wax} + 1284.11X_{EVA} + 3151.33X_{PMMA} - 11277.78X_{wax}X_{.EVA} + 2211.11X_{wax}X_{.PMMA} - 5522.22X_{EVA}X_{PMMA} - 44144.44X_{wax.}X_{EVA.}X_{PMMA}$ $(r^2 = 0.9100)$

Table IV(d): Two-way ANOVA for flexural stress data for the Wax/LLDPE/PMMA

Source	Sum of Squares	Degree of freedom	Mean Square	F-value	Probability
Wax*EVA	1.09	1	1.09	468.32	0.0021
Wax*PMMA	0.6612	1	0.6612	282.80	0.0035
Wax*PMMA	0.0621	1	0.0621	26.57	0.0356
Error	0.0047	2	0.0023		
Total	29.28	7			

$Y_{Stress} = 1.30X_{wax} + 42.31X_{EVA} + 13.14X_{PMMA} - 76.71X_{wax.}X_{EVA} + 32.07X_{wax}X_{PMMA} - 25.32 X_{EVA}X_{.PMMA}$ $(r^2 = 0.9998)$

Table IV(e): Two-way ANOVA for flexural strain data for the Wax/LLDPE/PMMA

Source	Sum of Squares	Degree of freedom	Mean Square	F-value	Probability
Wax*EVA	0.0141	1	0.0141	0.2353	0.7125
Wax*PMMA	0.0013	1	0.0013	0.0216	0.9071
EVA*PMMA	0.0032	1	0.0032	0.0536	0.8551
Wax*EVA*PMMA	0.0001	1	0.0001	0.0024	0.9691
Error	0.0600	1	0.0600		
Total	1.44	7			

$Y_{Strain} = 1.70X_{wax} + 16.37X_{EVA} + 0.70X_{PMMA} - 23.33X_{wax}X_{.EVA} - 1.67X_{wax}X_{.PMMA} - 13.33X_{EVA}X_{PMMA} + 8.33X_{wax.}X_{EVA.}X_{PMMA}$ $(r^2 = 0.9582)$

Table IV(f): Two-way ANOVA for flexural stress data for the Wax/LLDPE/PMMA

Source	Sum of Squares	Degree of freedom	Mean Square	F-value	Probability
Wax*EVA	1271.60	1	1271.60	0.1562	0.7604
Wax*PMMA	3276.26	1	3276.26	0.4025	0.6401
EVA*PMMA	104.05	1	104.05	0.0128	0.9283
Wax*EVA*PMMA	3766.77	1	3766.77	0.4627	0.6197
Error	8140.17	1	8140.17		
Total	3.334E+05	7			

$Y_{Modulus} = 38X_{wax} - 883.11X_{EVA} - 1405.33X_{PMMA} - 7002.78X_{wax}X_{.EVA} + 2648.61X_{wax}X_{.PMMA} + 2397.22X_{EVA}X_{PMMA} + 439006.94X_{wax.}X_{EVA.}X_{PMMA}$ $(r^2 = 0.9756)$

APPENDIX V: TGA and DSC curves of wax/EVA/PMMA and wax/LLDPE/PMMA blends

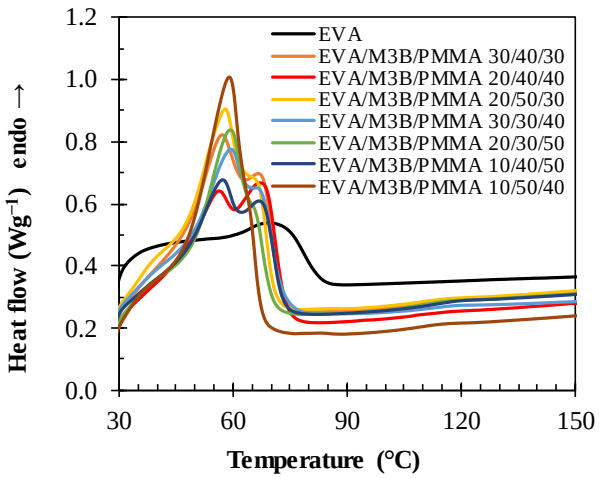

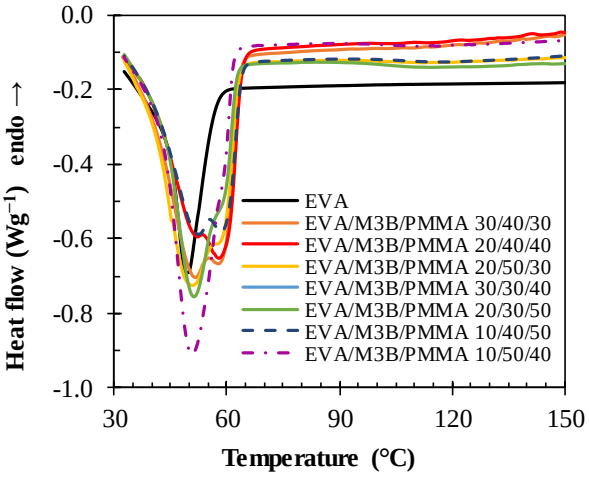

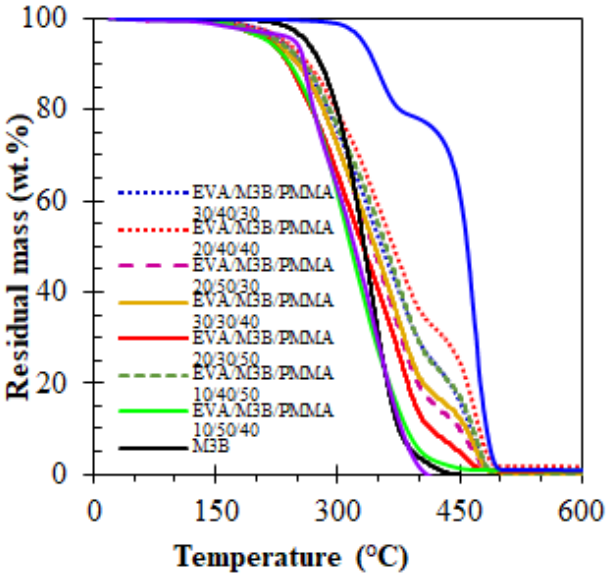

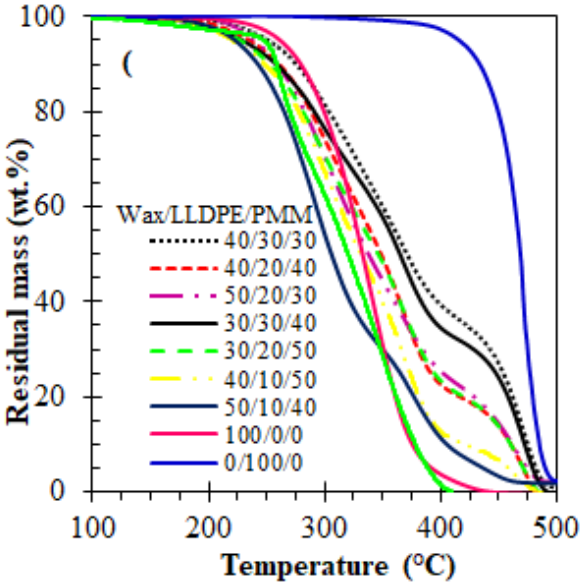

APPENDIX VI: Typical compounder settings, i.e. temperature profiles from hopper to die and screw speed used to compound wax/EVA/PMMA blends and wax/LLDPE/PMMA blends

The TX28P extrusion conditions to compound 40/30/30 wax/EVA/PMMA polymer blends

Conditions	**Zone 1 (°C)**	**Zone 2 (°C)**	**Zone 3 (°C)**	**Die**
Set	50	85	95	100
Read	52.5	85.7	94.2	102.3

The TX28P extrusion conditions to compound 40/20/40 wax/EVA/PMMA polymer blends

Conditions	**Zone 1 (°C)**	**Zone 2 (°C)**	**Zone 3 (°C)**	**Die**
Set	50	85	95	100
Read	56.3	86.4	94.6	102.7

The TX28P extrusion conditions to compound 50/20/30 wax/EVA/PMMA polymer blends

Conditions	**Zone 1 (°C)**	**Zone 2 (°C)**	**Zone 3 (°C)**	**Die**
Set	50	85	95	100
Read	55.3	86.3	97.1	102.6

The TX28P extrusion conditions to compound 30/30/40 wax/EVA/PMMA polymer blends

Conditions	**Zone 1 (°C)**	**Zone 2 (°C)**	**Zone 3 (°C)**	**Die**
Set	50	85	95	100
Read	55.9	87.2	96.2	103.2

The TX28P extrusion conditions to compound 30/20/50 wax/EVA/PMMA polymer blends

Conditions	**Zone 1 (°C)**	**Zone 2 (°C)**	**Zone 3 (°C)**	**Die**
Set	50	85	95	100
Read	56.1	87.3	94.7	103.2

The TX28P extrusion conditions to compound 40/10/50 wax/EVA/PMMA polymer blends

Conditions	**Zone 1 (°C)**	**Zone 2 (°C)**	**Zone 3 (°C)**	**Die**
Set	50	85	95	100
Read	56.3	86.7	94.3	103.1

The TX28P extrusion conditions to compound 50/10/40 wax/EVA/PMMA polymer blends

Conditions	**Zone 1 (°C)**	**Zone 2 (°C)**	**Zone 3 (°C)**	**Die**
Set	50	85	95	100
Read	56.1	86.3	94.6	103.2

The TX28P extrusion conditions to compound 40/30/30 wax/LLDPE/PMMA polymer blends

Conditions	**Zone 1 (°C)**	**Zone 2 (°C)**	**Zone 3 (°C)**	**Die**
Set	65	120	150	160
Read	72.1	122.3	150.9	163.1

The TX28P extrusion conditions to compound 40/20/40 wax/LLDPE/PMMA polymer blends

Conditions	**Zone 1 (°C)**	**Zone 2 (°C)**	**Zone 3 (°C)**	**Die**

Set	65	120	150	160
Read	72.4	122.5	151.7	163.1

The TX28P extrusion conditions to compound 50/20/30 wax/LLDPE/PMMA polymer blends

Conditions	**Zone 1 (°C)**	**Zone 2 (°C)**	**Zone 3 (°C)**	**Die**
Set	65	120	150	160
Read	69.6	121.9	152.9	162.9

The TX28P extrusion conditions to compound 30/30/40 wax/LLDPE/PMMA polymer blends

Conditions	**Zone 1 (°C)**	**Zone 2 (°C)**	**Zone 3 (°C)**	**Die**
Set	65	120	150	160
Read	70.9	121.7	153.9	163.7

The TX28P extrusion conditions to compound 30/20/50 wax/LLDPE/PMMA polymer blends

Conditions	**Zone 1 (°C)**	**Zone 2 (°C)**	**Zone 3 (°C)**	**Die**
Set	65	120	150	160
Read	70.9	121.7	153.9	163.7

The TX28P extrusion conditions to compound 40/10/50 wax/LLDPE/PMMA polymer blends

Conditions	**Zone 1 (°C)**	**Zone 2 (°C)**	**Zone 3 (°C)**	**Die**
Set	65	120	150	160
Read	72.1	122.3	152.7	162.4

The TX28P extrusion conditions to compound 50/10/40 wax/LLDPE/PMMA polymer blends

Conditions	Zone 1 (°C)	Zone 2 (°C)	Zone 3 (°C)	Die
Set	65	120	150	160
Read	72.3	122.1	152.7	162.1

APPENDIX: VII: Impact strength of characteristics of wax/EVA/PMMA blends and TMA penetration test sample graphs for wax/LLDPE/PMMA

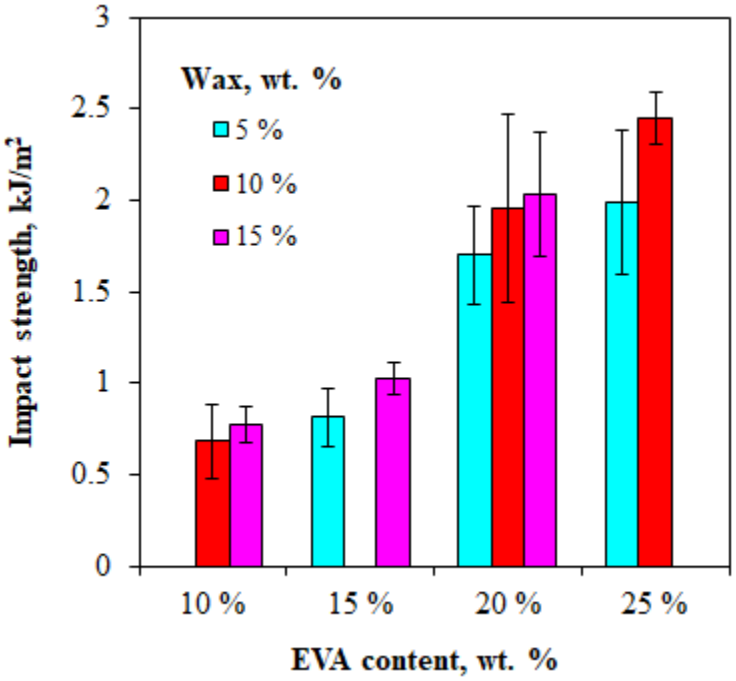

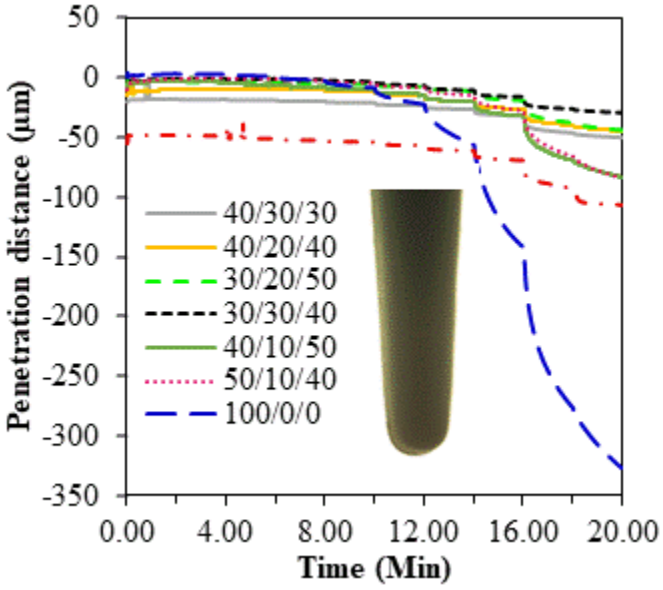

APPENDIX: VIII: SEM pictures of (a) PMMA; (b) EVA; (c)wax; (e) wax/EVA, (e-j) wax/EVA/PMMA and (k-n) wax/LLDPE/PMMA blends.

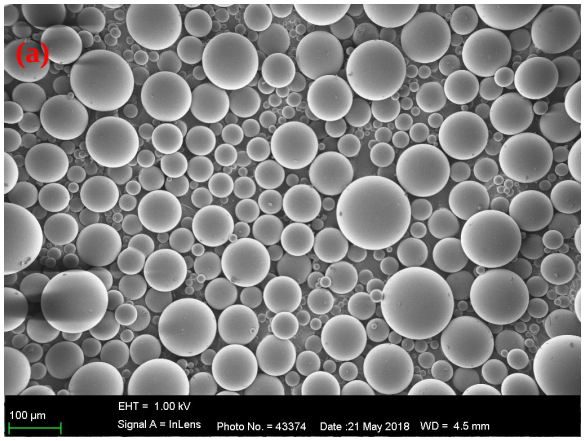

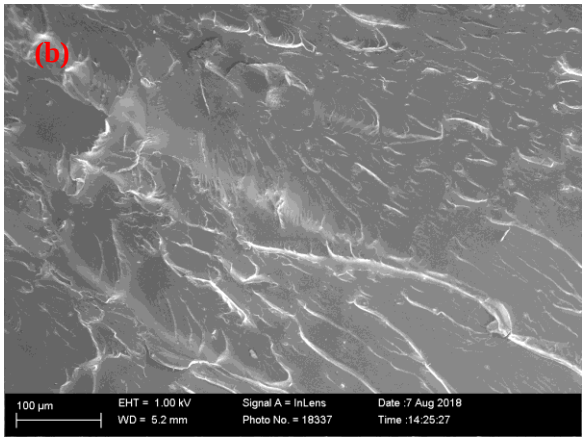

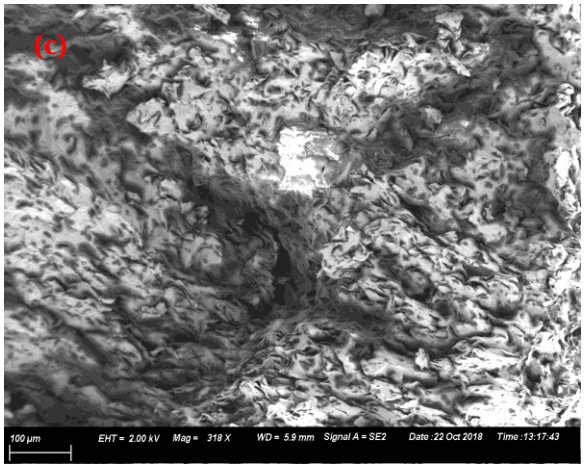

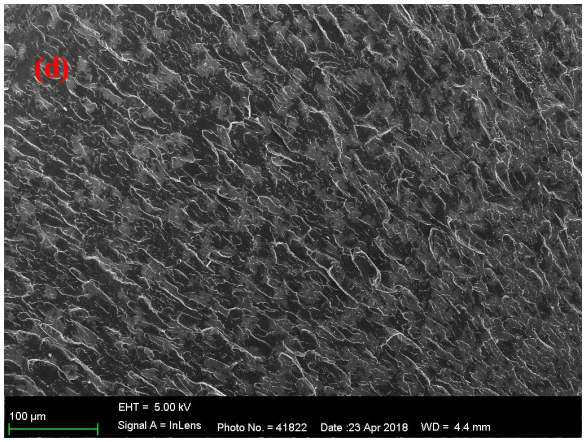

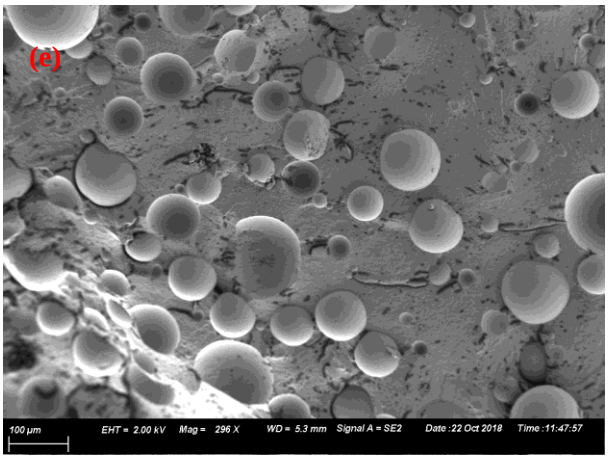

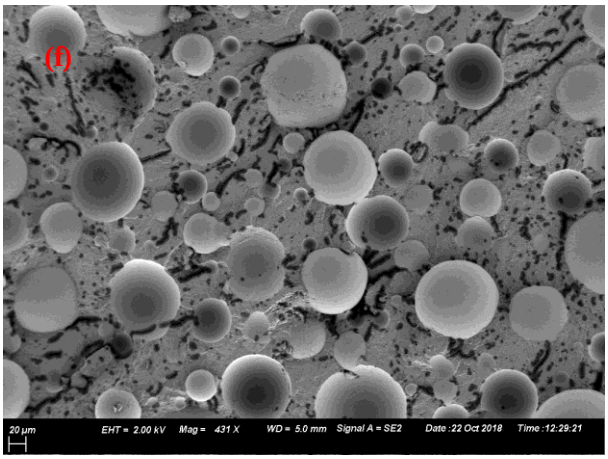

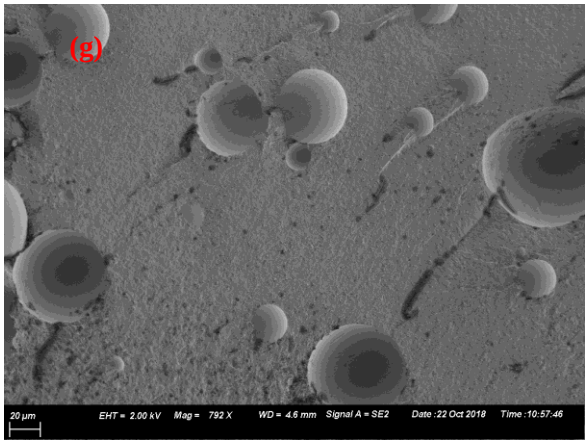
(g)
20 µm EHT = 2.00 kV Mag = 792 X WD = 4.6 mm Signal A = SE2 Date :22 Oct 2018 Time :10:57:46

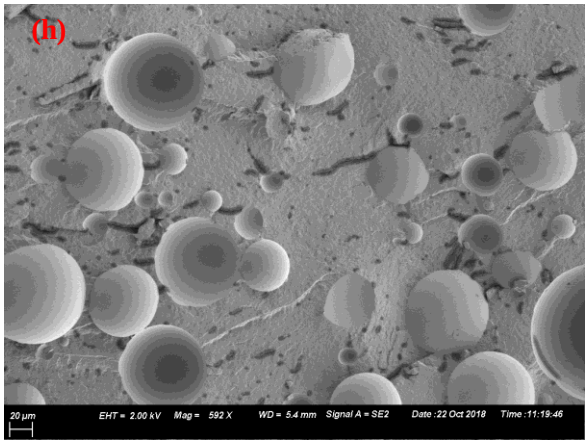
(h)
20 µm EHT = 2.00 kV Mag = 592 X WD = 5.4 mm Signal A = SE2 Date :22 Oct 2018 Time :11:19:46

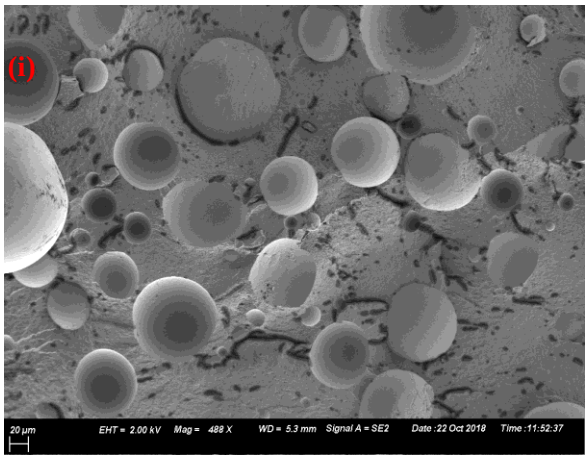
(i)
20 µm EHT = 2.00 kV Mag = 488 X WD = 5.3 mm Signal A = SE2 Date :22 Oct 2018 Time :11:52:37


(j)
20 µm EHT = 2.00 kV Mag = 639 X WD = 4.6 mm Signal A = SE2 Date :22 Oct 2018 Time :12:01:53

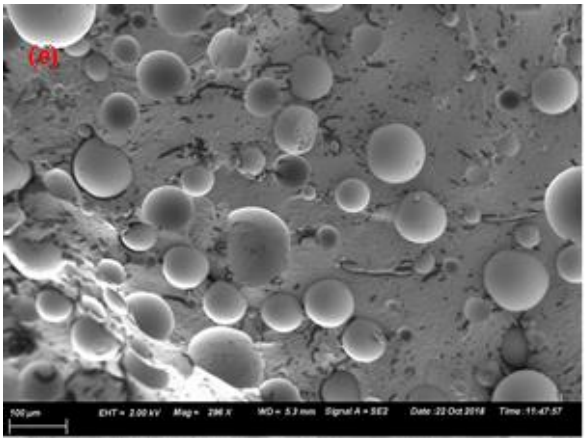
(e)

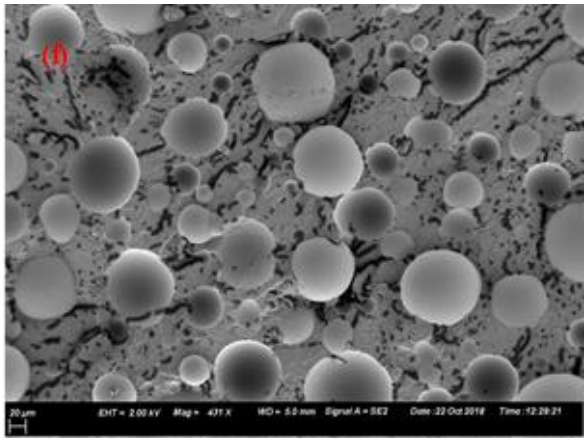
(f)


(g)
20 µm
EHT = 2.00 kV
Mag = 792 X
WD = 4.6 mm
Signal A = SE2
Date :22 Oct 2018
Time :10:57:46

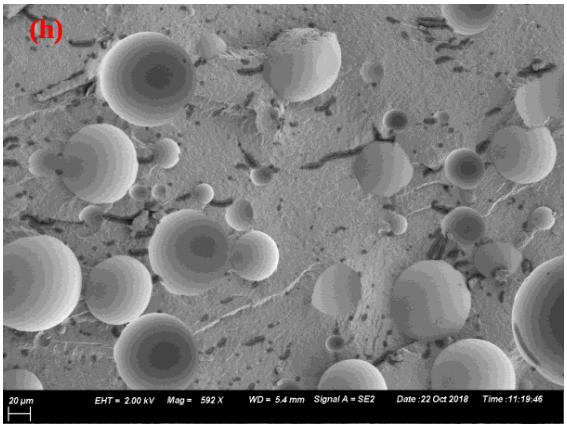
(h)
20 µm
EHT = 2.00 kV
Mag = 592 X
WD = 5.4 mm
Signal A = SE2
Date :22 Oct 2018
Time :11:19:46

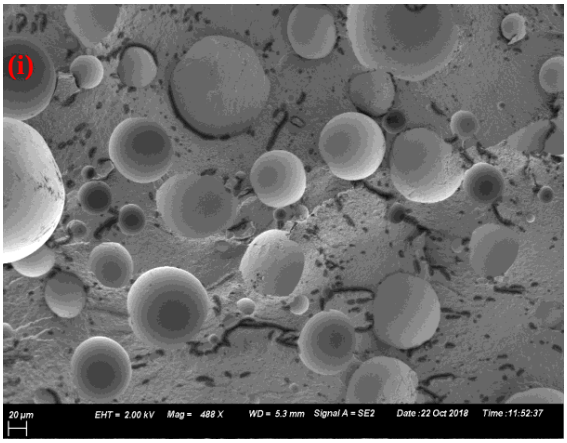
(i)
20 µm
EHT = 2.00 kV
Mag = 488 X
WD = 5.3 mm
Signal A = SE2
Date :22 Oct 2018
Time :11:52:37

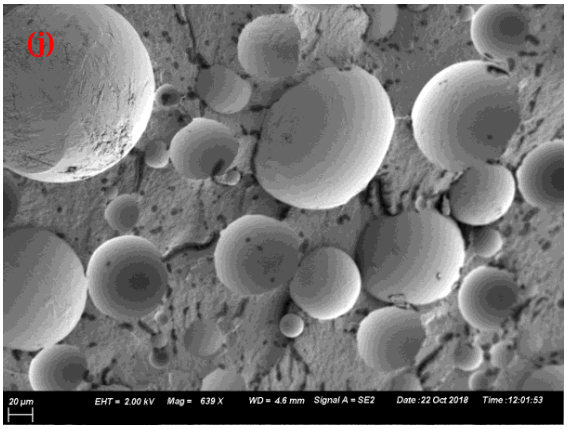
(j)
20 µm
EHT = 2.00 kV
Mag = 639 X
WD = 4.6 mm
Signal A = SE2
Date :22 Oct 2018
Time :12:01:53

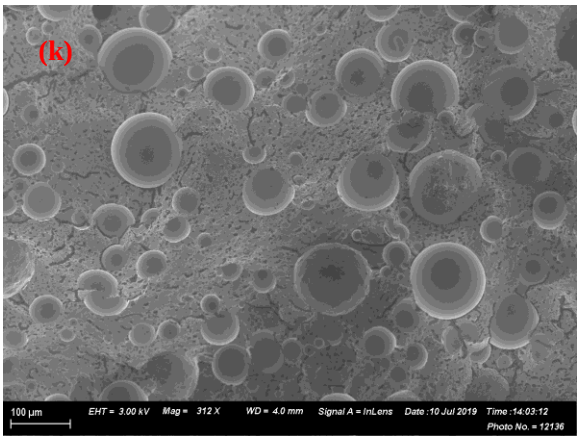
(k)
100 µm
EHT = 3.00 kV
Mag = 312 X
WD = 4.0 mm
Signal A = InLens
Date :10 Jul 2019
Time :14:03:12
Photo No. = 12136

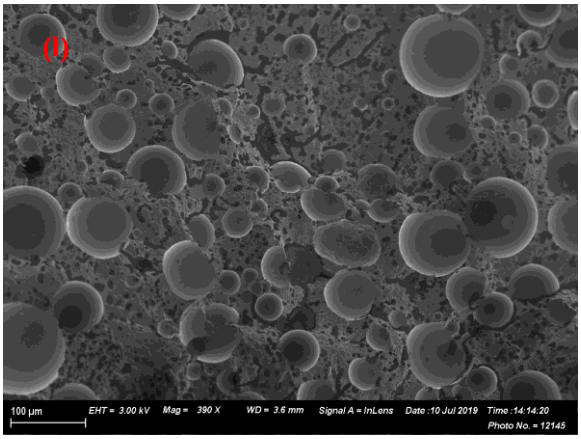
(l)
100 µm
EHT = 3.00 kV
Mag = 390 X
WD = 3.6 mm
Signal A = InLens
Date :10 Jul 2019
Time :14:14:20
Photo No. = 12145

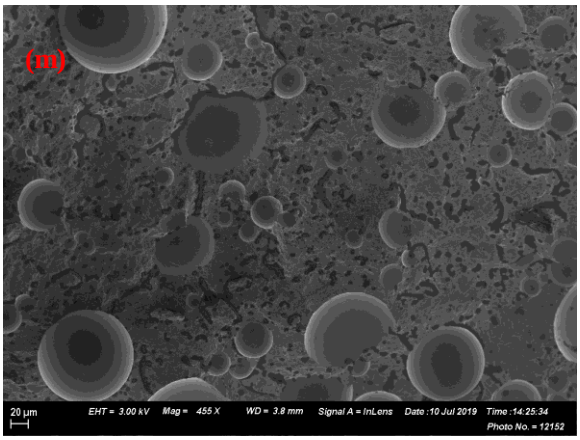
(m)
20 µm
EHT = 3.00 kV
Mag = 455 X
WD = 3.8 mm
Signal A = InLens
Date :10 Jul 2019
Time :14:25:34
Photo No. = 12152

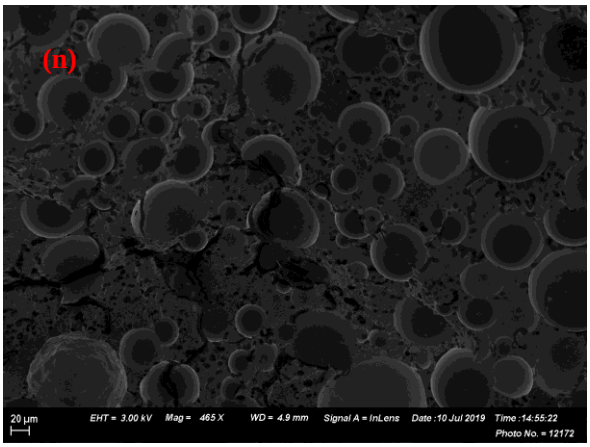
(n)
20 µm
EHT = 3.00 kV
Mag = 465 X
WD = 4.9 mm
Signal A = InLens
Date :10 Jul 2019
Time :14:55:22
Photo No. = 12172

APPENDIX: IX: MSDS Data sheets

POLYMETHYL METHACRYLATE CAS NO 9011-14-7	MATERIAL SAFETY DATA SHEET SDS/MSDS

SECTION 1: Identification of the substance/mixture and of the company/undertaking 1.1 Product identifiers

Product name : Polymethyl Methacrylate

CAS-No. : 9011-14-7

1.2 Relevant identified uses of the substance or mixture and uses advised against

Identified uses : Laboratory chemicals, Industrial & for professional use only.

1.3 Details of the supplier of the safety data sheet

Company : Central Drug House (P) Ltd
7/28 Vardaan House
New Delhi -110002
INDIA

Telephone : +91 11 49404040
Email : care@cdhfinechemical.com

1.4 Emergency telephone number

Emergency Phone # : +91 11 49404040 (9:00am - 6:00 pm) [Office hours]

SECTION 2: Hazards identification

2.1 Classification of the substance or mixture

Not a hazardous substance or mixture according to Regulation (EC) No. 1272/2008. **2.2 Label elements**

Not a hazardous substance or mixture according to Regulation (EC) No. 1272/2008.

2.3 Other hazards

This substance/mixture contains no components considered to be either persistent, bio accumulative and toxic (PBT), or very persistent and very bio accumulative (vPvB) at levels of 0.1% or higher.

SECTION 3: Composition/information on ingredients 3.1 Substances

Synonyms	:	Poly (methacrylic acid methyl ester) PMMA
Formula	:	(C5H8O2) n
CAS-No.	:	9011-14-7

No components need to be disclosed according to the applicable regulations.

SECTION 4: First aid measures 4.1 Description of first aid measures If inhaled

If breathed in, move person into fresh air. If not breathing, give artificial respiration.

In case of skin contact

Wash off with soap and plenty of water.

In case of eye contact

Flush eyes with water as a precaution.

If swallowed

Never give anything by mouth to an unconscious person. Rinse mouth with water.

4.2 Most important symptoms and effects, both acute and delayed

The most important known symptoms and effects are described in the labelling (see section 2.2) and/or in section 11

4.3 Indication of any immediate medical attention and special treatment needed

No data available

SECTION 5: Firefighting

measures 5.1 Extinguishing

media Suitable extinguishing

media

Use water spray, alcohol-resistant foam, dry chemical or carbon dioxide.

5.2 Special hazards arising from the substance or mixture

Carbon oxides **5.3 Advice for firefighters**

Wear self-contained breathing apparatus for firefighting if necessary.

5.4 Further information No data available

SECTION 6: Accidental release measures

6.1 Personal precautions, protective equipment and emergency procedures Avoid dust formation. Avoid breathing vapours, mist or gas. For personal protection see section 8.

6.2 Environmental precautions
No special environmental precautions required.

6.3 Methods and materials for containment and cleaning up

Sweep up and shovel. Keep in suitable, closed containers for disposal.

6.4 Reference to other sections for disposal see section 13.

SECTION 7: Handling and storage

7.1 Precautions for safe handling

Provide appropriate exhaust ventilation at places where dust is formed. Normal measures for preventive fire protection.
For precautions see section 2.2.

7.2 Conditions for safe storage, including any incompatibilities

Store in cool place. Keep container tightly closed in a dry and well-ventilated place.
Storage class (TRGS 510): Combustible Solids

7.3 Specific end use(s)
Apart from the uses mentioned in section 1.2 no other specific uses are stipulated

SECTION 8: Exposure controls/personal protection

8.1 Control parameters

8.2 Exposure controls

Appropriate engineering controls
General industrial hygiene practice.

Personal protective equipment Eye/face protection

Use equipment for eye protection tested and approved under appropriate government standards such as NIOSH (US) or EN 166(EU).

Skin protection

Handle with gloves. Gloves must be inspected prior to use. Use proper glove removal technique (without touching glove's outer surface) to avoid skin contact with this product. Dispose of contaminated gloves after use in accordance with applicable laws and good laboratory practices. Wash and dry hands.

Body Protection

Choose body protection in relation to its type, to the concentration and amount of dangerous substances, and to the specific work-place., The type of protective equipment must be selected according to the concentration and amount of the dangerous substance at the specific workplace.

Respiratory protection

Respiratory protection is not required. Where protection from nuisance le (EN 143) dust masks. Use respirators and components tested and approved under appropriate government standards such as NIOSH (US) or CEN (EU).

Control of environmental exposure No special environmental precautions required.

SECTION 9: Physical and chemical properties

9.1 Information on basic physical and chemical properties

a)	Appearance	Form: powder Colour: white
b)	Odour	odourless
c)	Odour Threshold	No data available
d)	pH	No data available
e)	Melting point/freezing point	No data available
f)	Initial boiling point and boiling range	No data available
g)	Flash point	> 250.00 °C - closed cup
h)	Evaporation rate	No data available
i)	Flammability (solid, gas)	No data available
j)	Upper/lower flammability or explosive limits	No data available
k)	Vapour pressure	No data available
l)	Vapour density	No data available
m)	Relative density	1.200 g/cm3
n)	Water solubility	insoluble
o)	Partition coefficient: n-octanol/water	No data available

p) Auto-ignition temperature 304 °C

q) Decomposition temperature No data available

r) Viscosity No data available

s) Explosive properties No data available

t) Oxidizing properties No data available

9.2 Other safety information No data available

SECTION 10: Stability and reactivity 10.1 Reactivity No data available **10.2 Chemical stability**
Stable under recommended storage conditions.

10.3 Possibility of hazardous reactions No data available **10.4 Conditions to avoid** No data available **10.5 Incompatible materials**
Strong oxidizing agents, Strong acids

10.6 Hazardous decomposition products

Hazardous decomposition products formed under fire conditions. - Carbon oxides
Other decomposition products - No data available
In the event of fire: see section 5

SECTION 11: Toxicological information 11.1 Information on toxicological effects Acute toxicity
No data available2-Propenoicacid, 2-methyl-, methyl ester, homopolymer

Skin corrosion/irritation
No data available (2-Propenoicacid, 2-methyl-, methyl ester, homopolymer)

Serious eye damage/eye irritation
No data available (2-Propenoicacid, 2-methyl-, methyl ester, homopolymer)

Respiratory or skin sensitization
No data available (2-Propenoicacid, 2-methyl-, methyl ester, homopolymer)

Germ cell mutagenicity
No data available (2-Propenoicacid, 2-methyl-, methyl ester, homopolymer)

Carcinogenicity

IARC: No component of this product present at levels greater than or equal to 0.1% is identified as probable, possible or confirmed human carcinogen by IARC.

Reproductive toxicity
No data available (2-Propenoicacid, 2-methyl-, methyl ester, homopolymer)

Specific target organ toxicity - single exposure
No data available (2-Propenoicacid, 2-methyl-, methyl ester, homopolymer)

Specific target organ toxicity - repeated exposure
No data available

Aspiration hazard
No data available (2-Propenoicacid, 2-methyl-, methyl ester, homopolymer)

Additional Information

RTECS: TR0400000

To the best of our knowledge, the chemical, physical, and toxicological properties have not been thoroughly investigated. (2-Propenoicacid, 2-methyl-, methyl ester, homopolymer)

SECTION 12: Ecological information

12.1 Toxicity
Nodata available

12.2 Persistence and degradability No data available **12.3 Bio accumulative potential** No data available **12.4 Mobility in soil**
No data available (2-Propenoicacid, 2-methyl-, methyl ester, homopolymer)

12.5 Results of PBT and vPvB assessment

This substance/*mixture* contains no components considered to be either persistent, bio accumulative and toxic (PBT), or very persistent and very bio accumulative (vPvB) at levels of 0.1% or higher.

12.6 Other adverse effects No data available

SECTION 13: Disposal considerations

13.1 Waste treatment methods Product

Offer surplus and non-recyclable solutions to a licensed disposal company.

Contaminated packaging
Dispose of as unused product.

SECTION 14: Transport information 14.1 UN number

ADR/RID: - IMDG: - IATA: -

14.2 UN proper shipping name
ADR/RID: Not dangerous goods IMDG: Not dangerous goods
IATA: Not dangerous goods

14.3 Transport hazard class(es)
ADR/RID: - IMDG: - IATA: -

14.4 Packaging group
ADR/RID: - IMDG: - IATA: -

14.5 Environmental hazards
ADR/RID: no IMDG Marine pollutant: no IATA: no

14.6 Special precautions for user No data available

SECTION 15: Regulatory information

15.1 Safety, health and environmental regulations/legislation specific for the substance or mixture
This safety data sheet complies with the requirements of Regulation (EC) No. 1907/2006.

15.2 Chemical safety assessment
For this product a chemical safety assessment was not carried out

SECTION 16: Other information Further information

The above information is believed to be correct but does not purport to be all inclusive and shall be used only as a guide. The information in this document is based on the present state of our knowledge and is applicable to the product with regard to appropriate safety precautions. It does not represent any guarantee of the properties of the product. Central Drug House (P) Ltd and its Affiliates shall not be held liable for any damage resulting from handling or from contact with the above product. See www.cdhfinechemical.com for additional terms and conditions of sale.

SABIC® LLDPE M500026
Linear low density polyethylene for masterbatch compounding

Description

SABIC® LLDPE M500026 is a high flow linear low-density polyethylene copolymer grade with a narrow molecular weight distribution.

Application

SABIC® LLDPE M500026 resin is recommended for injection moulding masterbatch where a high filler acceptance is required, combined with a good flow.

Processing conditions

Typical moulding conditions for SABIC® LLDPE M500026 are: material temperature 180 - 230 °C (355 - 450 °F).

Mechanical properties

Test specimen is prepared from compression moulded sheet made according to ASTM D-1928, procedure C.

Typical data. Revision 20060418

Properties	Units SI	Values	Test methods
Polymer properties			
Melt flow rate (MFR)			ASTM D 1238
at 190 °C and 2.16 kg	g/10 min	**50**	
Density	kg/m³	**926**	ASTM D 1505
Mechanical properties			
Tensile test			ASTM D 638
stress at yield	MPa	**13**	
stress at break	MPa	**12.4**	
strain at break	%	**120**	
secant modulus at 1% elongation	MPa	**354**	
Izod impact notched at 23 °C	J/m	**450**	ASTM D 256
Hardness Shore D	-	**55**	ASTM D 2240
ESCR	h	**2**	ASTM D 1693

Thermal properties			
Vicat softening temperature			ASTM D 1525
at 10 N (VST/A)	°C	**88**	
Brittleness temperature	°C	**<-75**	ASTM D 746

All information supplied by or on behalf of the SABIC Europe companies in relation to its products, whether in the nature of data, recommendations or otherwise, is supported by research and believed reliable, but the relevant SABIC Europe company assumes no liability whatsoever in respect of application, processing or use made of the afore-mentioned information or products, or any consequence thereof. The user undertakes all liability in respect of the application, processing or use of the afore-mentioned information or product, whose quality and other properties he shall verify, or any consequence thereof. No liability whatsoever shall attach to any of the SABIC Europe companies for any infringement of the rights owned or controlled by a third party in intellectual, industrial or other property by reason of the application, processing or use of the afore-mentioned information or by the user.

internet www.SABIC-europe.com email TCC.TM-PE@SABIC-europe.com

SABIC® LLDPE M500026
Linear low-density polyethylene for masterbatch compounding

General information. SABIC® LLDPE grades are available in a wide range of viscosities. Supplementary to this, various grades are also available in powder form. This unique combination makes SABIC® LLDPE grades extremely suitable for masterbatch and compounding applications.
The SABIC® LLDPE portfolio offers an excellent choice to find a good base resin for both additives, black, white and colour masterbatches, with varying amounts of additives and pigments.

Health, Safety and Food Contact regulations. Detailed information is provided in the relevant Material Safety Datasheet and or Standard Food Declaration, available on the Internet (www.SABIC-europe.com). Additional specific information can be requested via your local Sales Office.

Quality. SABIC Europe is fully certified in accordance with the internationally accepted quality standard ISO 9001-2000. It is SABIC Europe's policy to supply materials that meet customers specifications and needs and to keep up its reputation as a pre-eminent, reliable supplier of e.g. polyethylene.

Storage and handling. Polyethylene resins (in pelletized or powder form) should be stored in such a way that it prevents exposure to direct sunlight and/or heat, as this may lead to quality deterioration. The storage location should also be dry, dust free and the ambient temperature should not exceed 50 °C. Not complying with these precautionary measures can lead to a degradation of the product which can result in colour changes, bad smell and inadequate product performance. It is also advisable to

process polyethylene resins (in pelletized or powder form) within 6 months after delivery, this because also excessive aging of polyethylene can lead to a deterioration in quality.

Environment and recycling. The environmental aspects of any packaging material do not only imply waste issues but have to be considered in relation with the use of natural resources, the preservations of foodstuffs, etc. SABIC Europe considers polyethylene to be an environmentally efficient packaging material. Its low specific energy consumption and insignificant emissions to air and water designate polyethylene as the ecological alternative in comparison with the traditional packaging materials. Recycling of packaging materials is supported by SABIC Europe whenever ecological and social benefits are achieved and where a social infrastructure for selective collecting and sorting of packaging is fostered. Whenever 'thermal' recycling of packaging (i.e. incineration with energy recovery) is carried out, polyethylene -with its fairly simple molecular structure and low amount of additives- is considered to be a trouble-free fuel.

internet www.SABIC-europe.com email TCC.TM-PE@SABIC-europe.com

ELVAX™ 250

Ethylene Vinyl Acetate Copolymer

Description

Product Description	ELVAX™ 250 is an ethylene-vinyl acetate copolymer resin for use in industrial applications.

Restrictions

Material Status	Commercial: Active

Typical Characteristics

Composition	28% By Weight Vinyl Acetate comonomer content Thermal Stabilizer: BHT antioxidant
Applications	ELVAX™ resins can be used in a variety of applications involving molding, compounding, extrusion, adhesives, sealants, and wax blends.

Typical Properties

Physical	Nominal Values	Test Method(s)	
*Density ()	0.95g/cm³	ASTM D792	ISO 1183
*Melt Flow Rate (190°C/2.16kg)	25g/10 min	ASTM D1238	ISO 1133
Thermal	**Nominal Values**	**Test Method(s)**	
*Melting Point (DSC)	70°C (158°F)	ASTM D3418	ISO 3146
Vicat Softening Point ()	42°C (107.6°F)	ASTM D1525	ISO 306

Processing Information

*Maximum Processing Temperature	235 °C (455°F)
General Processing Information	ELVAX™ resins can be processed by conventional thermoplastic processing techniques, including injection molding, structural foam molding, sheet and shape extrusion, blow molding and wire coating. They can also be processed using conventional rubber processing techniques such as Banbury, two-roll milling and compression molding. ELVAX™ can be used in conventional extrusion equipment designed to process polyethylene resins. However, corrosion-protected

barrels, screws, adapters, and dies are recommended, since, at sustained melt temperatures above 455°F (235°C), ethylene vinyl acetate (EVA) resins may thermally degrade and release corrosive byproducts.

FDA Status Information

ELVAX™ 250 resin complies with Food and Drug Administration Regulation 21 CFR 177.1350(a)(1) - - Ethylene-vinyl acetate copolymers, subject to the limitations and requirements therein. This Regulation describes polymers that may be used in contact with food, subject to the finished food-contact article meeting the extractive limitations under the intended conditions of use, as shown in paragraph (b)(1) of the Regulation.

The information and certifications provided herein are based on data we believe to be reliable, to the best of our knowledge. The information and certifications apply only to the specific material designated herein as sold by Dow and do not apply to use in any process or in combination with any other material. They are provided at the request of and without charge to our customers. Accordingly, Dow cannot guarantee or warrant such certifications or information and assumes no liability for their use.

Regulatory Information

For information on regulatory compliance outside of the U.S.A., consult your local Dow representative.

Safety & Handling

THE IMPORTANCE OF PROPER HANDLING & STORAGE:

Maintaining proper handling and storage conditions for ELVAX™ resins is very important to ensure overall product quality and keep the resin in a free-flowing state. If the ELVAX™ resin is subjected to sunlight, rain or excessive temperatures, then the resin may not process properly or achieve the desired characteristics in the final product.

It is crucial for ELVAX™ resins to be kept under proper storage and handling conditions because improper storage and handling may cause the resin to “block” (massing of pellets into large clumps that can hinder the ease of material transfer) or lose the ability to flow freely.

Please refer to the ELVAX™ Handling Guide for additional information.

For additional information on appropriate Handling & Storage of this polymeric resin, please refer to the material Safety Data Sheet.

A Product Safety Bulletin, material Safety Data Sheet, and/or more detailed information on extrusion processing and/or compounding of this polymeric resin for specific applications are available from your Dow representative.

Product Stewardship

The Dow Chemical Company and its subsidiaries ("Dow") has a fundamental concern for all who make, distribute, and use its products, and for the environment in which we live. This concern is the basis for our Product Stewardship philosophy by which we assess the safety, health, and environmental information on our products and then take appropriate steps to protect employee and public health and our environment. The success of our Product Stewardship program rests with each and every individual involved with Dow products – from the initial concept and research, to manufacture, use, sale, disposal, and recycle of each product.

Customer Notice

Dow strongly encourages its customers to review both their manufacturing processes and their applications of Dow products from the standpoint of human health and environmental quality to ensure that Dow products are not used in ways for which they are not intended or tested. Dow personnel are available to answer your questions and to provide reasonable technical support. Dow product literature, including safety data sheets, should be consulted prior to use of Dow products. Current safety data sheets are available from Dow.

Medical Applications Policy

NOTICE REGARDING MEDICAL APPLICATION RESTRICTIONS: Dow will not knowingly sell or sample any product or service ("Product") into any commercial or developmental application that is intended for:

a. long-term or permanent contact with internal bodily fluids or tissues. "Long-term" is contact which exceeds 72 continuous hours (or for

PELLETHANE™ Polyurethane Elastomers only, which exceeds 30 days);

b. use in cardiac prosthetic devices regardless of the length of time involved ("cardiac prosthetic devices" include, but are not limited to, pacemaker leads and devices, artificial hearts, heart valves, intra-aortic

balloons and control systems, and ventricular bypass-assisted devices); c. use as a critical component in medical devices that support or sustain human life; or

d. use specifically by pregnant women or in applications designed specifically to promote or interfere with human reproduction.

Dow requests that customers considering use of Dow products in medical applications notify Dow so that appropriate assessments may be conducted.

Dow does not endorse or claim suitability of its products for specific medical applications. It is the responsibility of the medical device or pharmaceutical manufacturer to determine that the Dow product is safe, lawful, and technically suitable for the intended use. DOW MAKES NO WARRANTIES, EXPRESS OR IMPLIED, CONCERNING THE SUITABILITY OF ANY DOW PRODUCT FOR USE IN MEDICAL APPLICATIONS.

Disclaimer

NOTICE: No freedom from infringement of any patent owned by Dow or others is to be inferred. Because use conditions and applicable laws may differ from one location to another and may change with time, the Customer is responsible for determining whether products and the information in this document are appropriate for the Customer's use and for ensuring that the Customer's workplace and disposal practices are in compliance with applicable laws and other governmental enactments. Dow assumes no obligation or liability for the information in this document. NO WARRANTIES ARE GIVEN; ALL IMPLIED WARRANTIES OF MERCHANTABILITY OR FITNESS FOR A PARTICULAR PURPOSE ARE EXPRESSLY EXCLUDED.

NOTICE: If products are described as "experimental" or "developmental": (1) product specifications may not be fully determined; (2) analysis of hazards and caution in handling and use are required; (3) there is greater potential for Dow to change specifications and/or discontinue production; and (4) although Dow may from time to time provide samples of such products, Dow is not obligated to supply or otherwise commercialize such products for any use or application whatsoever. Additional Information

North America		Europe/Middle East		Latin America	
U.S. & Canada:	1-800-441-4369 1-989-832-1426 +1-800-441-4369	All Countries	+31-11567-2626 +800-3694-6367	Argentina: Brazil:	+54-11-4319-0100 +55-11-5188-9000
Mexico:		Italy:	+800-783-825	Colombia: Mexico:	+57-1-219-6000 +52-55-5201-4700
South Africa	+800-99-5078	Asia Pacific	+800-7776-7776 +60-3-7958-5392		

http://www.dow.com

SECTION 1. Identification of the substance/mixture and of the company/undertaking

Product identifier

Trade name	SASOLWAX FISCHER TROPSCH MEDIUM WAXES
Synonyms	SASOLWAX™: B28, B38, F5, M3C, M3E, M3HMA, M3M, M3MCB, M3X, M5, M5CB, M6, M3000, M3000X, SRB, SRW, 1742, 5501A, 5501B, 1824, IW2F, IW3F, 6530SA, WAKSOL 38, 505, M3B, M1T, M2F, M3F, Sasol wax 303, Sasol wax 305.

Relevant identified uses of the substance or mixture and uses advised against

Use	Industrial use.

Manufacturer or supplier's details

Company	Sasol Chemicals, a division of Sasol South Africa (Pty) Ltd
Address	Sasol Place, 50 Katherine Street Sandton 2090 South Africa
Telephone	+27103445000
E-mail address	sasolchem.info.sa@sasol.com
Emergency telephone number	+44 (0)1235 239 670 (Europe, Israel, Africa, Americas) +44(0)1235 239 671 (Middle East, Arabic African countries) +65 3158 1074 (Asia Pacific) +86 10 5100 3039 (China) +27 (0)17 610 4444 (South Africa) +61 (2) 8014 4558 (Australia)

SECTION 2. Hazards identification

Classification of the substance or mixture

	South Africa. GHS Classification and Labelling of Chemicals - SANS 10234
Classification	This substance is not classified as hazardous according to GHS.

Label elements

	South Africa. GHS Classification and Labelling of Chemicals - SANS 10234
Pictogram	Not applicable
Signal word	Not applicable
Hazard statements	This substance is not classified as hazardous according to GHS.

Precautionary statements

Prevention	This substance is not classified as hazardous according to GHS.
Response	This substance is not classified as hazardous according to GHS.
Storage	This substance is not classified as hazardous according to GHS.
Disposal	This substance is not classified as hazardous according to GHS.
Other hazards	No data available

SECTION 3. Composition/information on ingredients

Substance

Synthetic wax, Paraffinic hydrocarbons

Contents: 100.00 %W/W

CAS-No. 8002-74-2 Index-No. EC-No. 232-315-6

Other data MITI-No. 8-430

For the full text of the H-Statements mentioned in this Section, see Section 16.

SECTION 4. First aid measures

Description of necessary first-aid measures

Inhalation	Move to fresh air in case of accidental inhalation of vapours.
Skin contact	Cool melted product on skin with plenty of water. Do not remove solidified product. In case of burns by molten product medical treatment is necessary.
Eye contact	Rinse with water. If eye irritation persists, consult a specialist.
Ingestion	Never give anything by mouth to an unconscious person. If symptoms persist, call a physician.

Most important symptoms/effects, acute and delayed

SECTION 5. Firefighting measures

Suitable extinguishing media	Foam Dry powder
Unsuitable extinguishing media	Water spray.
Special hazards arising from the substance or mixture	Avoid contamination with oxidising agents
Special protective equipment for firefighters	In the event of fire, wear self-contained breathing apparatus. Use personal protective equipment.

SECTION 6. Accidental release measures

Personal precautions	No special precautions required.
Environmental precautions	Prevent release into the environment
Methods for cleaning up	Allow to solidify. Clean up all spills immediately. Control

personal contact with the substance, by using protective equipment.

Reference to other sections Refer to Section 8 and 13

SECTION 7. Handling and storage

Safe handling advice Provide sufficient air exchange and/or exhaust in work rooms.

Advice on protection against fire and explosion Keep away from open flames, hot surfaces and sources of ignition.

Requirements for storage areas and containers Keep in a dry, cool place.

Advice on common storage No data available

SECTION 8. Exposure controls/personal protection

Components with workplace control parameters

NATIONAL OCCUPATIONAL EXPOSURE LIMITS

Contains no substances with occupational exposure limit values.

Exposure controls

Engineering measures

Provide sufficient air exchange and/or exhaust in work rooms. Personal protective equipment

Respiratory protection	In case of insufficient ventilation, wear suitable respiratory equipment.
Hand protection	Leather gloves
Eye protection	Safety glasses
Skin and body protection	Overalls. PVC protective suit may be required if exposure is severe.
Hygiene measures	Wash hands before breaks and immediately after handling the product.

SECTION 9. Physical and chemical properties

Information on basic physical and chemical properties

Form	Coarse powder
State of matter	Solid; at 20 °C; 1,013 hPa
Colour	White to colourless
Odour	Odourless
Odour Threshold	No data available
Melting point/range	45 - 75 °C
Boiling point/boiling range	> 200 °C
Flash point	> 200 °C
Evaporation rate	No data available
Flammability (solid, gas)	No data available
Relative vapour density	No data available
Density	0.9 g/cm3; 25 °C
Water solubility	Insoluble

SECTION 10. Stability and reactivity

Reactivity	Stable under recommended storage conditions.
Chemical stability	Stable under recommended storage conditions.
Possibility of hazardous reactions	Hazardous polymerization does not occur.
Conditions to avoid	Heat
Materials to avoid	Oxidizing agents. Strong acids
Hazardous decomposition products	No data available

SECTION 11. Toxicological information

SECTION 14. Transport information

Acute oral toxicity

Synthetic wax, Paraffinic hydrocarbons:

LD50 Rat: > 2,000 mg/kg; GLP: no (literature value)

Acute dermal toxicity — Synthetic wax, Paraffinic hydrocarbons:

LD50 Rabbit: > 2,000 mg/kg; (literature value)

Eye irritation — Synthetic wax, Paraffinic hydrocarbons:

Rabbit: No eye irritation

SECTION 12. Ecological information

Other adverse effects This product has no known ecotoxicological effects.

SECTION 13. Disposal considerations

Product Dispose of in accordance with local regulations.

Marine pollutant Not a Marine Pollutant

Further Information Not classified as dangerous in the meaning of transport regulations.

SECTION 15. Regulatory information

Safety, health and environmental regulations/legislation specific for the substance or mixture

USA TSCA Inventory	All chemical constituents are listed in: USA TSCA Inventory (See chapter 3)
Canadian Domestic Substances List (DSL)	All chemical constituents are listed in: Canadian Domestic Substances List (DSL) (See chapter 3)
Australian Inv. of Chem. Substances (AICS)	All chemical constituents are listed in: Australian Inv. of Chem. Substances (AICS) (See chapter 3)
New Zealand Inventory of Chemicals (NZIoC)	All chemical constituents are listed in: New Zealand Inventory of Chemicals (NZIoC) (See chapter 3)
Jap. Inv. of Exist. & New Chemicals (ENCS)	All chemical constituents are listed in: Jap. Inv. of Exist. & New Chemicals (ENCS) (See chapter 3)
Japan. Industrial Safety & Health Law (ISHL)	All chemical constituents are listed in: Japan. Industrial Safety & Health Law (ISHL) (See chapter 3)
Korea. Existing Chemicals Inventory (KECI)	All chemical constituents are listed in: Korea. Existing Chemicals Inventory (KECI) (See chapter 3)
Philippines Inventory of Chemicals and Version 1.02	All chemical constituents are listed in: Philippines Inventory of Revision Date 08.02.2018
Chemical Substances (PICCS)	Chemicals and Chemical Substances (PICCS) (See chapter 3)
China Inv. Existing Chemical Substances (IECSC)	All chemical constituents are listed in: China Inv. Existing Chemical Substances (IECSC) (See chapter 3)

SECTION 16. Other information

Full text of H-Statements.

This substance contains no components with H-statement.

All reasonable efforts were exercised to compile this SDS in accordance with the Globally Harmonized System of Classification and Labelling of Chemicals (GHS). The SDS only provides information regarding the health, safety and environmental hazards at the date of issue, to facilitate the safe receipt, use and handling of this product in the workplace and does not replace any product information or product specifications. Since Sasol and its subsidiaries cannot anticipate or control all conditions under which this product may be handled, used and received in the workplace, it remains the obligation of each user, receiver or handler to, prior to usage, review this SDS in the context within which this product will be received, handled or used in the workplace. The user, handler or receiver must ensure that the necessary mitigating measures are in place with respect to health and safety. This does not substitute the need or requirement for any relevant risk assessments to be conducted. It further remains the responsibility of the receiver, handler or user to communicate such information to all relevant parties that may be involved in the receipt, use or handling of this product.

Although all reasonable efforts were exercised in the compilation of this SDS, Sasol does not expressly warrant the accuracy of, or assume any liability for incomplete information contained herein or any advice given. When this product is sold, risk passes to the purchaser in accordance with the specific terms and conditions of sale.